



Department of Cardiovascular Sciences

**Development of a Fluorescence Quantification
Assay for Mid to High Throughput Drug
Screening**

Pradeep Kaul

June 2017

**Dissertation submitted to the University of Sheffield for
degree of
Master of Philosophy**

Acknowledgements

First, I would like to profoundly thank my supervisor Dr. Tim Chico for his immense support. Not only do I extend my gratitude for his guidance but also for putting up with my rather erratic schedule. I will always be grateful for his patience.

I also want to thank Ms. Karen Plant for the help she provided throughout this period. She spent a lot of time teaching me various laboratory techniques at the start of the project. She was always ready to help whenever asked.

Dr. Stephen Brown from RNAi facility was immensely helpful. He helped with image acquisition and analysis. He was very kind to spare time to explain functioning of the plate-reader hardware and software.

Prior work done by Ms. Carolyn Gray and Peter Novodvorsky formed the basis of my project. Mr. Aaron Savage is another person I would like to mention for extending his help whenever I needed it.

I would like to thank my wife Stuti, who apart from supporting me emotionally had to bail me out financially for the year I spent in the laboratory. Lastly, I would like to acknowledge my sons Prannay and Ahaan who, many a time were at the receiving end of my frustrations.

Abstract

Background

In recent times zebrafish (*danio rerio*) has been used increasingly for drug screening, target identification, pharmacology and toxicology. Quantifying fluorescence emitted by fluorophores is a method that can be used to measure expression of a gene. I used a novel transgenic zebrafish line to develop a drug screening assay, using fluorescence quantification to assess expression of the atheroprotective *klf2a* gene, to which the fluorophore is tagged.

Materials and Methods

The novel transgenic zebrafish line (*klf2a:GFP;kdrl:RFP*) was developed in our laboratory for my experiments. To establish positive and negative controls for the assay, GFP fluorescence patterns, a surrogate for *klf2a* expression were observed in two days post fertilization (2dpf) embryos. Images were acquired using a fluorescence stereomicroscope. Green fluorescence was quantified using FIJI (ImageJ) software. GraphPad Prism was used for data analysis.

In order to prevent flow-dependent expression of *klf2a* in developing vasculature, 1 cell stage embryos were injected with 1nl of 0.2mM *tnnt2* morpholino into 1 cell stage embryos. No blood flow was established in these embryos. To switch off the flow-dependent expression of *klf2a* in zebrafish embryonic vasculature blood flow was interrupted at 1 day post fertilization stage, by treating embryos with anaesthetic drug, tricaine. To further examine the non-flow dependent *klf2a* expression tricaine-only treated embryos were compared with embryos treated with tricaine and lovastatin. Statins like lovastatin are known to upregulate *klf2* through non-flow dependent pathways.

Feasibility of using a plate-reader was established to further develop the assay for mid to high throughput drug screening.

Results

I replicated the results to substantiate that *klf2a* expression was dependent on flow in the vasculature. Lovastatin treatment significantly increased GFP fluorescence in 2dpf embryos as compared to DMSO (dimethyl sulphoxide) treated embryos.

I further showed that the assay was reproducible when used for a mid-throughput drug screening.

Aims

My aim was to develop a drug screening assay by fluorescence quantification of reporter gene GFP tagged to *klf2a* promoter in a double transgenic zebrafish line *klf2a:GFP;kdr1:RFP*.

Hypothesis

- A high throughput plate-reader can be used for optimal imaging and fluorescence measurements of zebrafish embryos in our transgenic line.
- In the double transgenic line used, GFP expression was flow-dependent.
- Lovastatin increased GFP fluorescence in these particular embryos.
- GFP fluorescence quantification can be used as a whole organism initial drug-screening assay.

Objectives

The points laid out in above hypothesis were tested as follows

- To assess the optimal way of imaging 1 and/or 2dpf embryos I compared imaging embryos using orientation tools in a 96 well plate with direct pipetting of embryos into the wells in a clear medium.
- I examined the effect of absent blood flow in embryos treated with tricaine and in *tnnt2* morphants on GFP expression.

- To see the effects of Lovastatin on GFP expression I performed a dose response exercise.
- The feasibility of using a high throughput plate-reader for drug screening was tested, first by establishing validity of positive and negative controls and then by using drugs from the Spectrum library for actual screening.

Table of Contents

i. Title Page

ii. Acknowledgements

ii. Abstract

iii. Aims, Hypothesis and Objectives

Table of Contents.....i

List of Figures.....vi

List of Abbreviations.....viii

Chapter 1

1. Introduction.....1

1.1 Krüppel like factors.....3

1.1.1 Krüppel like factors family of transcription factors.....3

1.1.1.1 Background.....3

1.1.1.2 Conservation and Phylogenetic analysis.....3

1.1.1.3 Structure of KLFs.....4

1.1.2 *KLFs* in organ development and tissue function.....6

1.1.2.1 Role in cardiovascular development.....6

1.1.2.2 *KLFs* and Endothelial Cells.....5

1.1.2.3 Role in development of other organs.....7

1.1.3 Krüppel Like Factors (<i>klf</i>) in zebrafish.....	7
1.1.3.1 Phylogeny of zebrafish <i>kfl</i> genes	7
1.1.3.2 <i>klf2a</i> and <i>klf2b</i> expression during development.....	8
1.1.4 Krüppel Like Factor 2 (<i>KLF2</i>).....	9
1.1.4.1 Role of <i>KLF2</i> in development.....	9
1.1.4.2 Role of <i>KLF2</i> in Endothelial Cell biology.....	9
1.1.4.3 Role of <i>KLF2</i> in leukocyte adhesion to endothelial cells.....	10
1.1.4.4 <i>KLF2</i> and thrombotic function.....	11
1.1.4.5 <i>KLF2</i> in angiogenesis and vasculogenesis.....	11
1.1.4.6 Role in regulating vascular tone.....	13
1.1.4.7 Role of <i>KLF2</i> in lung development.....	13
1.1.4.8 <i>KLF2</i> in erythropoiesis.....	14
1.1.4.9 Effects on immune system regulation.....	14
1.1.4.10 <i>KLF2</i> in metabolic regulation.....	14
1.1.5 Mechanisms regulating <i>KLF2</i>.....	15
1.1.5.1 Sensing of shear and stress by endothelial cells.....	15
1.1.5.2 Flow mediated regulation of <i>Klf2</i>	16
1.1.5.3 Non-flow dependent regulation of <i>Klf2</i>	18
1.1.6 <i>Klf2</i> and atherosclerosis.....	21
1.2 Zebrafish in drug screening.....	23
1.2.1 Zebrafish as a model of cardiovascular research.....	23
1.2.2 Chemical screening in zebrafish.....	24
1.2.3 Successes so far.....	26
1.2.4 Screens for mechanisms of action.....	28
1.2.5 <u>Uses in toxicology screening</u>.....	29

Chapter2

2. Materials and Methods.....	31
2.1 Zebrafish Husbandry.....	32
2.1.1 Background.....	32
2.1.2 Characteristics of zebrafish as an experimental model.....	32
2.1.3 Zebrafish Handling.....	33
2.1.4 Transgenic lines used.....	34
2.2 Collecting Zebrafish Embryos.....	35
2.2.1 Marbling.....	35
2.2.2 Pirmating.....	35
2.2.2.1 Materials.....	35
2.2.2.2 Method.....	36
2.3 Embryo Medium.....	37
2.4 Injecting zebrafish embryos.....	37
2.4.1 Embryos.....	37
2.4.2 Microinjection apparatus.....	37
2.4.3 Morpholinos.....	38
2.4.4 Method.....	38
2.4.4.1 Preparing morpholinos for injection.....	39
2.4.4.2 Preparing microinjection needles.....	39
2.4.4.3 Embryo collection.....	39
2.4.4.4 Microinjection of embryos.....	40
2.5 Screening for double transgenics.....	41

2.5.1 Materials	41
2.5.2 Methods	41
2.6 Dechoriation	42
2.6.1 Materials	42
2.6.2 Methods	42
2.7 Preparing agarose molds for embryo orientation	43
2.7.1 Materials	43
2.7.2 Methods	43
2.8 Preparing different treatments	43
2.8.1 Lovastatin	43
2.8.2 Tricaine	44
2.8.3 Lovastatin and Tricaine	44
2.8.4 DMSO	45
2.9 Treatment groups	45
2.10 Imaging embryos for GFP fluorescence	45
2.10.1 Phase 1	45
2.10.1.1 Materials.....	46
2.10.1.2 Methods.....	46
2.10.2 Phase 2	47
2.10.2.1 Materials.....	47
2.10.2.2 Methods.....	47
2.10.3 Phase 3	48
2.10.3.1 Materials.....	48
2.10.3.2 Methods.....	49

2.11 Algorithms used for image analysis.....	50
2.11.1 Simple Threshold technique.....	50
2.11.2 Customised segmentation algorithms.....	50

Chapter 3

3. Results and Development of assay.....	54
3.1 Introduction.....	55
3.2 Development of assay.....	55
3.2.1 Step1. Optimizing imaging method.....	55
3.2.1.1: 96 well plate vs 384 well plate.....	57
3.2.1.2 Using orientation tool for imaging.....	56
3.3 Step2. Finding optimal Lovastatin concentration.....	59
3.3.1 Comparing increase in GFP fluorescence pre an treatment.....	59
3.3.2 Mapping a dose response curve to find out the optimal Lovastatin dose for positive controls.....	61
3.4 Developing positive and negative controls.....	64
3.4.1 Validating positive and negative controls by examining effect of flow and Lovastatin on GFP fluorescence in 2dpf zebrafish.....	64
3.4.1.1 Using a fluorescent stereomicroscope.....	64
3.4.1.2 Validating positive and negative controls on plate-reader.....	69
3.5 Mid to High throughput assay for Drug Screening.....	71
3.6.1 Screening drugs from Spectrum SP100122 drug library.....	71

Chapter 4

4. Discussion.....	79
---------------------------	-----------

Chapter5

5. References.....	85
---------------------------	-----------

List of Figures

1.1 Phylogenetic groups of Krüppel Like Factors (<i>KLFs</i>).....	3
1.2 Structure of <i>KLFs</i>	4
1.3 Protein structure of <i>KLFs</i>	4
1.4 <i>KLF2</i> in vascular homeostasis.....	14
1.5 Pathways involved in up-regulation of <i>KLF2</i>	18
1.6 Pathways involved in down-regulation of <i>KLF2</i> expression.....	19
1.7 Cytokine mediated down-regulation of <i>KLF2</i>	21
1.8 Mevalonate pathway.....	22
1.9 Upregulatory functions of <i>KLF2</i>	23
2.1 Assembly of tanks in aquarium.....	38
2.2 Pair-mating assembly.....	40
2.3 Structure of Morpholinos.....	42
2.4. Injecting 1-cell stage embryos.....	41
2.5 Dechoriation.....	47
2.6 Zebrafish embryo orientation tools.....	48
2.7 Segmentation algorithm images.....	56
2.8 Multi-wavelength cell scoring model.....	58
3.1 Presentation of zebrafish embryos in microtitre plates.....	55
3.2 Images of 2dpf embryos of positive and negative controls in a 384 well plate.....	61
3.3 Graph comparing the presentation of zebrafish embryos in 96 and 384 well plates.....	62
3.4 Representative images of embryos using different mounting methods RFP.....	63

3.5 Column graph comparing the quality of images acquired with two techniques.....	63
3.6 Photograph of a 96 well plate with agarose molds.....	64
3.7 Picture panels showing relative increase in GFP fluorescence in controls and lovastatin treated embryos.....	66
3.8 Measuring fluorescence.....	66
3.9 Column graphs of pre and post treatment GFP fluorescence.....	67
3.10 Scatter plot of pre and post treatment fluorescence.....	67
3.11 Dose response curve for lovastatin.....	68
3.12 Lovastatin dose response graph.....	69
3.13 Lovastatin dose response using higher concentrations.....	70
3.14 Lovastatin dose response graph for higher concentrations.....	71
3.15 Measuring total fluorescence.....	74
3.16 Image panels of positive and negative control groups obtained using a fluorescent microscope.....	74
3.17: Graphs showing Corrected total fluorescence.....	75
3.18 Images panels of resveratrol treated embryos.....	76
3.19 Effect of resveratrol on GFP expression.....	76
3.20 Reconstruction of images of each well of a 96 well plate.....	77
3.21 Measuring fluorescence in a plate-reader.....	78
3.22 Scatter plot of fluorescence data acquired on ImageXpress.....	79
3.23 Spectrum library drug screening.....	81
3.24 Integrated intensity of different drug screen candidates.....	81
3.25 Representative images of drug screen	82
3.26 Blinded positive and negative controls.....	83
3.27 Revalidation of positive and negative controls.....	84

3.28 Representative images of mid-throughput screen of Spectrum 100122 (plate 8) candidates.....	86
3.29 Possible hits from the drug screen.....	86

List of Abbreviations

<i>KLFs</i>	Krüppel Like Factors
Sp1	Specificity Protein 1
GC	Guanine Cytosine
CTGF	Connective tissue growth factor
TGF β	Transformation Growth Factor β
c-DNA	Complementary DNA
C-	Carboxy-
N-	Amino-
hpf	hours post fertilization
dpf	days post fertilisation
E	embryonic day
VCAM	Vascular Cell Adhesion Molecule
IL	Interleukin
TNF	Tumor Necrosis Factor
LPS	Lipopolysaccharide
NF- κ B	Nuclear Factor
I κ B	Inhibitor of κ B
p	protein
CREB-	cAMP-response element-binding protein
SRC	Steroid receptor co-activator
CBP	CREB binding protein
PAR-1	Protease Activator Receptor-1
MCP-1	Monocyte Chemoattractant Protein
AP-1	Co-factor Activating Protein-1
SMAD	Sma gene, Mother against decapentaplegic
ATF2	Nuclear Activating Transcription Factor 2
NO	Nitric Oxide
tPA	Tissue Plasminogen activator
TM	Thrombomodulin
APC	Activated Protein C
PAI1	Plasminogen Activator Inhibitor 1
siRNA	small interfering Ribose Nucleic Acid
VEGFR2	Vascular Endothelial Growth Factor Receptor2
miRNA	micro Ribose Nucleic Acid
VSMC	Vascular Smooth Muscle Cell
Flk1	Fetal liver kinase 1
HIF	Hypoxia Inducible factor
eNOS	endothelial Nitric Oxide Synthetase.

ET-1	Endothelin-1
3T3-L1	3 day transfer, innoculum 3x10 mouse cell line
PPAR	Peroxisome proliferator-activated receptor
G Protein	Guanine nucleotide binding protein
MEF	Myocyte Enhancing Factor
MADS	MCM1, Agamous, Deficiens, Serum response factor
A/T	Adenine and thymine
ERK5	extracellular signal regulated kinase
PCAF	p300/CBP-associated factor
PI3K	Phosphoinositide-3 kinase
AMPK	AMP-activated protein kinase
HDAC	Histone deacylase
LDLR	Low density lipoprotein receptor
Nrf2	Nuclear factor erythroid related factor 2
ApoE	Apolipoprotein E
HSCs	Haemopoietic Stem Cells
BMP	Bone morphogenic protein
ALK2	Activin receptor like kinase2
PP2A	Phosphatase 2A
ALL	Acute Lymphoblastic leukemia
TnnT2	Troponin T2
MO	Morpholino
DMSO	Dimethyl sulphoxide
GFP	Green Fluorescent Protein
RFP	Red Fluorescent Protein
MCWS	Multi-wavelength cell scoring
Lova	Lovastatin

Chapter 1

Introduction

1.1 Krüppel Like Factors (*KLFs*)

1.1.1 Krüppel Like family of transcription Factors

1.1.1.1 Background

Krüppel like factors (*KLFs*) are a family of zinc finger containing transcription factors. These factors are associated with proliferation, differentiation, development and apoptosis. *KLFs* participate in physiological and pathophysiological functions of many organ systems like the cardiovascular, respiratory, blood and immune systems. *KLFs* are also involved in tumor biology. (Jiang et al., 2008, Nandan and Yang, 2009).

The first mammalian krüppel like factor was found in a mouse erythro-leukaemia cell line. (Miller and Bieker, 1993).

KLFs are a seventeen-member family of transcription factors that form a part of the Sp1/*KLF* group of transcription factors and share similar zinc finger structures. Krüppel Like factors are aptly named, as they are homologous to krüppel (German for “cripple”) protein in *Drosophila melanogaster*. Krüppel protein is a member of the “gap” class of proteins and its expression in *Drosophila melanogaster* embryos causes altered abdominal and thoracic segmentation resulting in death. (Nusslein-Volhard and Wieschaus, 1980, Schuh et al., 1986).

1.1.1.2 Conservation and Phylogenetic analysis

Genes coding for *KLF* proteins are highly conserved in mammals. Krüppel Like factors also have homologs in chicken (*Gallus gallus*), zebrafish (*Danio rerio*), frogs (*Xenopus laevis*) and nematodes (*Caenorhabditis elegans*). *KLF* expression varies in different tissues (Brey et al., 2009, Pearson et al., 2008).

On the basis of mode of function *KLFs* are divided into three different groups. (Pearson et al. (2008)).

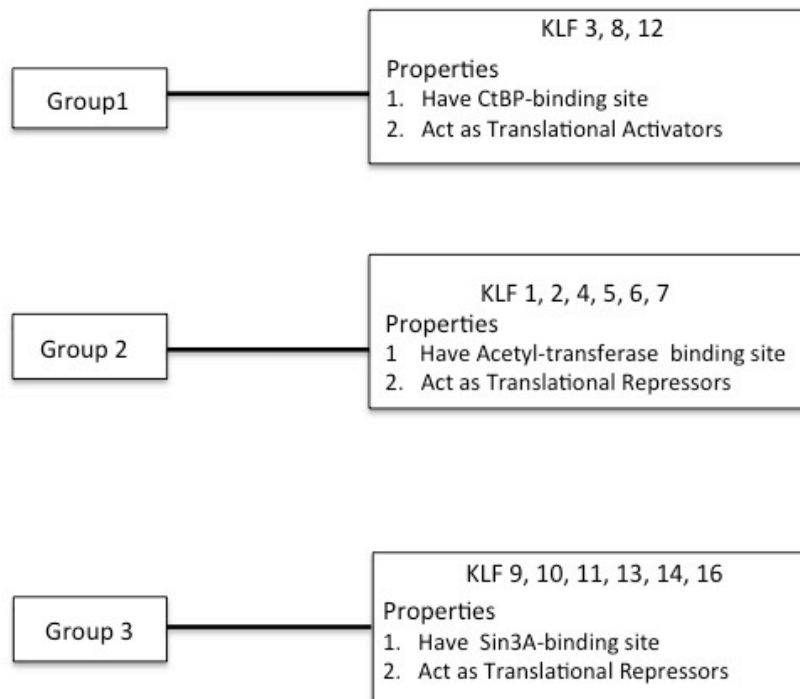


Figure 1.1 Phylogenetic groups of Krüppel like Factors (KLFs).

Figure showing three different groups of KLFs. Each group has a characteristic binding site and acts either as a translational repressor or a translational activator. CtBP (Carboxy-terminal Binding Protein).

KLFs 15 and 17 contain no specific protein interaction domain

1.1.1.3 Protein Structure of *KLFs*.

Zinc finger domains are a common feature of transcriptional factors. Several features distinguish *KLFs* from other zinc finger transcription factors. The carboxy-terminus of *KLF* proteins contains three (Cysteine)²-(Histidine)² zinc fingers. The first and second zinc fingers contain 25 amino acids and the third finger contains 23 amino acids. The

inter-finger space has a highly conserved 7 amino acid sequence. Each finger recognizes three base pairs in a DNA sequence and as such interact with 9 base pairs

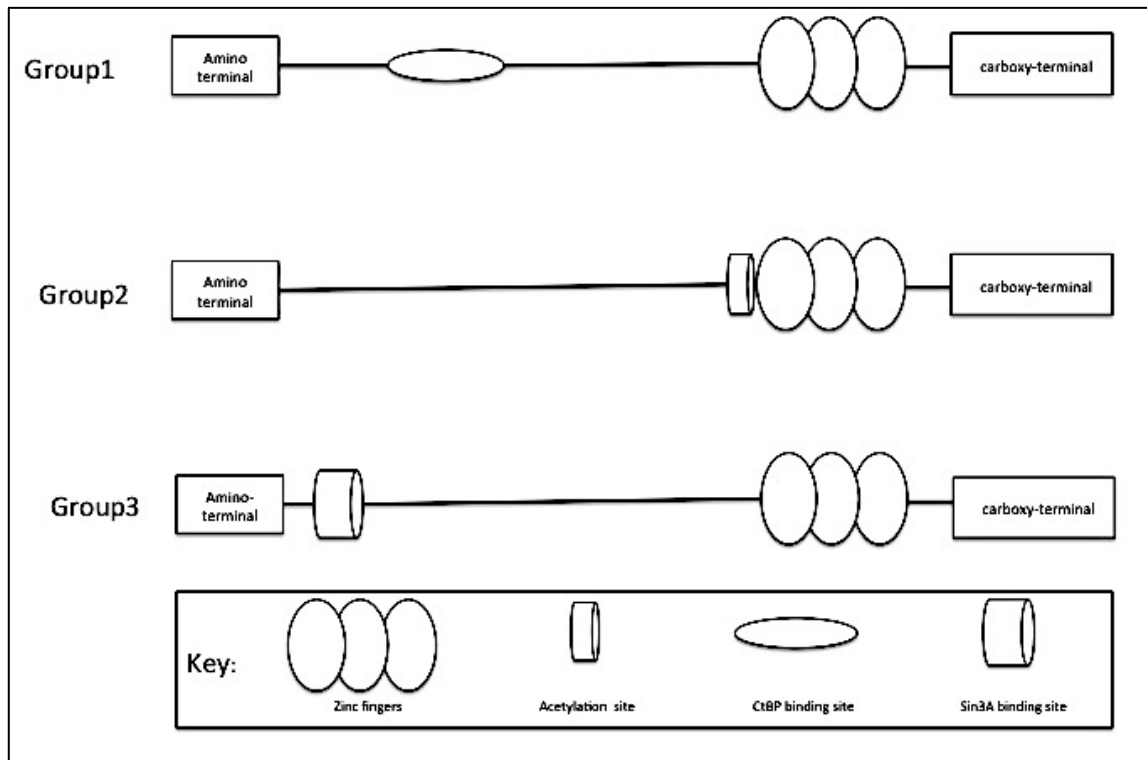


Figure 1.2 Structure of KLFs

Schematic representation of three groups of Krüppel Like Factors showing the position of activator and repressor binding domains.

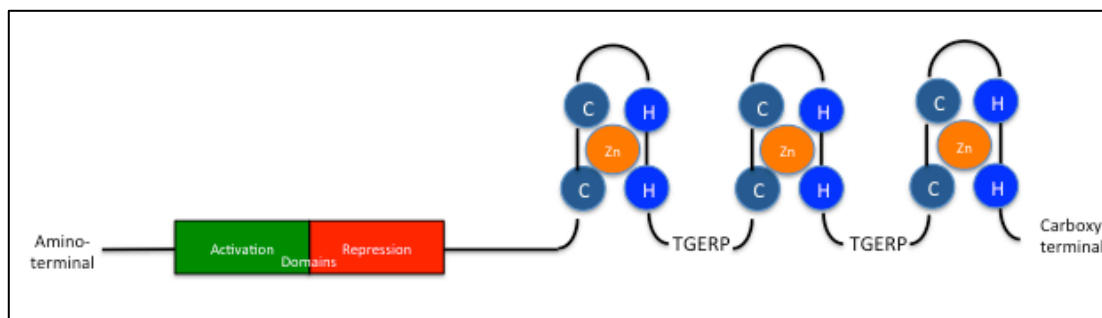


Figure. 1.3 Protein Structure of KLFs.

Schematic diagram of the structure of KLFs showing two C(Cysteine) and two H(Histidine) residues in each Zn (Zinc) finger and activation and repressor domains towards the amino-terminal.

(Dang et al., 2000). Zinc finger binding sites are similar among the *KLFs*. These include GC rich sequences like 5' CACCC-3' or the GT box. The members of *KLF* family have different amino-terminal regions, which impart functional diversity to them. This variation allows them to bind different co-activators, co-repressors and modifiers. Histone acetyl-transferase binding site, Carboxy-terminal Binding Protein (CtBP) site, and Sin3A binding site are found in Krüppel Like Factor groups 1,2 and 3 respectively. Zinc finger domains also play an important part in nuclear import of *KLFs* (Mehta et al., 2009).

Transcriptional regulation by *KLFs* is mediated by, modular activation and repression domains in their structure.

KLFs undergo posttranslational modifications by regulatory proteins through processes like acetylation, phosphorylation and ubiquitination (McConnell and Yang, 2010).

1.1.2 *KLFs* in organ development and tissue function

KLF family members play important regulatory parts at key stages of organ development, their physiology and pathophysiology.

1.1.2.1 Cardiovascular development

KLF2 and *KLF13* play a role in cardiovascular development. *KLF13* regulates cardiac cell proliferation (Martin et al., 2001). *KLF2* is an important, *in vivo*, regulator of haemodynamic shear stress necessary for normal cardiovascular development (Lee et al., 2006).

KLF15 is reduced in biopsy samples of patients with left ventricular hypertrophy (Fisch et al., 2007). Increased connective tissue growth factor (CTGF) expression and fibrosis was seen in *KLF15*^{-/-} mouse model, when, subjected to aortic banding. *KLF15* inhibits

binding of co-activator P/CAF thus suppressing CTGF expression, which in turn decreases cardiac fibrosis. (Wang et al., 2008). In contrast *KLF5* promotes fibrosis in myocardium (Shindo et al., 2002).

KLF10 prevents cardiac hypertrophy by unknown mechanisms (Rajamannan et al., 2007)

1.1.2.2 *KLFs* and Endothelial Cells

KLF2, 4 and 6 are expressed in endothelial cells (EC).

KLF4 reduces adhesion of inflammatory cells like neutrophils and platelets to vessel endothelium. It also prolongs clotting time (Hamik et al., 2007). *KLF6* induces several genes like, endoglin, collagen1, TGF β receptor type1, which are important for vascular remodeling after vessel injury (Botella et al., 2002).

***KLF2* will be discussed separately in subsequent sections.**

1.1.2.3 Role of *KLFs* in other organ system development.

KLFs play roles in development and maturation of respiratory, hematopoietic, immune, gastrointestinal, skeletal and nervous systems.

1.1.3 Krüppel Like Factors in Zebrafish (*Danio rerio*)

Zebrafish (*Danio rerio*) are a subclass of teleosts that have arisen from a common ancestor about 340 million years ago. This ancestor seems to have undergone an additional round of whole genome duplication also known as teleost specific genome duplication or TSD. As a result of TSD zebrafish possesses 26,206 protein coding genes, which is more than any other sequenced vertebrate species. Zebrafish also have a higher number of species specific genes as compared to humans. Human and zebrafish genomes, when directly compared, reveal that 71.4% of human genes have at least one zebrafish orthologue. Reciprocally, 69% of zebrafish genes have human orthologues.

47% of human genes have only one zebrafish orthologue. Many human genes have more than one orthologue in zebrafish genome, with an average of 2.28 zebrafish genes to one human gene (Vilella et al., 2009). The Online Mendelian Inheritance in Man (OMIM) database has 3176 human gene sequences that bear morbidity descriptions. 2601 (82%) of these genes have a zebrafish orthologue. This underlines the importance of zebrafish as a model to study various human diseases (Howe et al., 2013).

After gene duplication, usually one gene copy becomes functionally silenced and disappears overtime. This process is called non-functionalisation. Duplicate genes can also undergo neo-functionalization. Here the duplicate copies develop beneficial mutations in one or both copies that aid in evolution of new functions over time. Gene duplicates can also undergo sub-functionalization. In this case gene duplicates together perform the functions of a single copy mammalian orthologue.

Oates et al (Oates et al., 2001) hybridized a fragment of the c-DNA of mouse *Klf1* to an adult zebrafish kidney c-DNA, Sequence analysis demonstrated presence of five independent genes, each containing Krüppel like zinc finger motifs. These are *klf2a*, *klf2b*, *klf4*, *klf12* and *klfd*.

1.1.3.1 Phylogeny of zebrafish *klf* genes

In an amino acid sequence comparison with other members of *KLF* family C- terminals of five zebrafish genes have three tandem zinc fingers. The regions outside zinc finger domains have diverged significantly.

Zebrafish *klf2a*, *klf2b* and *klf4* proteins were similar to mammalian *Klf2* and *Klf4*. The zebrafish *klf* genes show more similarity to each other than to *Klf2* or *Klf4* resulting in a low boot- strap values. But examination of amino acid sequences at the N-termini of

proteins revealed five highly conserved blocks of residues separated by divergent regions.

The syntenic relations between the zebrafish and their closest mammalian homologs support the hypothesis that *klf2a* and *klf2b* are orthologs of *Klf2* and *klf4* is an ortholog of *Klf4*. Mammalian *Klf12* and zebrafish *klf12* are orthologous. *klfd* has no mammalian ortholog. (Oates et al., 2001)

1.1.3.2 *klf2a* and *klf2b* expression during development.

Klf2a and *klf2b* genes are expressed during gastrula stages in early epidermis in a partially overlapping pattern. *Klf2a* was detected in ventral, animal portion of the epiblast at 70% epiboly and extended vegetally as epiboly progressed. *Klf2b* had a similar expression pattern but in a slightly wider area. By the end of epiboly *klf2b* expression is lost in animal-most one third of the epiblast. *Klf2b* had higher expression in a lateral band extending around the dorsal midline of the embryo. Thus the domain of *klf2a* expression is enveloped by *klf2b*.

Klf2a expression was detected 24hpf around the anus and in small cluster of cells lateral to the posterior notochord. Expression was also noted in scattered cells in close vicinity of axial vessels, head vessels and heart. These expression patterns persist up to 48 hpf when signals for *klf2a* are detected in the caudal fin and in the pectoral fins.

Klf2b was expressed in the superficial layer of the epidermis, in large squamous cells present dorsally. At 36 hpf this expression is markedly decreased. *Klf2b* is present in higher levels at this stage, in two cords of cells anterior and ventral to the pectoral fin buds.

Zebrafish *klf2a* expression is seen in cells associated with blood vessels in head, trunk and tail, but not in intersegmental vessels, indicating that, a function in blood vessel development is ancestral for *KLF2* genes in vertebrates.

klf2b expression in differentiating epidermis is akin to *Klf4* in mouse. This may be because in mammalian lineage epidermal expression was lost in *KLf2* and retained by *Klf4*.

None of *klf2* genes were seen being expressed in developing thymus. Both *klf2* genes were expressed in pectoral fins and may have a role in differentiation of limb muscle.

Expression during erythrocyte development, as seen in zebrafish and mammals suggests that function in haematopoiesis is ancestral. (Oates et al., 2001)

1.1.4 Krüppel Like Factor 2 (KLF2)

Lingrel et al first cloned *KLF2* (Anderson et al., 1995). *KLF2* is a 354 amino acid protein, also called Lung Krüppel like protein because of its abundant presence in lung tissue. Human *KLF2* maps to chromosome 19p13.1. It has 85% homology to the mouse gene. 5' sequence in proximal promoter region and the 3' untranslated regions are conserved between the two species. Though the sequences in the proximal promoter show divergence between mouse and humans, a region of 75 base-pairs is conserved between the two species. This region functions as a novel transcriptional element important for *KLF2* gene expression (Wani et al., 1999a). Structural domain mapping has identified an N terminal activation domain between amino acids 1 and 110 and an inhibitory domain between amino acids 110 and 267. The inhibitory domain of *KLF2* interacts with WWP1, an E3 ubiquitin ligase, resulting in ubiquitination and proteasome mediated degradation of *KLF2* (Conkright et al., 2001, Zhang et al., 2004).

Using northern blot techniques on mouse embryos at 7,11,15 and 21 days of gestation, *Klf2* expression is evident in mouse embryos at embryonic day 7 (E7). The expression decreases by E11 and then increases around E15 (Anderson et al., 1995).

1.1.4.1 Role of *KLF2* in development

Target deletion studies have shown that *KLF2* regulates T-cell maturation, normal lung development, cardiovascular development and may have roles in maturation of other systems like nervous systems. The following sections will briefly describe role of *klf2* in development and pathophysiology (McConnell and Yang, 2010)

1.1.4.2. Role of *KLF2* in endothelial cell biology

KLF2 is the most studied *KLF* in vascular cell biology and patho-biology. *KLF2* is highly expressed in cultured endothelial cells when subjected to prolonged shear and stress due to laminar flow (Dekker et al., 2002, SenBanerjee et al., 2004).

In vivo studies have shown that *KLF2* is expressed in the endothelium of human aortae in regions exposed to prolonged laminar flow. *KLF2* is down regulated or absent in areas of non-laminar shear stress as is found at the origin of arterial branches. These branch points are more prone to early atherosclerosis (Dai et al., 2004).

1.1.4.3. Regulation of leukocyte adhesion to endothelial cells

Immune cells are recruited to vessel walls in response to the inflammatory stimulation of the endothelial cells. This sets the scene for a series of complex interactions which leads to development and progression of atherosclerosis. *KLF2* is an important transcriptional regulator that counteracts endothelial activation. *KLF2* inhibits cytokine mediated induction of adhesion molecules like Vascular Cell Adhesion Molecule (VCAM)-1 and E-selectin. This in turn reduces the attachment of inflammatory and immune cells to the endothelial cell lining of the vessel wall (SenBanerjee et al., 2004).

KLF2 prevents endothelial cell activation by interleukin -1 β (IL-1 β), Tumor necrosis factor- α (TNF- α), Lipopolysaccharide (LPS) and thrombin. The nuclear Factor- κ B (NF- κ B) pathway is the most important pro-inflammatory pathway affected by *KLF2* action. Normally in the absence of any pro-inflammatory stimuli NF- κ B stays in the

cytoplasm, inhibited by two inhibitors, I κ B and proteins, p100 and p105. On cellular stimulation these inhibitors are completely or partially broken down by phosphorylation. NF- κ B dimers p50/p65 thus formed move into the nucleus and alter gene expression. NF- κ B activity depends on other co-activator proteins like CREB-binding protein (CBP), Steroid receptor-coactivator-1 (SRC-1), IKK α and p300/CBP associated factor (Arany et al., 1994, Yamamoto et al., 2003).

KLF2 interacts with CBP/p300, a key co-factor for NF- κ B activity. *KLF2* reduces transcriptional activity of NF- κ B by competing with CBP/p300 co-activator and in this process reducing expression of target genes like VCAM-1 and E-selectin in response to inflammatory response. *KLF2* also inhibits protease activator receptor 1 (PAR-1). This in turn inhibits thrombin mediated induction of IL-6, IL-8 and monocyte chemoattractant protein-1 (MCP-1). Thus *KLF2* inhibits endothelial inflammation by inhibiting multiple pathways dependent on NF- κ B activity (Parmar et al., 2006).

Klf2 strongly inhibits Transformation Growth Factor- β signaling by two distinct mechanisms involving SMAD3/4 dependent transcriptional activation and by inhibiting co-factor activating protein-1 (AP-1). Endothelial cells overlying atherosclerotic plaques have increased levels of nuclear activating transcription factor 2 (ATF2). *KLF2* suppresses nuclear translocation of ATF2. (Boon et al., 2007, Fledderus et al., 2007).

1.1.4.4 *KLF2* and thrombotic function

Blood is maintained in a fluid state by factors like nitric oxide (NO), tissue plasminogen activator (tPA) and thrombomodulin (TM). Nitric oxide (No) inhibits platelet activation and prevents platelet aggregation. Tissue plasminogen activator (tPA) converts plasminogen into plasmin. Plasmin causes fibrinolysis and clot dissolution in injured blood vessels and re-establishing blood flow. Thrombomodulin (TM) is an integral membrane protein which acts as a cofactor for thrombin. This interaction changes

thrombin from a pro-coagulant to an anticoagulant factor. *KLF 2* can differentially regulate these key factors. By inducing TM expression *KLF2* augments antithrombotic function by activation of protein C to activated protein C (APC). Furthermore, *KLF2* overexpression inhibits procoagulant factors like tissue factor and plasminogen activator inhibitor1 (PAI1) and prolongs clotting time under flow condition. *KLF2* knockdown by small interfering RNAs (siRNAs) resulted in opposite effect, establishing *KLF2* as a key regulator of endothelial gene expression in thrombotic pathways (Lin et al., 2005).

1.1.4.5 *KLF2* in angiogenesis and vasculogenesis

Angiogenesis is important in physiological conditions like menstruation and wound healing and also in pathological conditions like chronic inflammation and tumors. *Klf2* has potent antiangiogenic effect. In nude mice models it has been demonstrated that overexpression of *KLF2* inhibits VEGF mediated angiogenesis and causes tissue oedema. At a molecular level *KLF2* at least partly inhibits expression of key VEGF receptor VEGFR2 by competing with SP1 for binding to VEGF promoter (Bhattacharya et al., 2005). Semaphorin-3F factor known to inhibit tumor cell migration is potently induced by *KLF2* (Dekker et al., 2006). *KLF2* by reducing endothelial cell migration and proliferation inhibits angiogenesis.

The above observations are contrary to the ones made in zebrafish by Nicoli et al. They found that *klf2a* in presence of flow induces microRNA126. miRNA 126 inhibits *spred1*, a negative regulator for VEGF expression thus promoting angiogenesis (Nicoli et al., 2010). The link between *KLF2* and microRNA126 induced VEGF upregulation has been seen in duodenal vessels of human cirrhotic patients (Kobus et al., 2012)

Homozygous deletion of *Klf2* causes normal vascular patterning but defective vascular morphology. There is deficient migration of vascular smooth muscle cells (VSMC) and

pericytes to vascular tubes resulting in defective tunica media that is not compact. These mice die around E12-E14 (Kuo et al., 1997). In *Xenopus* *KLF2* knockdown causes inhibition in Flk1 expression and results in gross abnormalities in vascular development (Meadows et al., 2009).

KLF2 inhibits hypoxia inducible factor (HIF)-1 α . *KLF2* knockdown increased expression of HIF-1 α and its target genes, IL-8, angiotensin II and vascular growth factor. Furthermore, *KLF2* inhibited hypoxia induced vascular tube formation (Kawanami et al., 2009)

Klf2^{-/-} and *Klf4*^{-/-} double knockout mice show defects in vascular integrity and die around day E10.5. The cross sectional structure of the vessels show disruptions of the endothelial cell layer. On a molecular level there is decreased expression of eNOS (endothelial nitric oxide), VEGFR2 and occludin, a tight junction protein. Interacting with other *KLFs*, *KLF2* plays a role in developing and maintaining vascular integrity (Chiplunkar et al., 2013).

1.1.4.6 *KLF2* in regulating vascular tone

Under physiological conditions vasodilatory factors like C-natriuretic peptide and eNOS are induced by laminar flow and help to regulate vascular tone. In pathological conditions expression of endothelin-1 (ET-1), a potent vasoconstrictor is increased. A single *KLF2* binding site is critical for the activation of eNOS promoter. This activation is brought about by *KLF2* which recruits co-activator CBP/p300 complex to eNOS promoter. *KLF2* can also inhibit expression of endothelin, adrenomedullin and angiotensin converting enzyme, three important genes regulating vascular tone. (SenBanerjee et al., 2004, Dekker et al., 2005).

KLF2 decreases the expression of caveolin1, which encodes a cell membrane protein. Caveolin1 is a negative regulator of eNOS in endothelial cells (Razani et al., 2001).

Mouse embryos lacking *KLF2* die around day E14 of heart failure due to high output state, due to lack of vascular tone. These physiological abnormalities are also observed in zebrafish embryos after morpholino knockdown of *klf2a* (Lee et al., 2006). This supports the fact that shear and stress causes changes in *KLF2* expression in vascular endothelium, which in turn regulates vascular tone to maintain normal physiological haemodynamics.

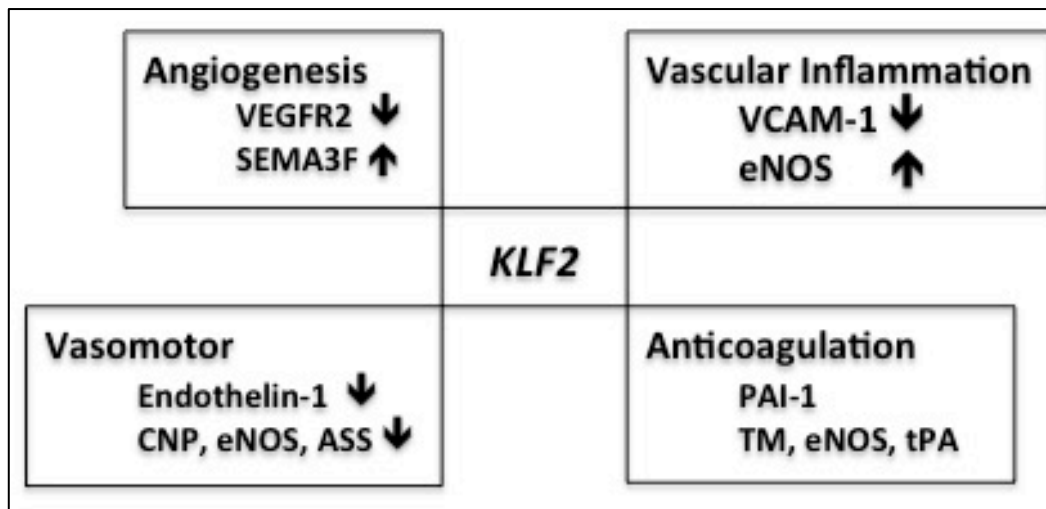


Figure 1.4 *KLF2* in vascular homeostasis

Figure representing mechanisms that are involved in various processes controlled by *KLF2* in maintaining vascular and endothelial homeostasis.

Abbreviations:

VEGFR2 (Vascular endothelial growth factor receptor-2), SEMA3F (Semaphorin-3F), VCAM-1 (Vascular cell adhesion molecule-1), eNOS (endothelial nitric oxide synthetase), CNP (C-type natriuretic peptide), ASS (arginosuccinate synthetase), PAI-1 (plasminogen activator inhibitor-1), TM (thrombomodulin), tPA (tissue plasminogen activator).

1.1.4.7 Role of *KLF2* in Lung development.

KLF2 is highly expressed in lung tissue. *KLF2* deficient mice die in utero between days E14. Hence, it is difficult to study the Role of *KLF2* in lung development. But, lung bud tissue cultures, from *KLF2*^{-/-} mice at age E11.5 grow normal tracheobronchial tree.

When chimeric mice were created by injecting *KLF2*^{-/-} embryonic stem (ES) cells into the blastocysts of wild type mice all organs except lung is developed normally. Animals that developed high chimerism died at birth with lungs that did not develop beyond late canalicular phase. (Wani et al., 1999b)

1.1.4.8 Role of *KLF2* in erythropoiesis

Klf2^{-/-} mice die during embryonic development between day E12.5 to E14.5. These embryos show intra-embryonic haemorrhage, anemia and growth retardation. *Klf2*^{-/-} embryos have significantly increased number of primitive erythroid cells that undergo apoptotic death (Basu et al., 2005). *KLF2* and *KLF1* might have redundant functions in regulating embryonic genes like β globin, primitive erythropoiesis and endothelial development.

1.1.4.9 *KLF2* in Immune system regulation.

Kuo et al ((Kuo et al., 1997) found that *KLF2* (*LKLF*) was needed to maintain single positive T-Lymphocytes in a quiescent state for their viability in peripheral organs and blood. *Klf2* is essential for T cell trafficking. *Klf2* deficient thymocytes show impaired expression of receptors like Sphingosine 1 phosphate ($S1P_1$), CD62L and $\beta 7$ integrin which are responsible for thymocyte migration and peripheral trafficking (Carlson et al., 2006). *KLF2* has been identified as a key transcriptional factor that prevents naive T cells from expressing inflammatory chemokine receptors necessary for acquiring migratory patterns of active T lymphocytes (Sebzda et al., 2008).

1.1.4.10 *KLF2* in metabolic regulation

Klf2 and *KLF3* inhibit adipocyte differentiation. In a 3T3-L1 model, levels of *KLFs* 2 and 3 are high in undifferentiated preadipocytes and not in mature adipocytes. *KLF2* is a down-regulator of adipogenesis. *KLF2* directly suppresses peroxisome proliferator-

activated receptor gamma (PPAR_γ) expression, and prevents differentiation of preadepocyte into mature adipocytes (Banerjee et al.,2003).

1.1.5 Mechanisms regulating *KLF2*

1.1.5.1 Sensing of shear and stress by endothelial cells

Several theories have been put forward to explain how various shear stress forces are sensed by endothelium. The theories proposed are,

- a) Ion channel activation
- b) Caveolae mediated regulation of Calcium
- c) G-protein coupled receptor activation
- d) Tyrosine kinase receptor activation
- e) Adhesive protein activation
- f) Glycocalyx elongation and
- g) Bending of primary cilia

The physico-chemical mechanisms involved in this endothelial mechano-transduction are incompletely understood. Current best evidence supports role of membrane cytoskeleton and membrane fluidity in shear-stress sensing by endothelium. ((Johnson et al., 2011)

1.1.5.2 Flow mediated regulation of *KLF2*

Kumar and colleagues provided the first insights into the mechanisms involved in *KLF2* expression. They identified a single consensus myocyte enhancing factor 2 (MEF2) – binding site in conserved region of the *KLF2* promoter. MEF2 is a member of MADS box (MCM1, Agamous, Deficiens, Serum response factor) family of transcription factors. MADS box factors bind to A/T rich sequences. (Kumar et al., 2005).

MEF2A and MEF2C are implicated as critical regulators of endothelial biology. MEF2A is associated with coronary artery disease and MEF2C plays a role in endothelial integrity and permeability (Hayashi et al., 2004, Wang et al., 2003). MEF2 null mice express similar phenotype to *Klf2* null mice and die in early embryonic age. This could be explained by the fact that *Klf2* and MEF2 are part of the same transcriptional axis (Bi et al., 1999). Berk et al, have previously shown that extracellular-signal regulated kinase (ERK5) is a highly flow induced factor thus linking MEF factors and *KLF2* regulation (Yan et al., 1999).

Using DNA affinity chromatography techniques, PCAF (p300/CBP-associated factor), heterogeneous nuclear ribonucleoprotein D and nucleolin have been identified as proteins that bind to *KLF2* promoter. These proteins bind the proximal *KLF2* promoter as part of phosphoinositide-3kinase (PI3K) dependent shear stress regulating complex (Huddleson et al., 2004).

Parmar and colleagues showed that flow responsive rise in *KLF2* expression is mediated via MEK5/ERK5/MEF2 transcriptional pathway (Parmar et al., 2006). Laminar flow through shear stress induces phosphorylation of ERK5 and MEF2, which is necessary for *KLF2* expression. These mechano-transduction events are suppressed by blocking AMPK (AMP-activated protein kinase) underlining the role of AMPK as part of the MEK5 and ERK5 pathway.

Laminar shear stress results in uncoupling of HDAC5 (Histone deacetylase 5) and MEF2 resulting in increase transcriptional activity of MEF2 and upregulation of *KLF2* and *enos* (Wang et al., 2010).

Thioredoxin inhibitory protein (TXNIP) suppresses *KLF2* expression and promotes monocyte adhesion to endothelial cells (Wang et al., 2012).

MicroRNAs are 18-24 base pair RNA fragments which are involved in post-transcriptional regulation of gene expression. Dicer, an important enzyme in microRNA synthesis, knockdown increased level of *KLF2* in human umbilical vein endothelial cells (HUVECs).

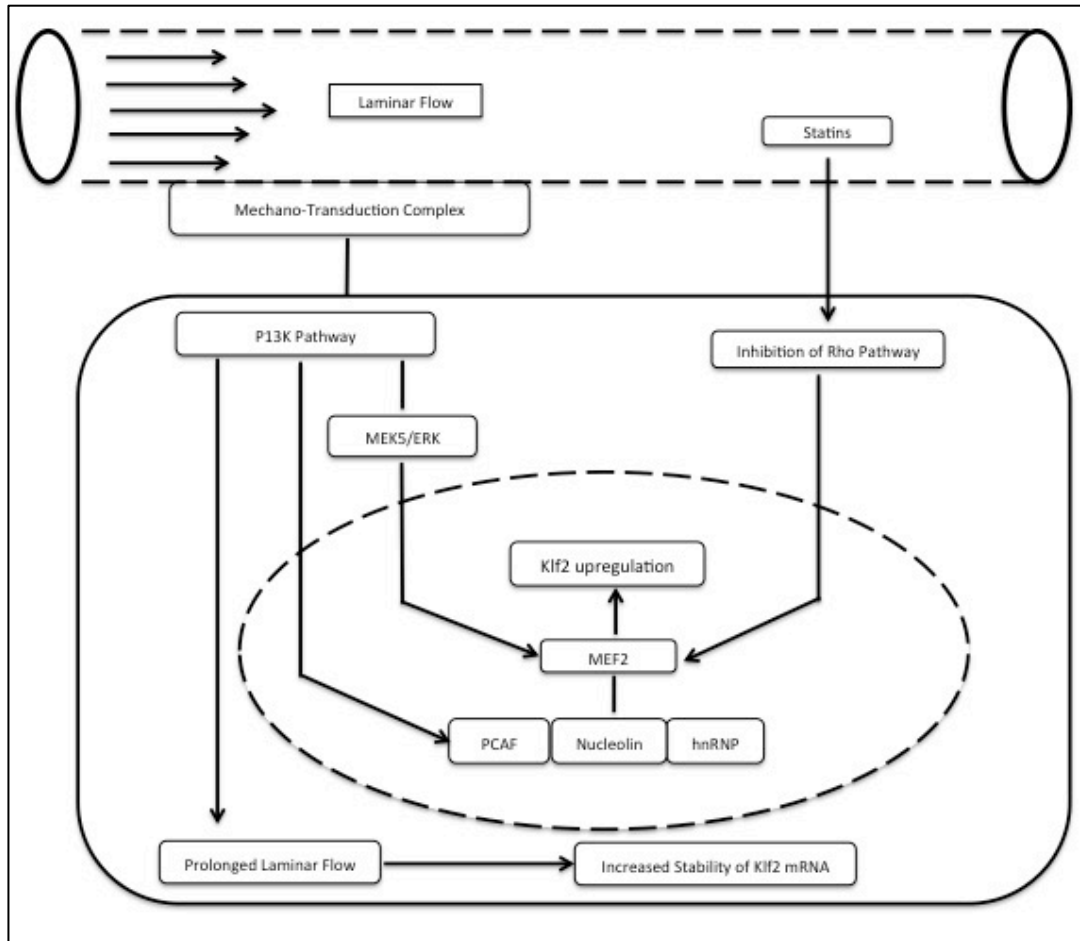


Figure: 1.5 Pathways involved in upregulation of *KLF2*.

Schematic representation of different pathways involved in upregulation of *KLF2*. Pathways on the left show processes involved in flow dependent upregulation. Right side of the figure shows how statins upregulate *KLF2* in a non-flow dependent manner through Rho pathway.

PI3K (Phosphoinositide-3-kinase), MEK (mitogen-activated protein kinase), ERK (extracellular signal regulated kinase 5), PCAF (p300/CBP associated factor), hnRNP (heterogeneous nuclear ribonucleoprotein), MEF2 (myocyte enhancer factor 2), Rho (Ras homologue gene family member A, *KLF2* (Krüppel like factor 2)

This suggests that microRNAS play a role in *KLF2* regulation. Laminar flow suppresses mirna92a and increases *KLF2* expression as shown by Bonaeur et al (Bonaeur et al, 2009, Fang and Davies, 2012).

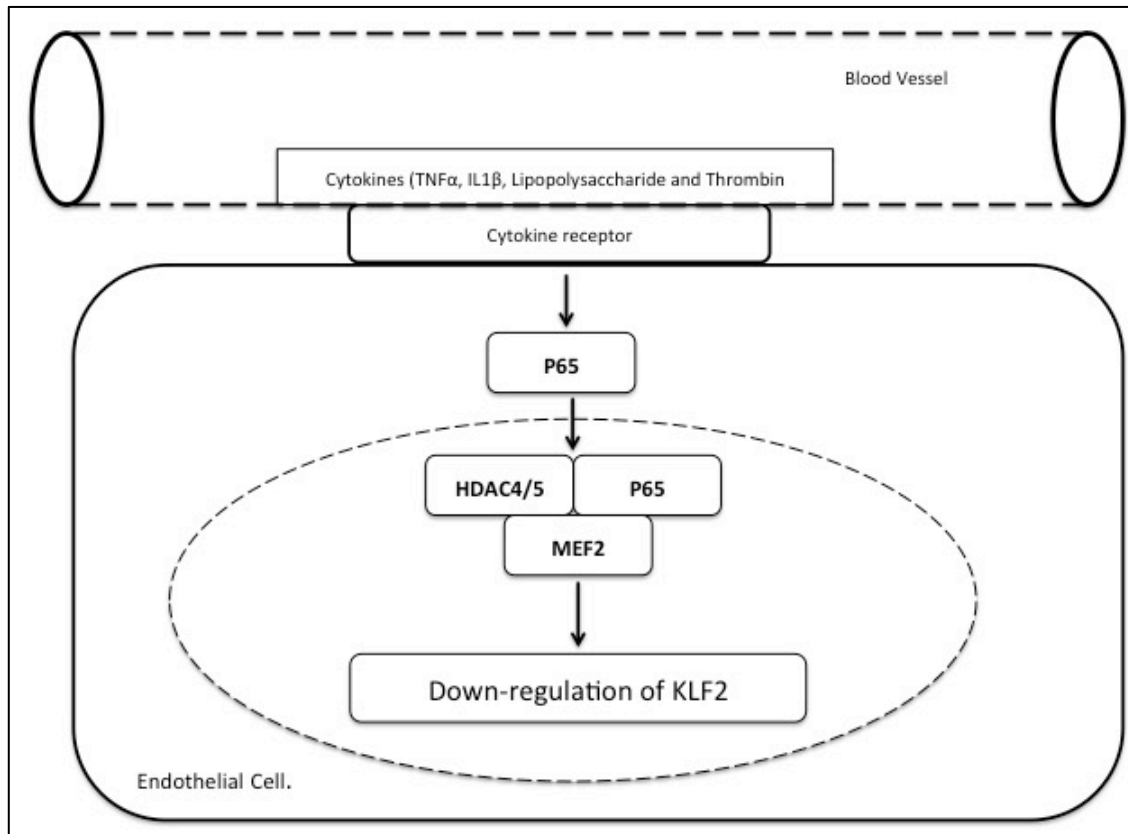


Figure 1.6 Pathways involved in downregulating *KLF2* expression.

Schematic representation of pathway responsible for the downregulation of *KLF2*.

TNF α (tumor necrosis factor α), IL1 β (Interleukin 1 β), P65 (nuclear factor- κ B p65), HDAC 4/5 (histone deacetylase 4/5), MEF2 (myocyte enhancer factor 2) *KLF2* (krüppel like factor 2)

Activin receptor-like kinase5 (Alk5) activation by shear stress in cardiovascular system causes ERK5 activation, by phosphorylation and subsequent induction of *KLF2* expression. *Klf2* in turn activates Smad 7 and forms a negative feedback loop to inhibit TGF- β cascade activation (Egorova et al., 2011). p21 activated kinase1 (PAK1) is a flow and statin responsive target of MEK5/ERK5 pathways. *KLF2* suppresses PAK1

expression and prevents ERK5 dependent endothelial cell migration, which is seen in pathological angiogenesis and plaque rupture in atherosclerotic lesions. (Komaravolu et al., 2015)

1.1.5.3 Non flow dependent regulation of *KLF2*

Proinflammatory stimuli to endothelial cells inhibit *KLF2* expression. Inhibiting *KLF2* results in allowing these inflammatory processes to carry on in an unimpeded manner. Kumar et al reported that, TNF- α through NF κ B and histone deacetylase pathways reduced *KLF2* expression. NF κ B inhibitor I κ B abolished this effect. Treatment of HUVECs with trichostatin A, which inhibits histone decetylase resulted in no effect on *KLF2* expression by TNF- α . Histone deacetylase 4 and 5 and p 65, a component of NF κ B, form a trimolecular complex with MEF2 factors on *KLF2* promoter and inhibit the ability of MEF2 to induce *KLF2* expression (Kumar et al., 2005). Endothelial activation by inflammatory cytokines causes *KLF2* suppression and uninhibited activity of deleterious NF κ B pathways.

Apart from lowering cholesterol, class of drugs called statins, exert an atheroprotective effect by de novo upregulation of *KLF2*. The up-regulatory effects of statins on *KLF2* are due to inhibition of 3-hydroxy-3-methylglutaryl coenzyme A (HMG CoA). The statin mediated effect on HUVECs (Human Umbilical Vein Endothelial Cells) was abrogated by adding mevalonate to statin treated HUVEC cultures. Isoprenoids, geranylgeranyl pyrophosphate (GGPP) and farsenyl pyrophosphate (FPP) are down-stream products of mevalonate pathway. These isoprenoids help in tethering important signaling proteins like Ras and Rho to cell membranes and regulating their activity. To further elucidate the down stream pathways, HUVECS were treated with geranylgeranyl pyrophosphate (GGPP) and farsenyl pyrophosphate (FPP). GGPP treated HUVECs showed complete reversal of statin mediated *KLF2* induction and FPP treated cells showed a modest

reduction in *KLF2* expression. Geranyl transferase (GGT) and Farsenyl transferase (FT) are the enzymes that covalently bind these isoprenoids to proteins Rho and Ras. The HUVECs cultures were treated with the inhibitors of these transferases. GGTI treated cell cultures showed *KLF2* upregulation that was comparable with statin treated cells. FTI treated cells were not able to reproduce this upregulation of *KLF2* at similar concentrations of the inhibitor. This confirms that GGPP associated Rho pathways are mediators of statin induced *KLF2* induction (Parmar et al., 2005). MEF2 binding site of *KLF2* promoter is necessary for *KLF2* upregulation by statins (Sen-Banerjee et al., 2005)

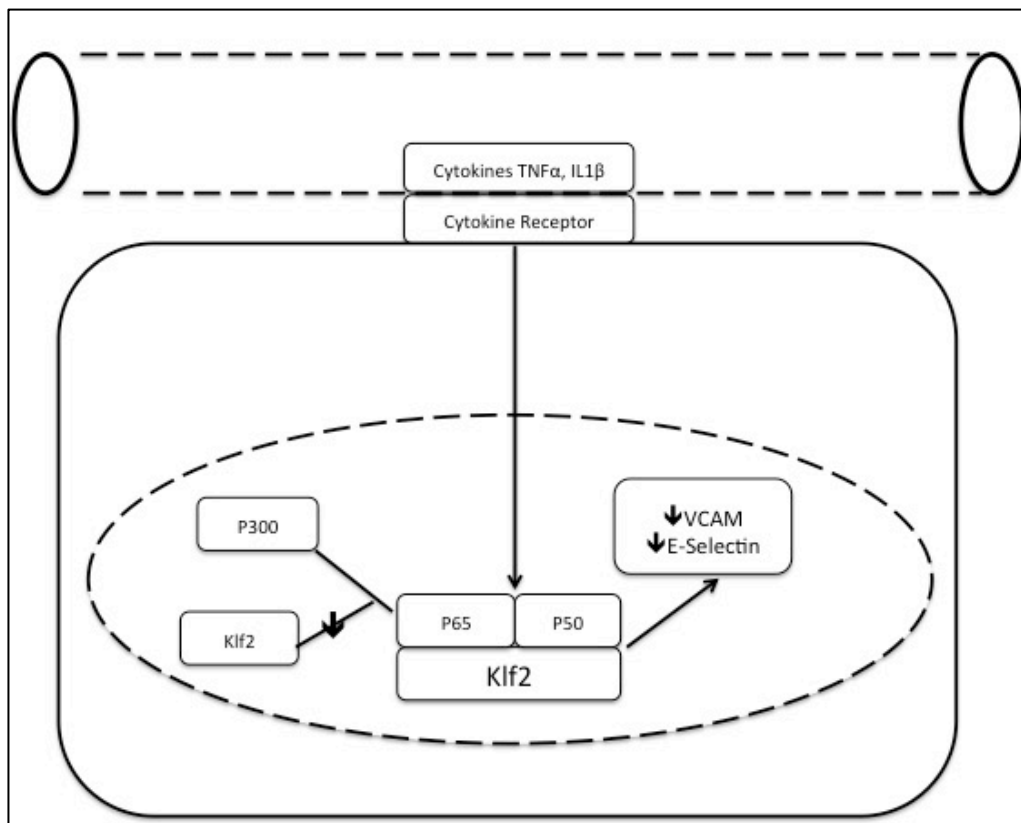


Figure 1.7 Cytokine-mediated down regulation of *KLF2*.

TNFα (tumor necrosis factor alpha), IL1β (interleukin1β), P300 (E1A binding protein 300), P50 (nuclear factor κB transcription factor 50), VCAM (vascular adhesion molecule), *KLF2* (Krüppel like factor2),

Resveratrol is a stilbenoid (a type of naturally occurring plant phenol). It activates Sirtulin1 (SIRT1), a nicotinamide adenine dinucleotide (NAD) dependent deacetylase, which, in turn induces KLF2 upregulation. *KLF2* upregulation occurs via a MAPK 5 (mitogen activated protein kinase 5)/MEF2 pathway.

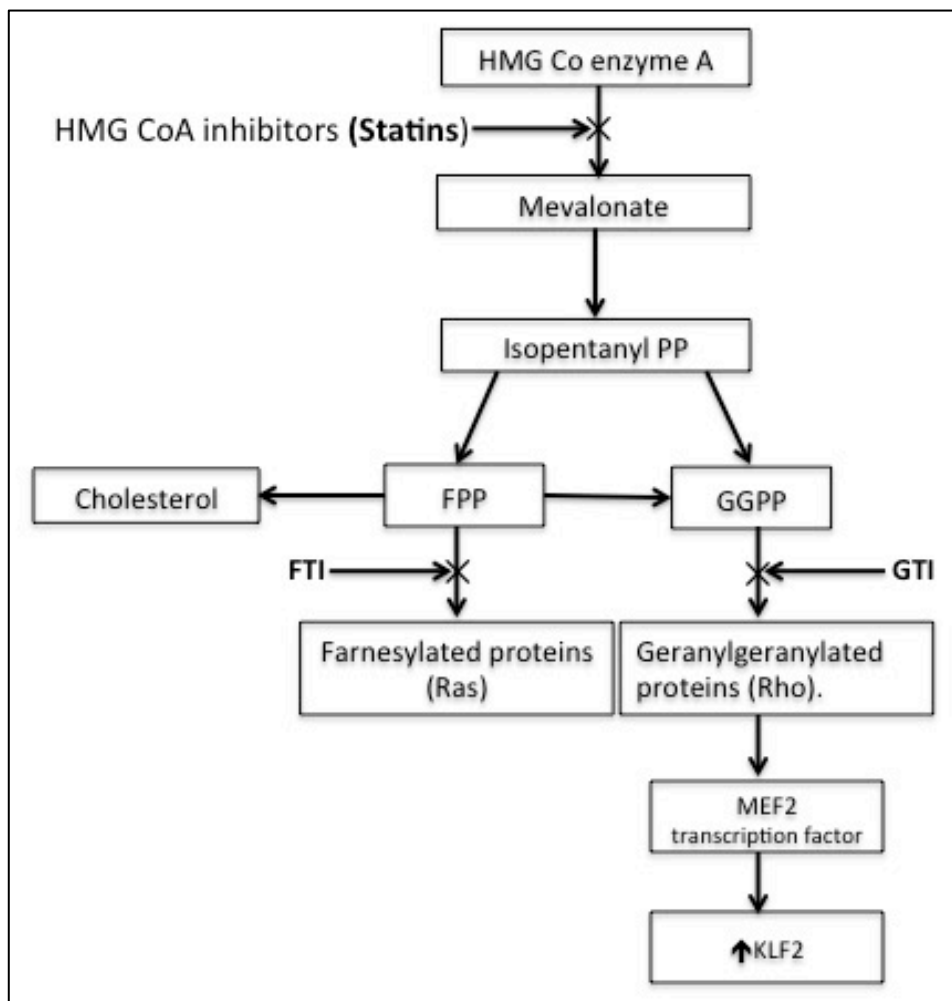


Figure 1.8: Mevalonate pathway and KLF2 expression.

Figure shows steps in mevalonate pathway and site of action of statins and farnesyl and geranyl transferase inhibitors.

HMG Co enzyme A: (3-hydroxyl-3-methylglutaryl coenzyme A), Isopentanyl PP (isopentanyl pyrophosphate), FPP (Farnesyl Pyrophosphate); GGPP (Geranylgeranyl Pyrophosphate); GTI (Geranyl transferase inhibitor); FTI (Farnesyl Transferase inhibitor), KLF2 (krüppel like factor2)

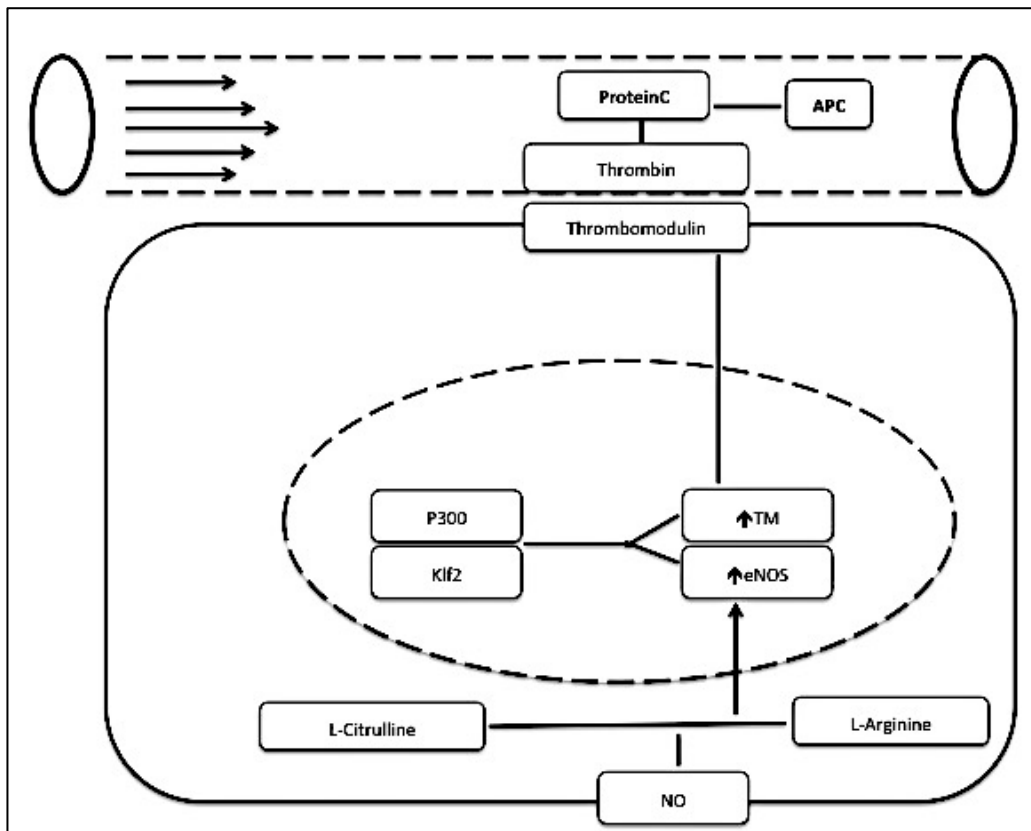


Figure 1.9 Upregulatory functions of *KLF2*

Induction of vasoprotective substances as induced by *KLF2*.
 APC (activated protein C), P300 (E1A binding protein 300),
 TM (thrombomodulin), *KLF2* (kruppel like factor2),
 eNOS (endothelial nitric oxide), NO (nitric oxide).

1.1.6 *KLF2* and Atherosclerosis.

Atherosclerosis is the most common pathology of large and medium size vessel resulting in vital organ ischaemic damage. “Lipid insudation” and “fibrin encrustation” are old hypotheses put forward to explain pathogenesis of atherosclerosis. Recent hypotheses have qualified vascular endothelium as a “dynamically mutable interface”, responsible for reacting to a variety of local and systemic stimuli. Manifestations of endothelial dysfunction include glycoprotein permeability and oxidation, enhanced mononuclear leucocyte adhesion and intimal accumulation, altered extra cellular matrix metabolism and dysregulation of haemostatic- thrombotic balance.

Pathophysiological stimuli for arterial endothelial dysfunction relevant to atherogenesis are pro-inflammatory cytokines, bacterial products, viruses, advanced glycation end products, hypercholesterolaemia and oxidized lipo-proteins, that accumulate in the vessel wall (Gimbrone and Garcia-Cardena, 2013).

It has been observed for a long time now that the earliest lesions of atherosclerosis develop in a distinct non-random pattern, in areas of arterial tree that are subjected to changes in flow patterns, as near branch points. This observation has led scientists to explore links between atherosclerosis and blood flow patterns (Cornhill and Roach, 1976).

Laminar shear- stress as found in unbranched tubular arteries that carry uniform laminar flow are typically protected from early atherosclerosis. Presence of various endothelial mechano-transducers and down-stream signaling pathways link externally applied mechanical stimuli to intracellular and intranuclear events that bring about complex system of biomechanical endothelial gene regulation (Davies et al., 2013, Davies, 1995).

Dai et al analysed flow patterns using three-dimensional (3D) fluid dynamic analysis. They characterized an “atheroprone” pattern in carotid sinus region and “atheroprotective” pattern in distal internal carotid artery. Human cultured endothelial cells were subjected to these two flow patterns. Exposure to atheroprone flow induced dysregulation of expression and organization of cytoskeletal and junctional proteins and activated deleterious NFκB pathways. The gene that was most differentially regulated between two flow patterns was *KLF2* (Dai et al., 2004). The focal nature of atherosclerosis in human arteries and its long established correlation between particular haemodynamic environment might be explained by the spatial patterns of *KLF2* expression.

The following evidence further makes a case for links between *KLF2* expression and atherosclerosis. ApoE null mice bearing a hemizygous deficiency of *Klf2* exhibited a 31-37% increase in atherosclerotic lesion area as compared to littermate controls (Atkins et al., 2008). Myeloid cell-specific *KLF2* inactivation leads to an increase in atherosclerosis in LDLR^{-/-} murine model (Lingrel et al., 2012). *KLF2* suppression in T cells and monocytes leads to a proinflammatory phenotype in these cells (Das et al., 2006).

Atheroprotective flow upregulates certain antioxidant genes and strongly activates, transcription factor, nuclear factor erythroid-2-related-factor-2 (Nrf2). *KLF2* and Nrf2 act synergistically to activate the expression of a substantial fraction of flow-dependent atheroprotective genes (Fledderus et al., 2008).

KLF2 and Nrf2 at present seem to be two “critical regulatory nodes” in vascular homeostasis and may be relevant targets for pharmacological agents (Rader and Daugherty, 2008).

There is experimental evidence that *KLF2* expression triggers production of extracellular vesicles containing microRNAs. These exert a paracrine effect on adjacent vessel wall components and reduce atherosclerosis in murine ApoE^{-/-} model (Hergenreider et al., 2012).

1.2 Zebrafish in drug screening

1.2.1 Zebrafish as a model for cardiovascular research

In the last decade zebrafish has been increasingly used in investigating human diseases and biological processes. Zebrafish (*Danio rerio*), originally natives of the tropical southeast Asian rivers, are available throughout the world. Apart from following the trend of using least sentient organisms in science, zebrafish provide certain scientific advantages. These are:

a) Genetic similarity to humans

Zebrafish are vertebrates, hence share a high degree of sequence and functional homology with humans.

b) Easier to house and care

Due to their small size and relatively simple living environment it is easier to house and raise zebrafish.

c) Easy to see

Zebrafish embryos are transparent, hence impact of any genetic manipulation or drug effect is easy to see and capture with various imaging modalities.

d) Fecundity

Zebrafish lay upto 300 eggs per week, as such are capable of large number of offsprings as compared to rodents. Embryos are externally fertilized by males and grow very quickly.

e) Easier to induce genetic changes

Genetic changes can be brought about by injecting embryos at 1 cell stage with relevant genetic constructs or by simply adding mutagen to the medium.

f) does not need circulation during embryonic development

In the initial days of development 2-4mm zebrafish embryos are not dependent on circulation for growth. Embryos continue to grow as they gain sufficient oxygen through diffusion.

Zebrafish screens are typically carried out in live fish embryos or larvae exhibiting fully integrated vertebrate organ system and exhibiting diverse biological processes.

These advantages make zebrafish a very attractive model for cardiovascular research. Cardiovascular development can be imaged whilst it is happening in wild type or transgenic zebrafish using fluorescent reporters. Zebrafish do not spontaneously develop cardiovascular diseases analogous to those seen in humans. However mechanisms postulated to play a role in human disease can be modeled and studied. Successful zebrafish models have been described to study thrombosis, arteriogenesis, inflammation, cardiomyopathy and cardiac regeneration (Chico et al., 2008).

1.2.2 Chemical screening in zebrafish

Traditional methods of small molecule discovery involved trial and error testing of chemical compounds on phenotypic outcomes in animals and in cell cultures. But in past decades emphasis has been laid on “target driven approaches”, which seek to identify novel therapeutics based on prior knowledge about the single biological target. This technique has delivered far fewer first in class drugs (Swinney and Anthony, 2011).

Phenotype-driven approaches seem to have done better for following probable reasons.

1. Phenotype-driven approaches can identify disease modifying drugs even in the absence of a validated target. For example, ezetimibe was discovered for its cholesterol lowering effects years before its target Niemann-Pick C1-like protein 1 (NPC1L1).
2. Most efficacious drugs may benefit from activity at multiple targets and thus be a “magic shotgun rather than a magic bullet” for a polygenetic disorder (Roth et al., 2004).
3. Small molecules derived from phenotypic screens often have been further selected for positive pharmacological properties such as low toxicity, ability to make it to the appropriate target site and also have the ability to avoid or exploit endogenous enzymes or transporters.
4. Whole organ phenotypic screening holds further advantages, as this approach is target agnostic and holistic. Such screens not only include targets relevant to disease but also to chemical activation, transport, toxicity and other side effects. They also offer screening and counter screening in the same assay resulting in discovering compounds with desirable effects and passing out compounds with undesirable qualities.
5. As a consequence, compounds advancing from phenotypic screens are often of higher quality than hits from *in vitro* target based screens.

Live zebrafish were used for the first time for drug screening in a 96 well plate, in the year 2000, by adding small amounts of compound to fish water. Small molecules found this way are helpful in understanding vertebrate development and identifying novel genes involved (Peterson et al., 2000).

There are hundreds of examples of small molecules that have conserved effects in both humans and zebrafish. It is, therefore, reasonable to assume that many bioactive compounds identified in zebrafish screens will maintain their activity in humans.

There is now a strong evidence about mechanisms that regulate drug distribution across physiological barriers like blood brain barrier and tissue-specific transporters in zebrafish (Fleming et al., 2013) (Popovic et al., 2014). Small molecule testing in zebrafish not only replicated the effects of individual human drugs but, drug – drug interactions were also mimicked. This would suggest that drug distribution, metabolism and excretion studies are also possible in zebrafish (Chng et al., 2012).

Though zebrafish possess a full complement of cytochrome P450 (CYP) genes, genome duplication and functional redundancy have hampered a thorough study of conservation of metabolism of small molecules in zebrafish. In spite of the reasonable evidence of functional parallels, extrapolation must be carried out carefully as drug metabolism may vary at different stages of development and a part of a particular pathway may not reflect the whole pathway.

1.2.3 Successes so far

66 drug screens have been reported in zebrafish so far. These screens have had diverse phenotypic targets ranging from embryo morphology to cardiac physiology and sleep. Some have shown new effects of existing drugs whereas others have discovered novel compound classes.

Therapeutic potential of Prohema, a stabilized version of prostaglandin E2 (PGE₂) was first discovered in zebrafish. In situ hybridization in embryos showed that Prohema boosts number of haemopoietic stem cells (HSCs). After phase II clinical trials, it is used for pre-treatment ex vivo conditioning of umbilical cord blood in patients receiving

hematopoietic stem cell transplant for leukaemia or lymphoma (Lord et al., 2007, Cutler et al., 2013).

Other compounds that were discovered are:

Dorsomorphin, a pyrazolopyrimidine, inhibits bone morphogenetic protein (BMP) receptor, which is an activin receptor like kinase 2 (ALK2) in humans and Alk8 in zebrafish. Dorsomorphin and its derivatives like LDN-193189 are being tested to treat fibro-osseous dysplasia and anaemia of inflammation (Yu et al., 2008). Dorsomorphin was discovered in a zebrafish drug screen seeking molecules that affected normal body organization during embryogenesis.

Proto-1 and its derivatives are benzothiophene carboxamides which are being investigated to prevent effect of aminoglycoside antibiotics which kill hair cells in internal ear and cause hearing loss (Owens et al., 2008). Again the otoprotective effect of Proto-1 was discovered in a 10,960 compound screen in zebrafish.

Both these compounds have been approved for preclinical studies.

Transgenic and mutant zebrafish screens have unveiled new effects that a drug already in use can have. AML1-ETO is a transgenic zebrafish model incorporating leukemia oncogene AML1-ETO. Cyclooxygenase inhibitors were found to suppress leukaemogenesis in these fish. WNT- β -catenin pathway was implicated in self renewal of leukaemia stem cells. This has been confirmed in murine models. As the cyclooxygenase inhibitors are already approved for safe human use, Phase 1 clinical studies to confirm these effects will be replicated in humans were easily set up. (Klimek et al., 2012).

Another such example is promise shown by glucocorticoids in treating long QT (LQT) syndrome. Zebrafish model for long QT syndrome was created by *kcnh2* gene mutation. Drug screening of existing drugs identified fludrenolide as a potent suppressor of

LQT like phenotype. Clinical trials started subsequently show a probable role for dexamethasone in LQT syndrome (Peal et al., 2011).

1.2.4 Screens for mechanism of action

Discovering mechanism of action of small molecules discovered in zebrafish drug screens remains one of the most substantial hurdles. Phenotype-based drug screens, many a times throw up unexpected and transformative new insights into disease under investigation. Computational, biochemical and genetic techniques can be used to discover mechanism of action. All these techniques can be applied to the zebrafish small molecule screens.

Affinity chromatography and mass spectroscopy techniques have identified protein phosphatase2A (PP2A) and mitochondrial malate dehydrogenase as targets for perphenazine and visnagin for their actions in T-Cell acute lymphoblastic leukemia (T-Cell ALL). and doxorubicin induced cardiomyopathy respectively (Gutierrez et al., 2014, Asimaki et al., 2014).

One of the most effective tools in zebrafish screening is a large collection of phenotypes associated with specific gene mutations and knockdowns. Identifying similarity between drug effect, induced phenotype and genetic phenotype, can provide clues towards principal drug target. Dorsomorphin phenocopies *loss of fin* mutant indicating a BMP pathway for its effect. Similarly Kalihinol-F causes several effects on zebrafish embryos like undulation of notochord, defective neural development and haematopoiesis, which mimics *calamity* mutants with disrupted function of Copper transporting ATPase, *atp7a*. This led to hypothesis that kalihinol F chelates copper. This was biochemically proven as exogenous copper rescued the mutation (Sandoval et al., 2013). Another example of multi-dimensional phenotype matching and pheno-

clustering is Fumagillin an antiangiogenic compound known for more than 60 years. Zebrafish embryos treated with Fumagillin showed phenotypes similar to WNT5 mutants that have cranio-facial and skeletal developmental abnormalities (Zhang et al., 2006).

The number and variety of phenotypes that can be distinguished in a whole organism greatly exceeds the number distinguishable in cultured cells. Phenotype matching can be a powerful way of determining mechanism of action of small molecules.

1.2.5 Use in Toxicology screens

Zebrafish as opposed to mammalian models can be deployed very early in a toxicology screen. Zebrafish toxicology screens that are run parallel, can help in eliminating toxic compounds at a very early stage and prioritize “hits” for further development. This approach will help toxic compounds “failing fast”.

Zebrafish have been shown to replicate mammalian models for cardiotoxicity, hepatotoxicity, nephrotoxicity and reproductive toxicity (Ducharme et al., 2015, Driessen et al., 2015).

Aims

My aim was to develop a drug screening assay by fluorescence quantification of reporter gene GFP tagged to *klf2a* promoter in a double transgenic zebrafish line *klf2a:GFP;kdrl:RFP*.

Hypothesis

- A high throughput plate-reader can be used for optimal imaging and fluorescence measurements of zebrafish embryos in our transgenic line.
- In the double transgenic line used, GFP expression was flow-dependent.
- Lovastatin increased GFP fluorescence in these particular embryos.
- GFP fluorescence quantification can be used as a whole organism initial drug screening assay.

Objectives

The points laid out in above hypothesis were tested as follows

- To assess the optimal way of imaging 1 and/or 2dpf embryos I compared imaging embryos using orientation tools in a 96 well plate with direct pipetting of embryos into the wells in a clear medium.
- I examined the effect of absent blood flow in embryos treated with tricaine and in *tnnt2* morphants on GFP expression.
- To see the effects of Lovastatin on GFP expression I performed a dose response exercise.

- The feasibility of using a high throughput plate-reader for drug screening was tested, first by establishing validity of positive and negative controls and then by using drugs from the Spectrum library for actual screening.

Chapter 2

Materials and Methods

2.1 Zebrafish Husbandry

2.1.1. Background

Zebrafish (*Danio rerio*) is a teleost fish of Cyprinid family in the class *Actinopterygii* (ray-finned fish). The lineages leading to cyprinids and mammals split about 450 million years ago.

Zebrafish genome is 1.7 gigabases in size and is divided into 25 chromosomes. Zebrafish genome is about half the size of human genome and has been completely cloned. There are two homologues of the mammalian equivalent. Gene duplication accounts for only 20% of zebrafish genes identified. This suggests that functioning of the ancestral genes in teleosts may be shared by two different genes. Each of these genes have a more restricted function than the original gene. This can help in studying gene function in zebrafish as the function of each gene will be less complex.

Streisinger first used zebrafish to study vertebrate development in 1981. Soon after that zebrafish embryology was studied and using genetic manipulation methods thousands of mutant lines were characterized. There are several hundred laboratories in the world where zebrafish models are used to unravel various gene functions. Sanger center in the UK alongwith groups in Tubingen (Germany) and Utrecht (Netherlands) have completed sequencing whole zebrafish genome.

2.1.2 Characteristics of Zebrafish as an experimental model

The zebrafish embryo has the following characteristics that make it ideal for studying embryonic development. Fertilization of eggs and further development are external. Embryos are relatively large and transparent, which allows direct visualization of organogenesis. Development is rapid and in two days all features of vertebrate body can be seen. Most of organ systems are smaller and less complex versions of mammalian

organs needing far fewer cells in an organ to perform requisite function. For example zebrafish kidney consists of a single glomerulus and bilateral ducts that run throughout the trunk. Also zebrafish larvae are able to swim and search for food in 5 days post-fertilization. A number of unique features in zebrafish facilitate genetic analysis, inbreeding schemes and stock-keeping. The advantages score over the fact that generation time of 2-4 months is not small. (Streisinger et al., 1981)

2.1.3 Zebrafish Handling

Our institution has a state of art zebrafish aquarium. All animal work was done by following home office regulations. I always worked with Ms. Karen Plant, who held the requisite license.

The water temperature and room temperature is maintained between 25-27 degrees Celsius. Zebrafish are kept on a fourteen-hour light and 10 hour dark cycle using appropriate timers. The water supply to the aquarium is maintained by recycling it through a big common filter. From the filter, water is pumped up to a reservoir kept above the racks of aquaria in the fish room. From the reservoir water is distributed to the aquarium by gravity flow. Flow rate can be adjusted for each row. An exchange rate of about three volume changes per hour is recommended. Water is kept in constant motion and debris is removed automatically. All the fish are kept in serial tanks or overflow containers. Fish are fed twice a day on the weekdays and once a day over the weekends. Laboratory Squeeze bottles are used to squirt the food into the tanks. Fish are usually fed dry food flakes and live brine shrimps (*Artemia nauplia*).



Figure 2.1: Assembly of tanks in aquarium

Image showing assembly of breeding tanks in the aquarium with continuous water supply at the top and flows to the lower racks

2.1.4 Transgenic lines used

Nacre Wild type zebrafish which are depleted of any melanin were used for outcrossing.

Double transgenic line, *klf2a:GFP;kdrl:RFP*, used was engineered by Ms. Caroline Gray in our laboratory. BAC transgenesis was used to generate a construct driving GFP expression under control of the native zebrafish *klf2a* promoter with Tol2 transposase flanking sequences. This was injected into 1cell stage zebrafish embryos that were raised to adulthood. F0 founders identified by PCR and subsequent outcrossing isolated a single transgenic line *klf2a:GFP*. The single transgenic line thus produced was outcrossed with *kdrl:RFP* transgenics expressing RFP in endothelial cells. The double transgenics thus founded, were raised to adulthood.

2.2 Collecting zebrafish embryos

2.2.1 Marbling

Marbling tanks have an inner plastic tank in which bottom is replaced by a fine wire grid having a pore size of roughly 2mms. A few glass marbles are placed in the tank. Zebrafish are very aggressive and the marbles provide hiding places for the fish. The inner tank is placed in an outer plastic tank. There is about 2 cm space between the mesh and bottom of the outer tank. The tops of the two tanks are flush so that the fish do not fall in between the two tanks and eat the eggs. This assembly is lowered into the large serial tanks the previous evening (Day -1). Embryos are collected the following morning after the lights are switched on and 20 to 30 minutes of undisturbed mating are allowed.

2.2.2 Pairmating

The embryos I used were mostly obtained by pair-mating technique.

2.2.2.1 Materials

- **Pair-mating tanks**

Pair-mating tanks have an inner acrylic, mating sleeve with multiple holes in the bottom. The mating sleeves also have a groove in the middle to house a separator. The mating sleeve is housed in a one litre plastic tank. Both the containers are level at the top so that the fish do not escape into the outer box. This design helps the eggs to sink to the bottom of the outer tank and prevent the adults from eating the eggs.

- **Plastic Tea-strainer**

A plastic tea strainer was used to strain embryos from the pair-mating tanks.

- **Petri dish:**

90mm petri dish was used for collecting the embryos.

- **Squeeze bottles**

Squeeze bottles containing fish water were used to gently wash embryos into 90mm petri dish.

2.2.2.2 Method.

Male and female zebrafish were identified. Usually, one female and one male was placed in the two compartments created by the separator in the pair-mating tanks. 12 to 16 such pairs were set up.



Figure. 2.2 Pair-mating assembly.

Pair-mating assembly showing, an inner plastic sleeve with a separator and a lid housed in a 1 litre plastic tank. The bottom of the plastic tank is fenestrated. These fenestrations let the eggs through to the outer tank and prevent adult fish from eating the eggs.

2.3 Embryo medium

E3 was used as a medium in which embryos were incubated for up to 5 days post-fertilization. Embryos were euthanized by putting them into household bleach.

E3 medium was made from a 10X stock solution.

1X E3 medium contains the following reagents:

Sodium Chloride (NaCl)	5mM
Potassium Chloride (KCl)	0.17 mM,
Calcium Chloride (CaCl ₂)	0.33mM
Magnesium Sulphate MgSO ₄	0.33mM
Methylene blue	3 drops in 1000mls

2.4 Injecting zebrafish embryos.

Following materials and methods were used for micro-injection of zebrafish embryos.

2.4.1 Embryos

Embryos were collected and screened for 1-2 cell stage under a stereo-microscope (Leica) with a long working distance. These embryos were injected with troponin T2 (tnnt2) and standard control morpholinos.

2.4.2 Microinjection apparatus

- Stereomicroscope with a long working distance
- Pneumatic injector, Picopump PV 820 (Precision Instruments)
- 1mm glass capillary tubes (TW100F-4 by World Precision Instruments).
- Micro-pipette needle puller (Sutter Instruments P-97).
- P10 pipette

- Number 5 Dupont Microforceps (World Precision Instruments)
- Graticule (PYSER- SGI)
- Immersion oil.
- Microscope slide
- Plastic pipette

2.4.3 Morpholinos

Morpholinos are synthetic nucleic acid analogs approximately 25 base pairs long. In a morpholino standard nucleic acid bases are attached to a methylene-morpholine ring linked through phosphorodiamidate groups. Morpholinos act by binding to a target sequence within a RNA, preventing other molecules that might otherwise interact with the sequence for successful translation. Morpholinos also function by modifying

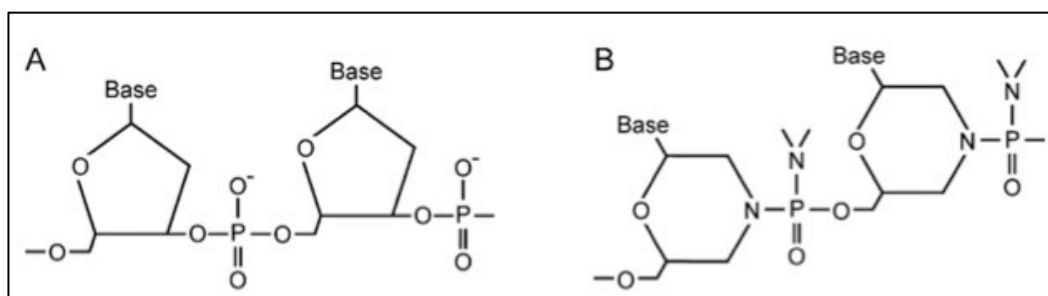


Figure 2.3 Structure of Morpholinos.

The above figure compares

- Basic structure of DNA
- Morpholino containing a hexa-carbon morpholine ring and phosphodiamidate bonds.

pre-mRNA splicing by preventing small nuclear ribonucleoproteins (snRNP) from binding to their targets at the borders of the introns on a pre-mRNA strand. (Summerton and Weller, 1997)

2.4.4 Methods

2.4.4.1 Preparing Morpholinos for injection

As shown in the table below standard control and troponint2 (tnnt2) were used in my project. Morpholinos were sourced from Gene Tools.

MO Name	Sequence (5'-3')	Amount injected	function
Standard Control MO	CCTCTTACCTCAGTTACAA	1nl (0.2mM)	none
Tnnt2 MO	CATGTTTGCTCTGATCTGACACGCA	1nl (0.2mM)	Translation block

Table 1: Structure of morpholinos used.

Molecular structure of standard control and Tnnt2 morpholinos used in experiments.

Morpholinos were diluted to a stock concentration of 1mM and stored at room temperature. 0.2mM solution of morpholinos was prepared as follows:

4 μ ls of 1mM stock solution of Morpholinos was pipetted out into an eppendorf tube containing 10 μ ls of milliQ water and 6 μ l of 1in10 phenol red (1%). The solution thus prepared was placed first on a vortex and then in a centrifuge (Genfuge) and spun at 10000 rpm for 30 seconds. The eppendorf (EPPENDORF) tube was then placed in a warm bath at 65^oC for 5 minutes to make sure there was no aggregation. The 0.2mM solution thus prepared was stored at room temperature and used for injecting embryos.

2.4.4.2 Preparing microinjection needles

1mm outer diameter glass capillary tubes were placed in a needle puller (Sutter instruments P-97). Micropipette puller was programmed to following settings heat 350, pull 60 and velocity 80. The needles thus produced were stored in a 90 mm petridish (STERILIN) on a rolled paper tape with sticky side up.

2.4.4.3 Embryo Collection

Once the lights were turned on in the morning separators were removed from the 5-6 pair-mating tanks and 20 -30 minutes of undisturbed mating time was allowed. Embryos were collected using a plastic sieve. These were washed into a petridish using aquarium water in a squeeze bottle.

After quick screening, under microscope one cell stage embryos were lined up against one side of a glass slide placed in an inverted petridish lid. The embryos were lined up in a single file using a plastic pipette and a seeker. Excess water was removed by pressing down on the glass slide and sucking water by a plastic pipette.

2.4.4.4 Microinjection of embryos

2-3 μ ls of 0.2mM tnnt2 Morpholinos was pipetted into the microinjection needles using a micropipette tip. The needles were shaken a few times to make sure that the morpholinos were loaded into the tip without any air bubbles.

The loaded needle was mounted onto a picopump. The tip of the needle was carefully snipped off under a microscope using number 5 micro-forceps. Pneumatic pump was activated using a foot pedal.

A drop of immersion oil was placed on the micrometer (graticule PYSER-SGI). It was subsequently placed under the microscope. The volume of injection was calibrated by adjusting air pressure and the injection time. The drop of morpholino spanning one millimeter on the micrometer gave an injecting volume of 500 picolitres.

1 nanolitre (nl) of 0.2mM Tnnt2 morpholino was injected into the yolk sac area of embryos already lined up against a microscope slide.

The process was repeated to inject another batch of embryos with 1nl of 0.2mM standard control morpholino. Once injected embryos were plated, labeled and incubated at 28^o C.

Morpholinos (MO) used in the experiment were standard control morpholino and Tnnt2 morpholino

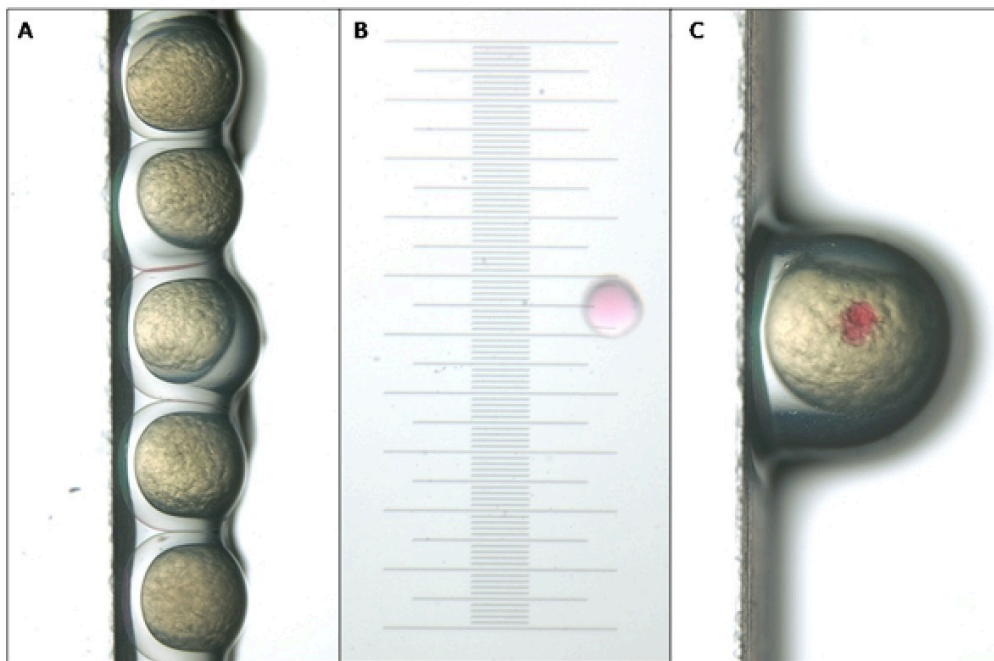


Figure 2.4. Injecting 1-cell stage embryos.

- A. Showing arrangement of embryos lined up against a glass slide
- B. Shows calibrating the micro-injector to inject a volume of 500 picolitres per injection.
- C. An embryo injected with morpholino. Phenol red added to the morpholino solution acts as an indicator to confirm the injection.

2.5 Screening for double transgenics:

2.5.1 Materials

- Fluorescent microscope (Zeiss, Axio Zoom V16)
- Seeker
- Plastic pipette (STARLAB Ltd)
- Petri dish (STERILIN)
- E3 medium

2.5.2 Method

All embryos collected were plated onto petridishes with 50 embryos in each petridish. After incubating overnight, injected and uninjected embryos were screened. Only double transgenics , i.e, red and green fluorescence positive, embryos were identified and used in subsequent experiment

All embryos were observed under fluorescence stereomicroscope (Zeiss, Axio Zoom V16) at 50X to 70X magnification. Embryos that were red and green fluorescence positive were selected for rest of the experiments. A seeker was used to bunch these embryos to one side of the petridish and plastic pipette was used to aspirate out the embryos into petridishes containing fresh E3 without methylene blue.

2.6 Dechoriation

2.6.1. Materials

- Long focal distance stereomicroscope (Leica S6E, Leica Microsystems)
- Seeker
- No 5 Dupont micro-forceps (World Precision Instruments) X2

2.6.2 Method

Embryos were placed under the microscope in a petridish. Each embryo was steadied with one pair of microforceps and the chorion was entered carefully with the tips of the other microforceps, thus releasing the embryos.

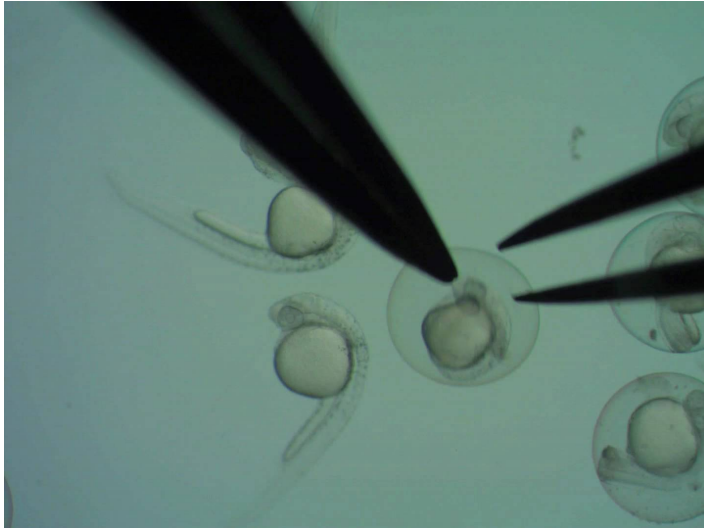


Figure 2.5 Dechoriation
Image showing the process of dechoriation of 1dpf embryos with two pairs of micro-forceps. Released embryos are seen in the same field.

2.7 Preparing agarose molds for acquiring images

2.7.1 Materials.

- Black-walled clear bottom 96 well plate (Greiner)
- 3-D printed mold (3-D printed in RNAi lab, University of Sheffield)
- Flat reagent dish (Oxford Lab Equipment)
- Micropipette (P200, Sutter Instruments P-97)

2.7.2 Method

Wittbrodt described the method to create agarose molds for uniform and correct orientation of zebrafish embryos for imaging (Wittbrodt et al., 2014). Steps of the process I followed are as follows,

1. Previously prepared 1% LMP agarose (Sigma- Aldrich) was heated in a microwave till it became liquid.
2. It was allowed to cool and then poured it into a flat reagent dish and allowed to cool.
3. 50µls of liquid agarose was added to each well in one column of a black walled clear bottom, 96 well plate (Greiner)
4. Agarose was allowed to cool off in the wells for 30 seconds to 1minute.
5. The 3-D printed mold was gently lowered into the column of wells containing agarose.
6. The mold was removed after after 30 minutes.
7. The tip of a P200 pipette was cut for facilitating, atraumatic, aspiration of zebrafish embryos.
8. Each embryo was aspirated in 200µls of clear E3 medium and placed in the well
9. Zebrafish embryos were prodded into these molds using a microinjecting needle under a brightfield microscope.

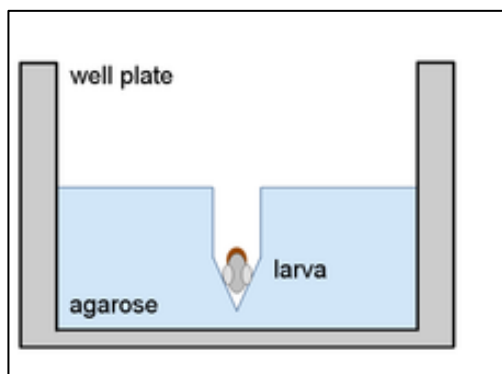
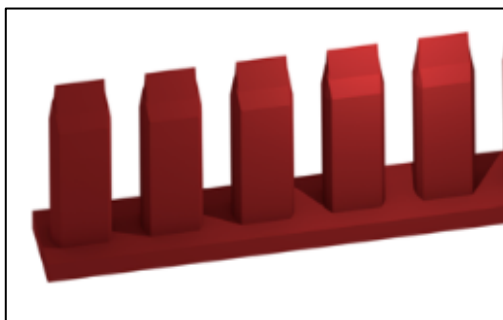


Figure 2.6. Zebrafish embryo orientation tools.

Top figure: 3-D printed orientation tool.

Bottom figure: Schematic cross sectional-image of a 96 plate well showing a zebrafish within the agarose mold created by the orientation tool for optimal imaging.

(Westhoff et al., 2013)

2.8 Preparing different treatments.

2.8.1 Lovastatin

Materials required

- Lovastatin (Sigma-Aldrich, CAS #75330-75-5)
- Analytical balance (Oxford Lab Equipment)
- DMSO (Sigma-Aldrich # 67-68-5)
- Micropipettes (World Precision Instruments)
- Falcon tubes (50 milliliters) (Oxford Lab Equipment)
- 10 millimeter glass pipette
- Electric pipette aspirator (Isolab)

Lovastatin (Sigma- Aldrich) was purchased. One gram of Lovastatin was weighed using an analytical balance. 50 milliliters (ml) of DMSO (dimethyl sulphoxide) was pipetted out using an electric pipette puller into a 50ml falcon tube. Lovastatin was added to DMSO to give a concentration of 50mM (millimolar). The solution was placed on a vortex to ensure complete mixing of lovastatin. This 50mM stock solution was stored in 10 microliters (μ l), 50 μ ls and 2 ml aliquots in appropriate sized eppendorf tubes. The tubes were covered in a silver foil and stored at -80° C.

To prepare Lovastatin 4 μ M for treatment, 50mM stock solution was thawed at room temperature. 3.2 μ L of 50mM lovastatin was diluted in 300 μ L of DMSO. This was added to 40mls of clear E3 solution in a falcon tube. This gave a final Lovastatin concentration of 4 μ M.

2.8.2 Tricaine

1. Tricaine (MS222, Sigma) stock solution (4mg/ml)
2. E3 medium

3. 10 ml glass Pipette
4. 50 ml Falcon tubes (Oxford Lab Equipment)
5. Electric pipette aspirator (Isolab)

33.4 mls of clear E3 solution was pipetted out using a 10ml pipette with an electric puller. 6.6 mls of stock solution of tricaine was added to give a final concentration of 0.66mg/ml.

2.8.3 Lovastatin + Tricaine

33.4 mls of E3 were pipetted out into a falcon tube. 6.6 mls of tricaine stock solution (4mg/ml) were added to E3 medium. 3.2 μ l of 50mM lovastatin stock was added to 300 μ ls of DMSO and mixed on a vortex for few seconds. This was then added to E3 and tricaine solution. The final concentration of lovastatin was 4 μ M and that of tricaine was .66mg/ml.

2.8.4 DMSO

40 mls of clear E3 were pipetted out into a falcon tube. 300 μ ls of DMSO (Sigma-Aldrich) were added to E3.

2.9 Treatment groups:

The double transgenics isolated were divided equally into following treatment groups

- **Treated with DMSO only**
- **Treated with Lovastatin 4 μ M**
- **Treated with tricaine (0.66mg/ml) only**
- **Treated with Lovastatin (4 μ M) + tricaine (0.66mg/ml)**
- **Standard control morpholino injected**
- **Tnnt2 morpholino injected.**

All the above groups were incubated in respective treatment solutions overnight at 28°C.

2.10 Imaging embryos for GFP fluorescence

As will be discussed in chapter 3 the development of the screen went through three phases.

2.10.1 Phase 1

Imaging on Axio-Zoom V16 fluorescence stereomicroscope (Zeiss)

2.10.1.1 Materials

- 2dpf embryos
- Plastic pipettes (Oxford Lab Equipment)
- Seeker
- Watch glass
- Zeiss Axio Zoom V16 fluorescence stereomicroscope (Zeiss)
- ZenPro (Zeiss) software

2.10.1.2 Method

0.5ml to 1ml of tricaine was added to each petri dish containing embryos in various treatment groups. 5 embryos were randomly selected from each group and imaged as follows.

Each embryo was transferred into a watch glass with a drop of clear E3. Seeker was used to line up the embryos in a horizontal plane under the microscope. On a Axio Zoom V16 fluorescent stereomicroscope following settings were used to acquire images

Magnification 75%

Exposure 5400 milliseconds

White settings 16383

Black settings 3000

Gamma set to 1.0

Five embryos from each group were imaged. The metadata of files were stored as .czi files (**Zenpro, Zeiss**). All the images were opened using FIJI software. Images were analysed to measure integrated density (fluorescence) and saved as jpegs for reconstruction and reproduction.

The data obtained was analysed using **GraphPad** Prism software. Mean integrated densities and Standard error of means (SEM) were calculated. The results were further analysed using Ordinary one-way ANNOVA.

2.10.2 Phase2

Assessing plate-reader feasibility

2.10.2.1 Materials

- 2 dpf embryos
- Black-walled clear bottomed 96 well plate (Greiner)
- P200 micropipettes and pipette tips (World Precision Instruments)
- Tricaine stock solution (Sigma-Aldrich)
- A white board (workstation)
- Seekers
- Hairtools
- Thermancol box
- ImageXpress plate-reader (Molecular Devices)
- MetaXpress5.0 software for analyzing images.

2.10.2.2 Method

A black-walled clear bottom 96 well plate (Greiner) was placed on a lit white board workstation. A plate plan was noted down.

Three embryos from different treatment groups were placed in each well of the 96 well plate in 225µl of clear E3 medium. 25µl of tricaine (4mg/ml) were pipetted into each

well. Embryos were moved to the centre of the well using a hair-tool. 96 well plate was placed in a polystyrene box to avoid temperature changes and spillage.

96 well plate was loaded onto ImageXpress, (Molecular Devices) high throughput fluorescence plate-reader.

Following settings in the plate acquisition part of:

Objective: 2X

Exposure: 1500 milliseconds for RFP (red) channel

2000 milliseconds for GFP (green) channel

Focus Focus on well bottoms

Each well was divided into four quadrants to capture all the embryos in the well.

Once pretreatment images were acquired, 200µls of E3 medium was pipetted out of each well, leaving behind 50 microlitres of E3 medium. 100 µls of E3 medium was added to each well and a further 100 µl of treatment solutions of lovastatin, tricaine, lovastatin and tricaine and DMSO were added to the wells as per the plate plan. The 96 well plate was incubated overnight at 28^o C.

Images were analysed using MetaXpress 5.0 software. The multi-wavelength cell scoring (MWCS) algorithm (described later) provided in the software was customized and used to calculate integrated intensity of each quadrant. Integrated intensity for each well was calculated by adding the mean integrated intensity of each quadrant. Data acquired was analysed using GraphPad Prism statistical software. Mean integrated densities and Standard error of means (SEM) were calculated. The results were further analysed using Ordinary one-way ANNOVA.

2.10.3 Phase 3

Using the assay for screening drugs from Spectrum (SP100122) library

2.10.3.1 Materials

- Double transgenic 2 dpf embryos
- Black-walled clear bottomed 96 well plate (Greiner)
- Spectrum SP100122 drug library test plate (Sigma)
- P200 micropipettes and pipette tips (World Precision Instruments)
- Tricaine (stock solution) (Sigma-Aldrich)
- A back-lit whiteboard workstation
- Seekers
- Hairtool
- Thermanacol box
- ImageXpress plate-reader (Molecular Devices)
- MetaXpress5.0 software for analyzing images.

Spectrum drug library is dispensed in sealed 96 well plates. Columns 1 and 12 are mostly empty. Wells A01, A12, H01 and H12 contain DMSO only. Thus each plate has 80 drugs for screening purposes. Each well contains 5 μ ls of a drug in 25mM concentration.

2.10.3.2 Method

After noting down a plate plan, spectrum library test plate was thawed at room temperature. 95 μ ls of clear E3 were added to each well to make a total volume of 100 μ ls. 1dpf embryos were screened for double transgenic embryos. Three, 30 hpf (hours post fertilization) embryos were placed in wells of a 96 well plate in 150mls of E3. 100 μ ls of drug solution was added to respective wells. The 96 well plate was given a good shake to achieve good mixing of the drug with E3 in the well. This gave a 2.5 times dilution to give a final concentration of 10 μ M. The 96 well plate was placed in an incubator overnight at 28^o C.

On day 2, 25 μ ls of tricaine (4mg/ml) was added to each well to anaesthetize the embryos. A hair-tool was used to bring the embryos to the centre of the wells for best capture while imaging. Images were acquired on ImageXpress (Molecular Devices) fluorescent plate-reader using the same settings as were used for acquiring pretreatment images. Images were reconstructed using FIJI (NIH) and Powerpoint (Microsoft) software programmes.

The images thus obtained were analysed using MetaXPress 5.0 software using a customized MWCS (multi wavelength cell scoring) algorithm. Intergrated intensity for each well was calculated and data acquired was analysed using GraphPad Prism software. Mean integrated density and standard error of mean was calculated. The results were further analysed using One way ANNOVA statistical test.

2.11 Algorithms used for Image analysis.

2.11.1 Simple threshold technique

Initially, I used FIJI software to analyse the images. I used the “Threshold method” the simplest form of segmentation techniques for image analysis.

2.11.2 Customised segmentation algorithm.

MetaXpress 5.0 software was used to analyse images and quantify GFP florescence. It was very evident after initial image acquisition and analyzing using the threshold techniques that there were issues of autofluorescence, particularly in the yolk sac area of zebrafish embryos. To prevent this over-estimation of fluorescence I used segmentation methods to customize an algorithm, which excluded the yolk sac area from fluorescence quantification. This algorithm used an initial red fluorescent protein image which defined the zebrafish vasculature. A segmentation image of the vasculature

was thus created. Images taken with a green filter for GFP fluorescence were segmented as well. The two images were subtracted. The final image as shown in the figure below was used to measure GFP expression in the vasculature avoiding areas of autofluorescence.

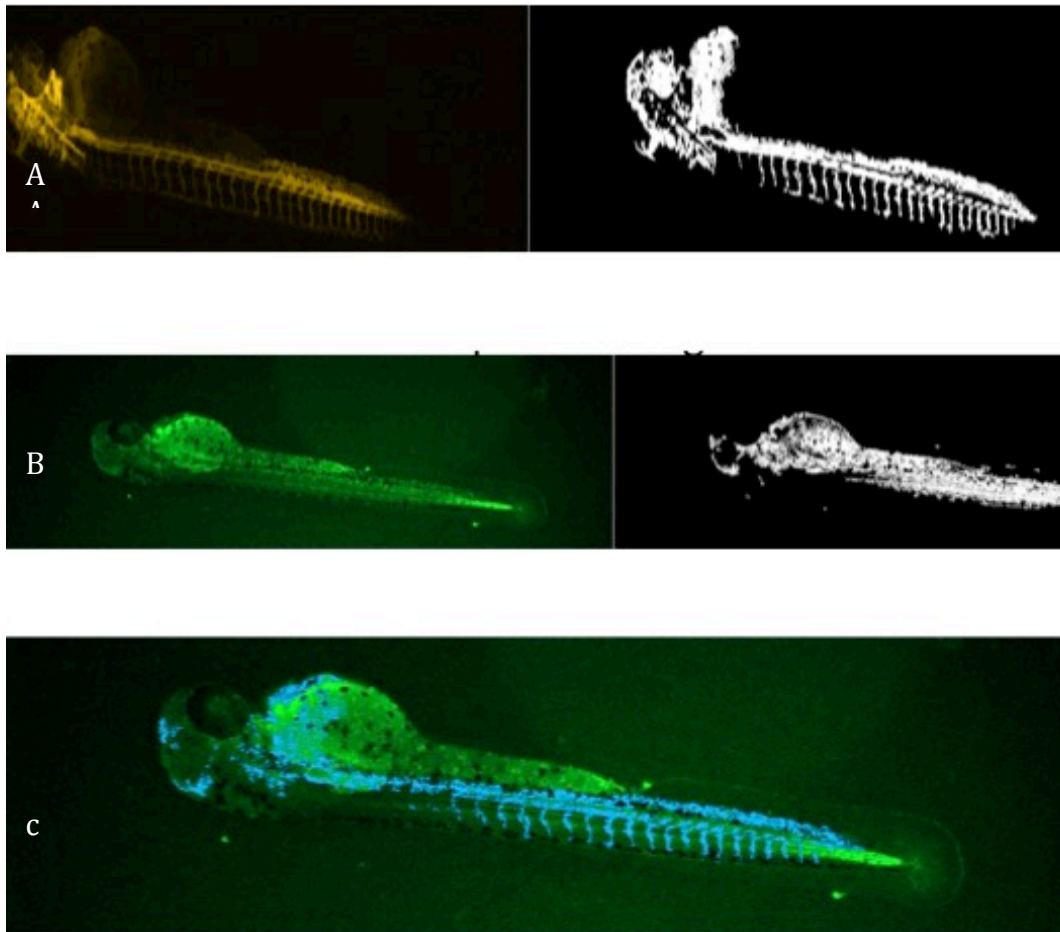


Figure 2.7 Segmentation algorithm images.

Image panels showing different steps in developing a segmentation algorithm to create a mask of zebrafish vasculature. The mask thus created is superimposed on GFP picture to calculate fluorescence, avoiding areas of auto-fluorescence.

- A. RFP segmentation image
- B. GFP segmentation image
- C. Masked image.

I soon found that this algorithm would work only if we used only one zebrafish embryo per well. If more than one fish was imaged in one well, we had to line the fish perfectly to be able to use this subtraction algorithm. For a high throughput assay this would prove to be cumbersome and time consuming.

Therefore we customized Multi-Wavelength Cell Scoring (MWCS) algorithm which was more efficient and easy to use for our assay. This was also based on segmentation concept. This algorithm is used in cell fluorescence assays. The steps involved in creating this algorithm are as follow

- Select RFP image which is called all nuclei
- Specify the size range of the nuclei
- Choose the second image that contains positive stain, which is GFP in this case.
- Select stain area
- Specify the size and range of cells.

This algorithm identifies GFP positive areas as cells of various sizes. The minimum and maximum width helps the software to determine what is considered a GFP positive cell. A range of intensity is determined by hovering the cursor over the lowest intensity GFP positive cell and the highest intensity GFP positive cell. This is usually much above the background fluorescence. Defining these parameters helps the software to calculate GFP signal that is not affected by background fluorescence.

- Perform a multi-parameter analysis to obtain wavelength specific average intensity of GFP positive cells.

A line graph function was used to assess background intensity. It was also used to define the limits of the gray scale values in the GFP image for calculations.

A

B

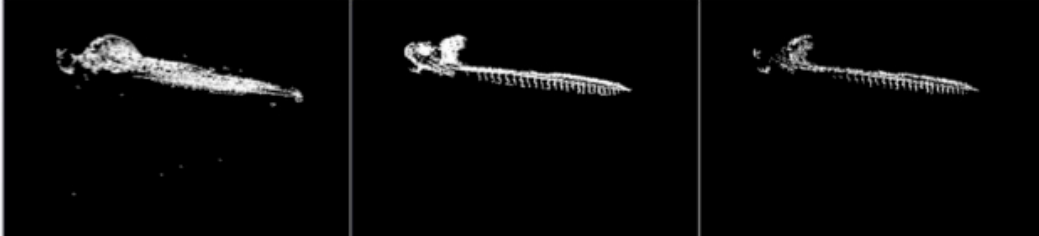


Figure:2.8 Multi-Wavelength Cell Scoring in our model.

Image A. GFP (G Fluorescent Protein) image showing GFP positive areas. Auto-fluorescence can be seen in yolk sac and the tail areas. This was used as second image.

Image B: RFP (Red Fluorescent Protein) image showing vasculature in 2dpd embryos. This was used as the all nuclei image in the algorithm

Panel C: The right-most image in the panel shows the areas in which the GFP stain was calculated. It is obvious from the image that the areas of auto-fluorescence were avoided.

Chapter 3

Results and Development of Assay

3.1 Introduction

Zebrafish are increasingly used for initial drug screening as alluded to earlier. Quantifying fluorescence emitted by tagged reporter genes is increasingly used in whole organism drug screening (White et al., 2016).

I used a double transgenic (*klf2a*:GFP; *kdrl*:RFP) zebrafish (*Danio rerio*) line, developed in our laboratory, to develop an assay which could lead to a mid to high throughput whole organism screening.

3.2 Development of assay

This assay was developed in the following steps. These are

1. Finding the most feasible imaging method
2. Finding optimal Lovastatin concentration
3. Developing positive and negative controls
4. Customizing an algorithm for quantifying GFP fluorescence.
5. Actual drug screening from Spectrum Drug Library (Sigma)

3.2.1 Step 1: Optimizing imaging method

3.2.1.1: Comparing 96 well plate with 384 well plate.

To assess images taken in a 384 well plate and a 96 well plate, I compared the images of the embryos in a 384 well and a 96 well plate. The images of the embryos that were in focus were comparable. Similarly embryos presenting themselves dorsally or ventrally were comparable.

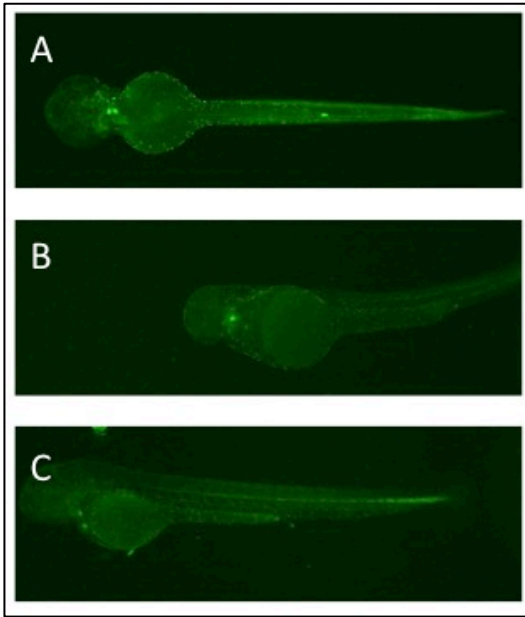


Figure 3.1 Presentation of embryos in microtitre plates.

Images showing possible presentations when imaged in a microtitre plate

- A. Dorsal presentation
- B. Ventral presentation
- C. Lateral presentation

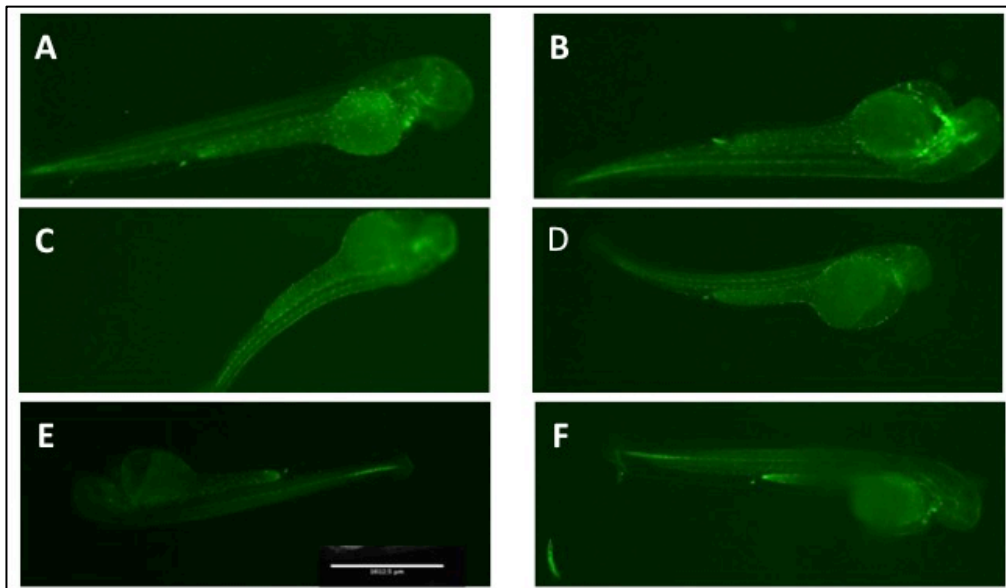


Figure 3.2 Images of 2dpf embryos of positive and negative controls in a 384 well plate.

Representative images of 2dpf embryos of different treatment groups in a 384 well plate.

- | | |
|----------------------------------|--------------------------------|
| A. DMSO treated. | B. Lovastatin treated |
| C. Lovastatin + Tricaine treated | D. Tricaine treated |
| E. Tnnt2 morpholino injected | F. Control morpholino injected |
- Scalebar (3.22 μ m =1 pixel)

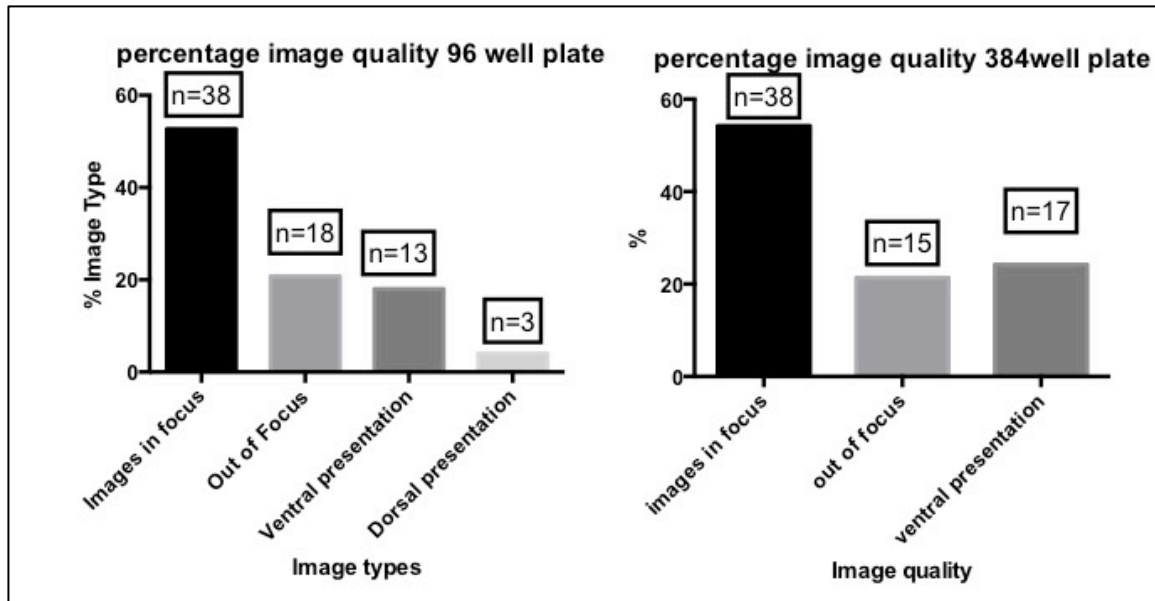


Figure 3.3 Graph comparing the presentation of zebrafish embryos in 96 and 384 well plates.

The two column graphs comparing images obtained from embryos in a 96 well plate (left graph) and 384 well plate (right graph). There was no obvious difference in two techniques. (none of the embryos were found in dorsal presentation in the 384 well plate)

However, embryos could not be manipulated into a more lateral position in a 384 well plate, I decided to use 96 well plate with clear bottom and black walls.

3.2.1.2 Using orientation tool for imaging.

To further find an optimal method of imaging zebrafish embryos, I compared the following two methods.

- a. Direct imaging of embryos immersed in clear E3 solution with tricaine in 96 well plate with black walls and a clear bottom (Greiner). Images were obtained using ImageXpress (Molecular Devices) plate reader using a 2X objective.

- b. 96 well compatible zebrafish orientation tools have been described. I used 3D printed molds to make agarose wells in a 96 well plate to orientate zebrafish embryos for optimal imaging.

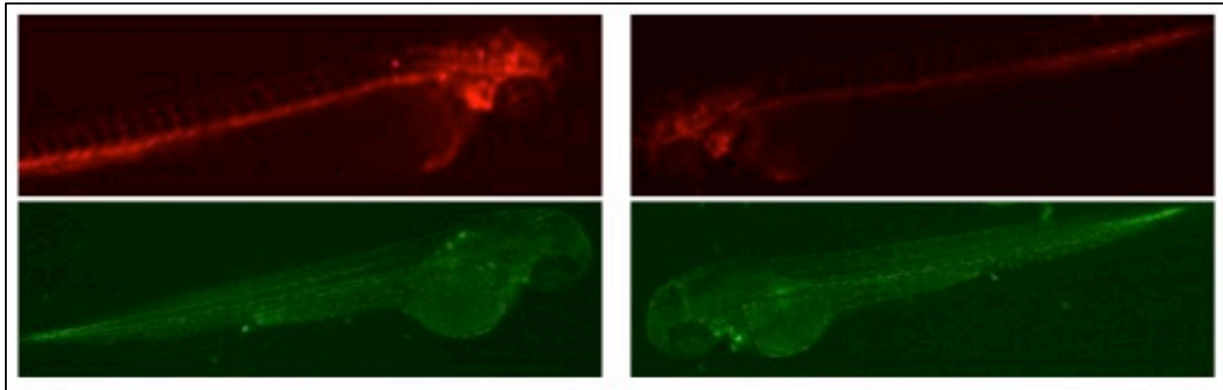


Figure 3.4 Representative Images of embryos using different mounting methods.

Left panel shows a representative RFP and GFP images of embryos imaged in a 96 well plate containing clear E3 medium. Right panel shows RFP and GFP images in agarose molds made in wells using orientation tools.

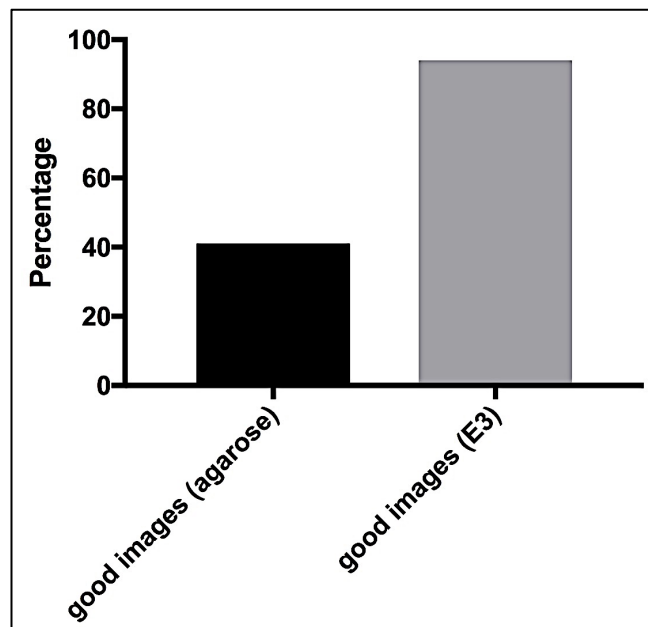


Figure 3.5 Column graph comparing the quality of images acquired with two techniques.

Column graph showing obvious superiority of images obtained by imaging embryos with clear E3 medium in the well as compared to the images obtained by placing embryos in agarose wells.

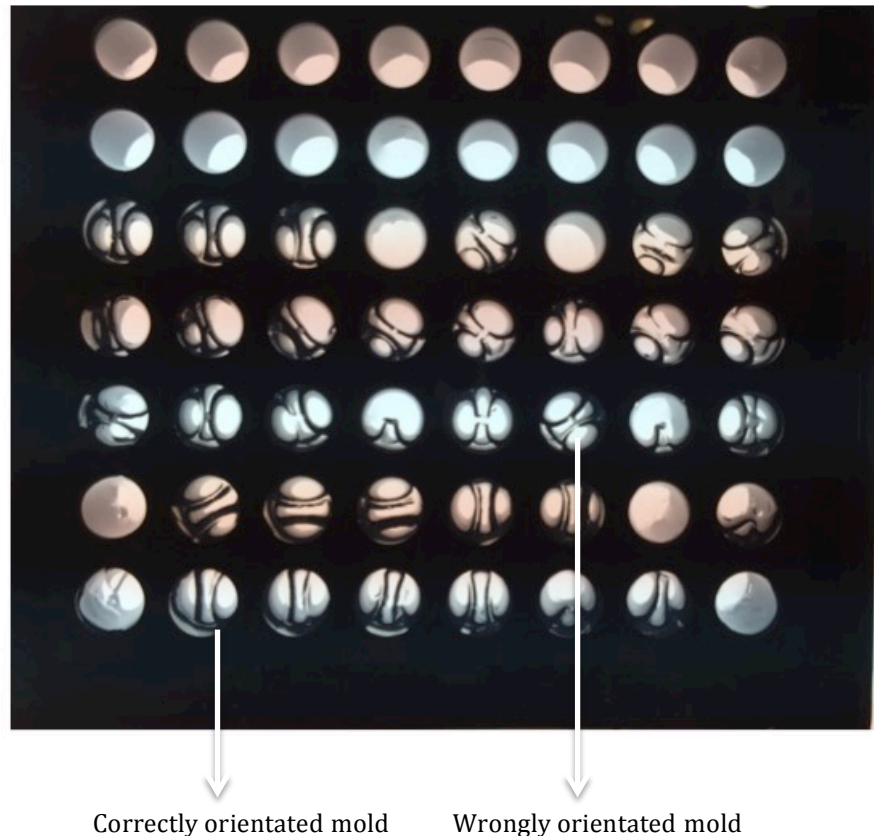


Figure 3.6 Photograph of a 96 well plate with agarose molds
 Image of a 96 well plate bottom, showing a well-orientated agarose mold (short white arrow). Many of the agarose molds are mal-rotated (long white arrow), precluding optimal imaging of the embryos.

I found the following pitfalls in using agarose molds for imaging,

- a. Some agarose came out stuck to the molds when plastic molds were removed.
- b. On adding E3 to the wells the agarose molds rotated in the wells thus resulting in mal-orientation of zebrafish embryos.
- c. On adding E3 embryos floated out of the molds.
- d. Prodding embryos into the molds was time consuming.

Conclusion

The obvious conclusion from the above experiment was that imaging 2dpf zebrafish embryos in agarose molds was not feasible. Therefore, I transferred the embryos into

the 96 well plate by pipetting out embryos in clear E3 medium and let the embryos settle on to the clear glass bottom of the well. I also used a hair tool to orientate zebrafish embryos horizontally. 25 micro-litres of stock solution of Tricaine was added to each well to anaesthetize the embryos whilst imaging. This facilitated the pre-treatment and post-treatment imaging.

3.3 Step 2. Finding optimal Lovastatin concentration.

3.3.1 Comparing relative increase in GFP fluorescence pre and post treatment with lovastatin.

1day post fertilization (dpf) embryos were divided into four groups. Each group consisted of five embryos. One embryo from each group was plated in a small petri dish and labeled. DMSO controls were labeled as DMSO 1, DMSO 2 and so forth. Lovastatin treated embryos were labeled as Lova 21, Lova22 and so forth. In lovastatin treated groups the first number was concentration in μM and second digit was the number assigned to the embryo. The embryos were imaged on a fluorescence stereomicroscope before any treatment. The embryos were treated with varying concentrations of Lovastatin and control group was treated with DMSO. Embryos were incubated overnight and post-treatment images were obtained. FIJI (Image J) was used to quantify fluorescence and GraphPad Prism software was used for analyzing the data.

All images were acquired on the fluorescent stereomicroscope fluorescent microscope (Zeiss Axio Zoom V16) using following settings,

Exposure was set at 5400 milliseconds. Black and white values were set at 3000 and 16383 respectively. Gamma was set at 1.

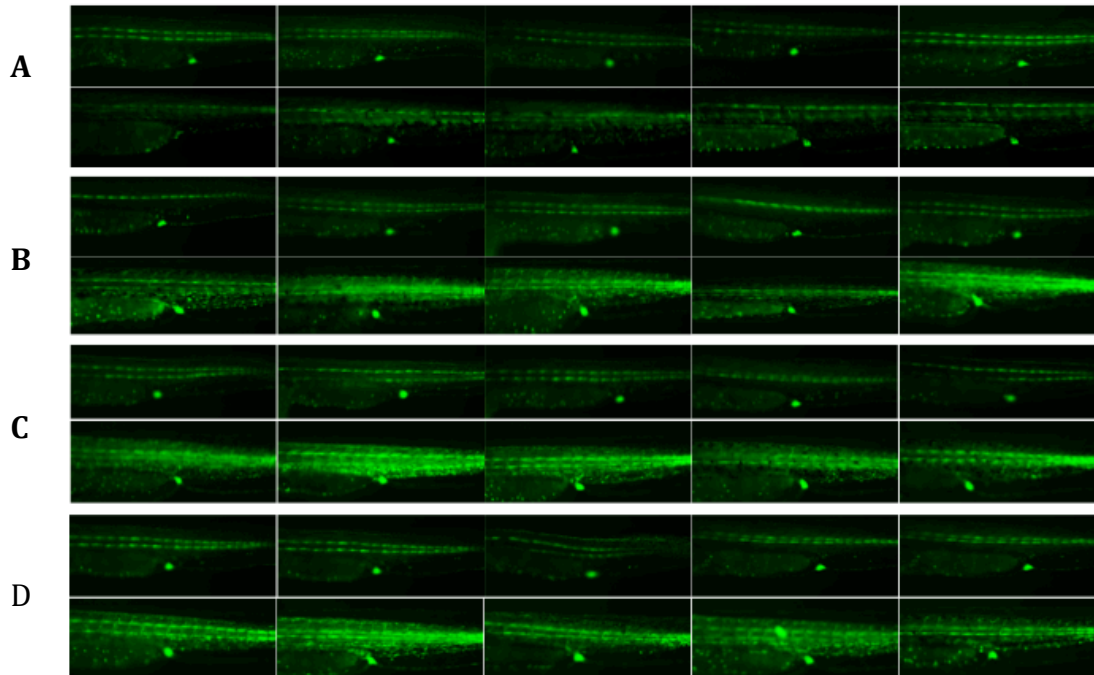


Figure 3.7 Picture panels showing relative increase in GFP fluorescence in controls and Lovastatin treated embryos.

Comparing relative increase in fluorescence in lovastatin treated zebrafish embryos and DMSO treated controls at 1dpf stage (pretreatment) and at 2dpf stage (post treatment). Upper images in panels are pre-treatment images and lower images are post-treatment images.

A. DMSO controls **B.** Lovastatin 2µM **C.** Lovastatin 3µM **D.** Lovastatin 4µM
 {Image acquisition Settings : Exposure 5400 milliseconds, Black 3000, White 16383
 Magnification set at 75}

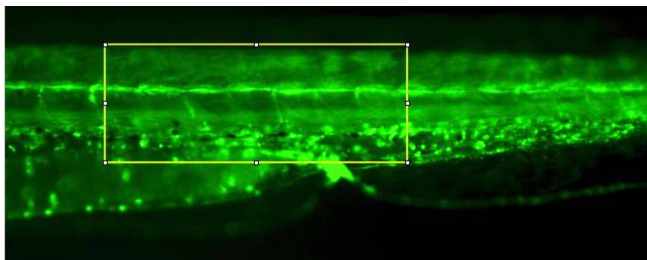


Figure 3.8 Measuring Fluorescence.

Rectangular area over body of embryo was selected for measuring GFP fluorescence using FIJI (ImageJ)

To answer the question whether the increase in fluorescence was simply as a result of normal growth in the embryos from 1dpf stage to 2dpf stage. The panel of images in figure 3.6 shows similar fluorescence in 1dpf embryos in all the groups. There is an obvious increase in green fluorescence in 2dpf embryos treated with different concentrations of Lovastatin as compared with 2dpf embryos treated with DMSO alone.

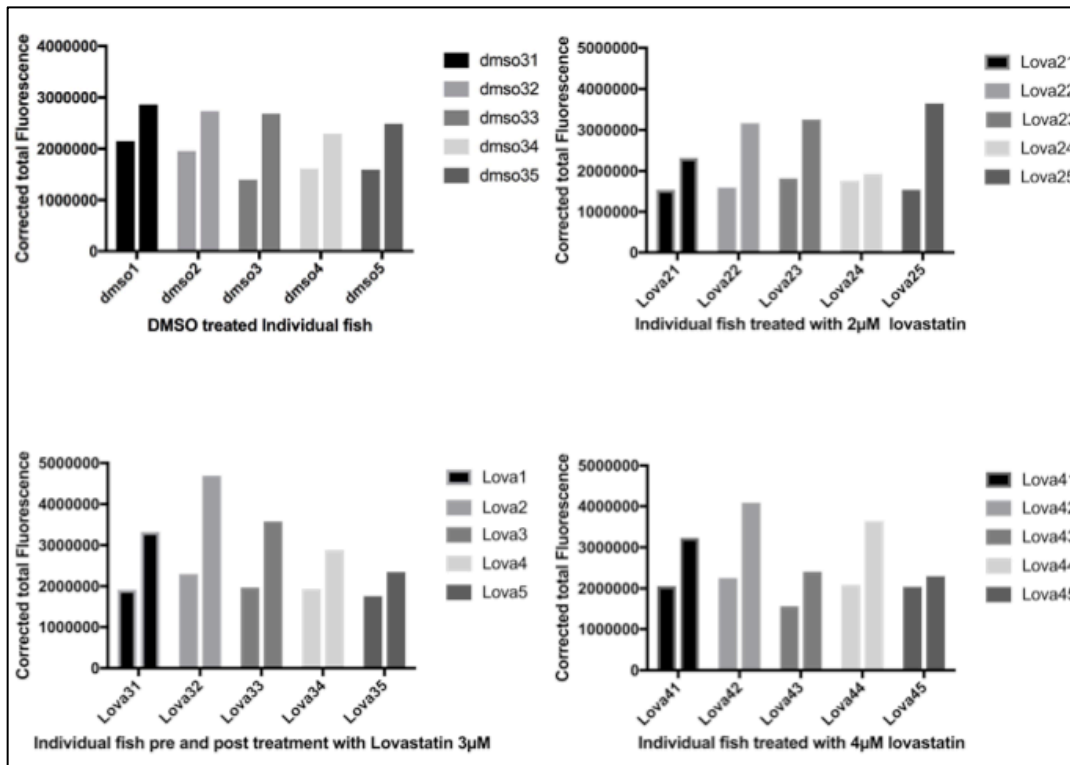


Figure 3.9 Column graphs of pre and post treatment fluorescence

Graphs showing the level of GFP fluorescence in individual zebrafish embryos pre (1dpf) and post-treatment (2dpf) with different concentrations of Lovastatin. (2dpf embryos). (p=ns)

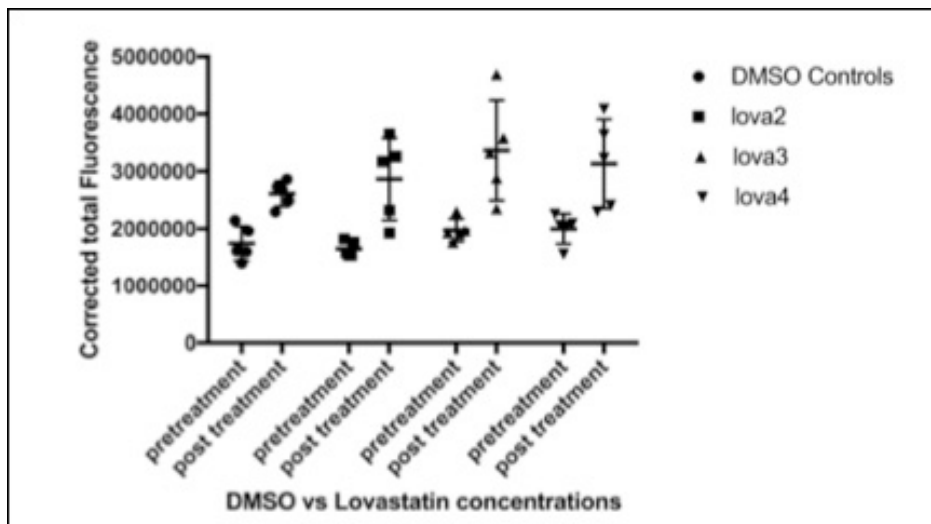


Figure 3.10: Scatter plot of pre and post treatment fluorescence.

Comparing 1dpf (pretreatment) and 2dpf (post-treatment) fluorescence in different treatment groups . (p=ns).

DMSO (Dimethyl sulphoxide), Lova (Lovastatin; the digits at the end show the concentration of lovastatin in μM).

(Mean corrected total fluorescence (pre/post treatment): DMSO (1742316/2610477), Lovastatin $2\mu\text{M}$ (164663/2863135), Lovastatin $3\mu\text{M}$ (1974817/3363774), Lovastatin $4\mu\text{M}$ (1997505/3130338). {(p=ns) One way ANOVA}

Conclusion

The above set of data showed that the relative increase in fluorescence was greater in lovastatin treated embryos as compared to the DMSO treated embryos in the control group. Though this increase was not statistically significant.

3.3.2 Mapping a dose response curve to find out the optimal Lovastatin dose for positive controls.

After screening and identifying double transgenic embryos, I treated 1dpf zebrafish embryos with Lovastatin in concentrations ranging from 1 μM to 5 μM . The embryos were then incubated at 28^o C overnight for 16 hours. The control group was treated with DMSO alone. Images of different groups (n=5) and controls (n=5) were obtained using fluorescent stereomicroscope (Zeiss Axio Zoom V16) and Zenpro (Zeiss) software. Images thus obtained were analysed using FIJI (National Institutes of Health, USA) software. Corrected total fluorescence was calculated for each group and the results were statistically analysed using ordinary one way ANOVA in GraphpadPrism.

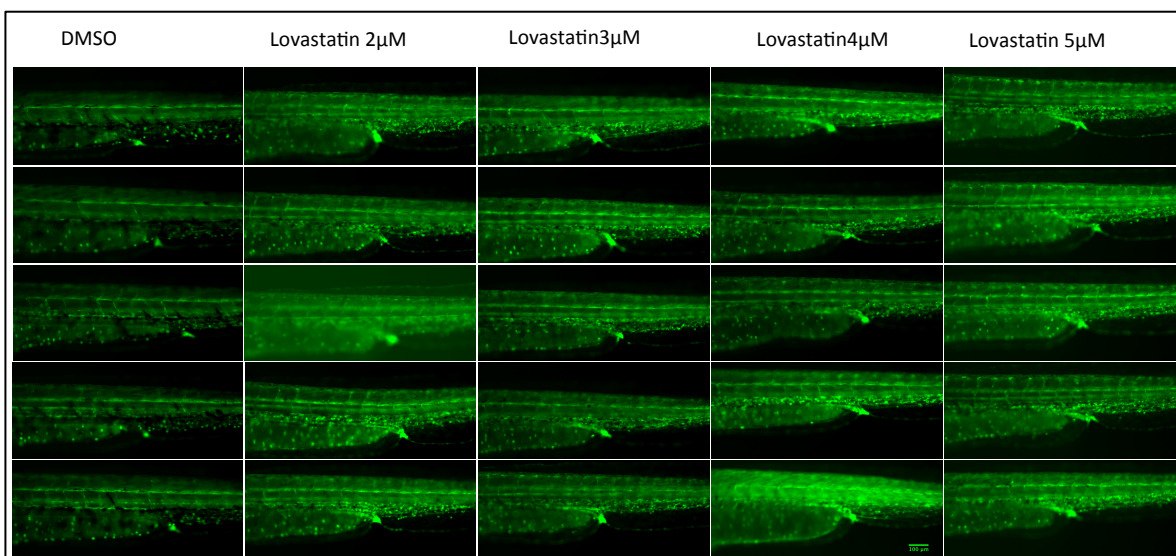


Figure 3.11 Dose response curve for Lovastatin.

Vertical picture panels showing increase in GFP fluorescence in 2dpf embryos treated with increasing doses of Lovastatin when compared with DMSO treated embryos (first vertical panel).

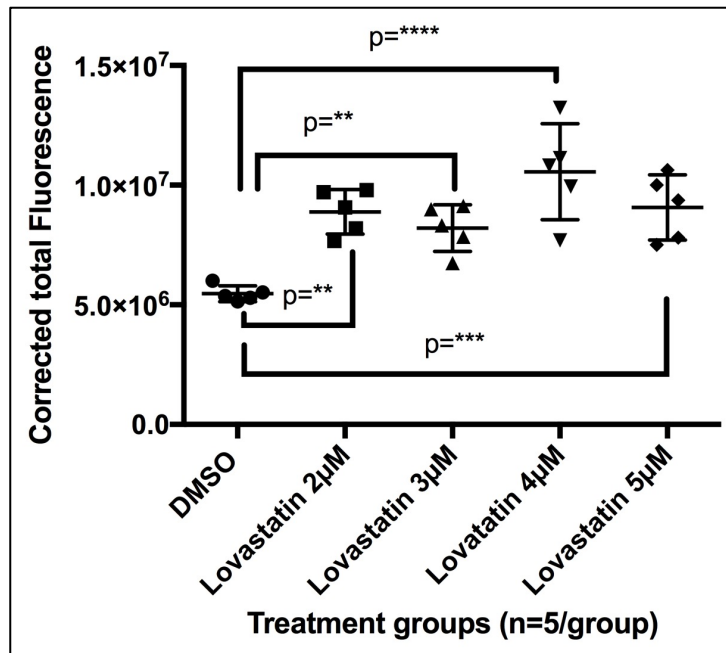


Figure 3.12 Lovastatin dose response graph

Scatter plot showing significant increase in corrected total fluorescence in 2dpf embryos treated with increasing concentrations of lovastatin. Graph showing a maximum increase in mean GFP fluorescence (105621625) in embryos treated with 4µM Lovastatin as compared with DMSO (546555)

I repeated the experiment using 4µM, 5µM, 6µM, 7µM and 8µM concentrations of lovastatin. The aim was to find the concentration of lovastatin that could result in maximum increase in GFP signal. 1 dpf embryos were treated with the above concentrations of lovastatin and were incubated overnight at 28 °C with DMSO treated controls. 2 dpf embryos from each group (n=5) were imaged on the fluorescent stereomicroscope (Axio Zoom V16, Zeiss). Corrected total fluorescence was calculated by analysing the images using FIJI (NIH) software. Statistical analysis was performed using One-way ANOVA in Graphpad Prism software.

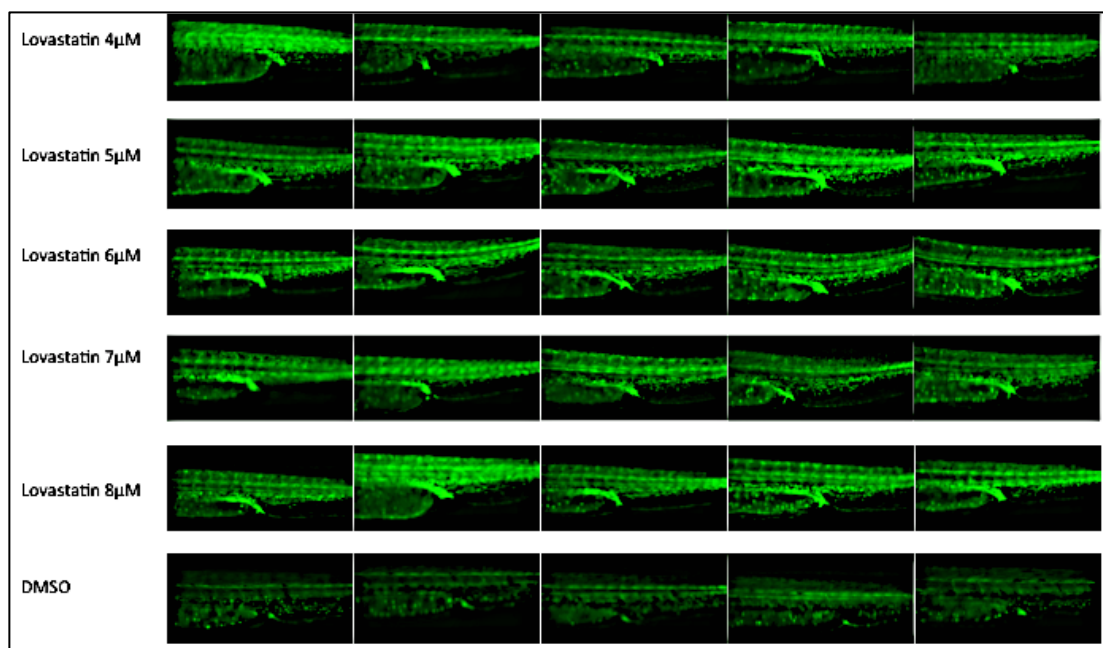


Figure 3.13 Lovastatin dose response using higher concentrations
 Increased expression of GFP in 2dpf embryos treated with Lovastatin in 4 μ M to 8 μ M concentration as compared to DMSO treated controls (Lowest panel).

Conclusion

The dose response plot showed that there was no linear correlation between lovastatin dose and GFP signal. Results revealed that maximum GFP signal was obtained when lovastatin was used in 4 μ M concentration. For subsequent experiments Lovastatin was used in 4 μ M concentration as a positive control.

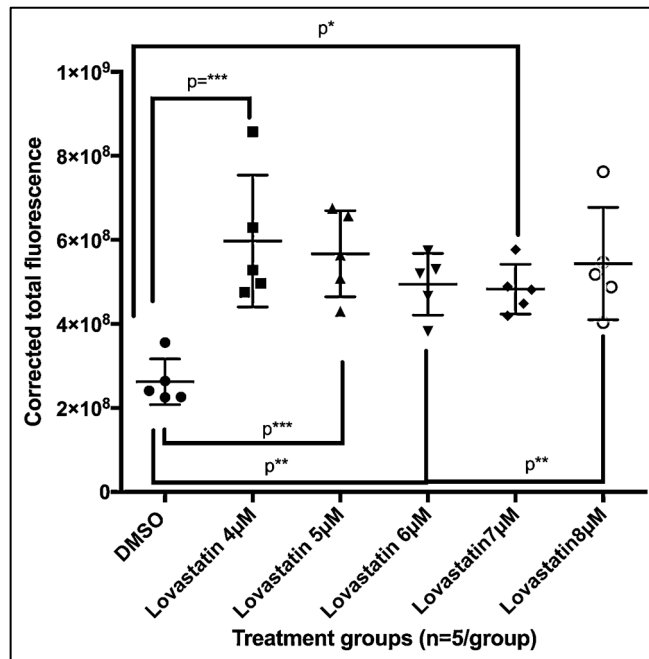


Figure 3.14 Lovastatin dose-response graphs for higher concentrations

A scatter plot showing mean corrected total fluorescence in 2dpf embryos. The graph shows a significant increase of GFP fluorescence in embryos treated with lovastatin. Maximum increase is seen in embryos treated with 4µM concentration of Lovastatin (597453880) as compared with DMSO treated group (262388980).

3.4 Developing positive and negative controls

We already know that *klf2* is a mechano-transduction gene expressed in endothelial cells and responds to flow patterns in blood vessels. Laminar flow patterns enhance *klf2* expression and non-laminar or turbulent flow suppresses *klf2* expression. If the zebrafish do not develop any blood flow, vascular *klf2* expression is almost completely suppressed. Statins are known to increase *klf2* expression through flow independent pathways by inhibiting Rho enzymes.

I used the above mentioned characteristics to develop positive controls involving flow and non flow dependent pathways for *Klf2a* expression. Zebrafish embryos were treated with Lovastatin to augment *klf2a* expression. I also used *tnnt2* morphants developed by

injecting 1-2 cell stage embryos with *tnnt2* morpholino. These embryos do not develop any blood flow due to loss of myocardial development resulting in significant decrease in *klf2a* expression in vascular endothelium.

I also treated 1dpf embryos with tricaine, a local anaesthetic, to arrest cardiac contractility and thus blood flow. Another group of 1dpf embryos was treated with tricaine and lovastatin to assess direct effect of lovastatin on *klf2a* expression in the absence of blood flow.

Two groups of 1dpf zebrafish embryos were used as negative controls. One group was treated with DMSO and the second injected with the standard control morpholino.

3.4.1 Validating positive and negative controls, by examining effect of flow and Lovastatin on GFP fluorescence in 2dpf zebrafish.

3.4.1.1 Using a fluorescent stereomicroscope (Axio Zoom V 16 Zeiss)

After embryo collection, I injected two groups of 1-2 cell embryos with 1nanoliter (nl) of standard control morpholino (0.2mM) and 1 nanolitre (nl) of *tnnt2* morpholino (0.2mM). The rest of the embryos were plated in groups of 50 embryos per petri dish. All the embryos were incubated at 28⁰ C overnight in E3 medium with methylene blue.

1dpf embryos in all the groups were screened for green and red fluorescence. Embryos positive for red and green fluorescence were divided into following treatment groups,

- i. DMSO only treated
- ii. Control morpholino injected
- iii. Tricaine only
- iv. Tricaine + lovastatin treated
- v. Lovastatin only
- vi. *tnnt2* morpholino injected.

Five embryos from each group were imaged for green fluorescence on stereomicroscope (Axio Zoom V16 by Zeiss). Zenpro (Zeiss) software was used to acquire images. Images thus obtained were analysed using FIJI (ImageJ) software. The total fluorescence values thus measured can be affected by autofluorescence, as in the yolk area of the embryos and by background fluorescence. In order to remove these errors corrected total fluorescence was calculated as follows

1. I selected a rectangular area of interest over 4-5 myotomes in the trunk area of the 2dpf embryo.
2. In FIJI, I set the analyse menu to measure area of the rectangle drawn, integrated density of the area and mean gray scale value.
3. I repeated these measurements by drawing a rectangle of the same size outside the embryo. This gave the values for the background fluorescence.
4. Corrected total fluorescence was calculated using the formula

$$\text{Corrected total fluorescence} = \text{Total Integrated density} - (\text{Area of embryo selected} \times \text{Mean gray scale value of the background})$$

Total corrected fluorescence was calculated over a selected area over the aortic region in the body of 2 dpf embryos. Corrected total fluorescence was also calculated over a selected area over the body including myotomes of 2dpf embryos. An area of same size was used for fluorescence calculations in all the embryos imaged. Data thus obtained was analysed using One-way ANNOVA test in GraphPad Prism statistical software

Corrected total fluorescence =
Total Integrated density - (Area of embryo selected X Mean gray scale value of the Background)

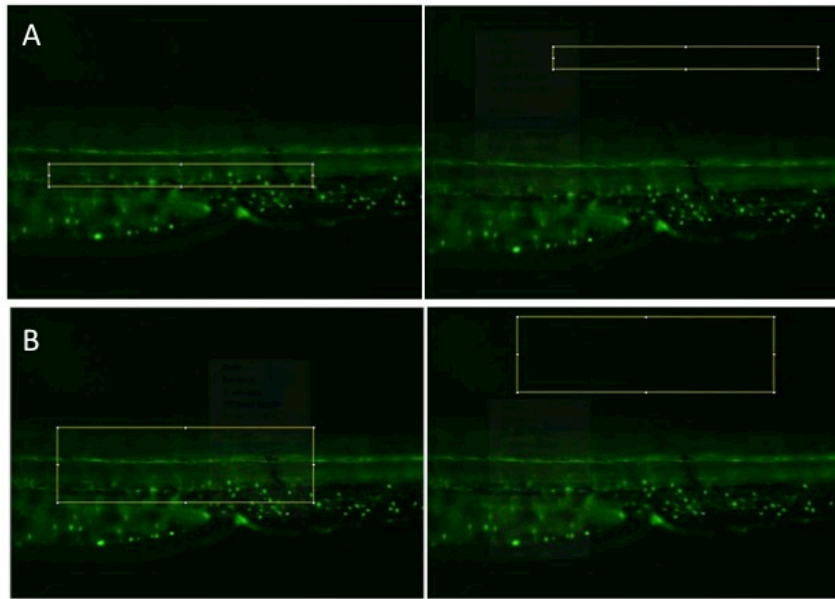


Figure 3.15 Measuring total corrected fluorescence.

Panel A: Shows a rectangular area drawn over aorta to calculate total fluorescence. Similar area drawn outside the embryo (left image) was used to measure background fluorescence.

Panel B: Rectangular areas drawn over myotomes to calculate total fluorescence and background fluorescence.

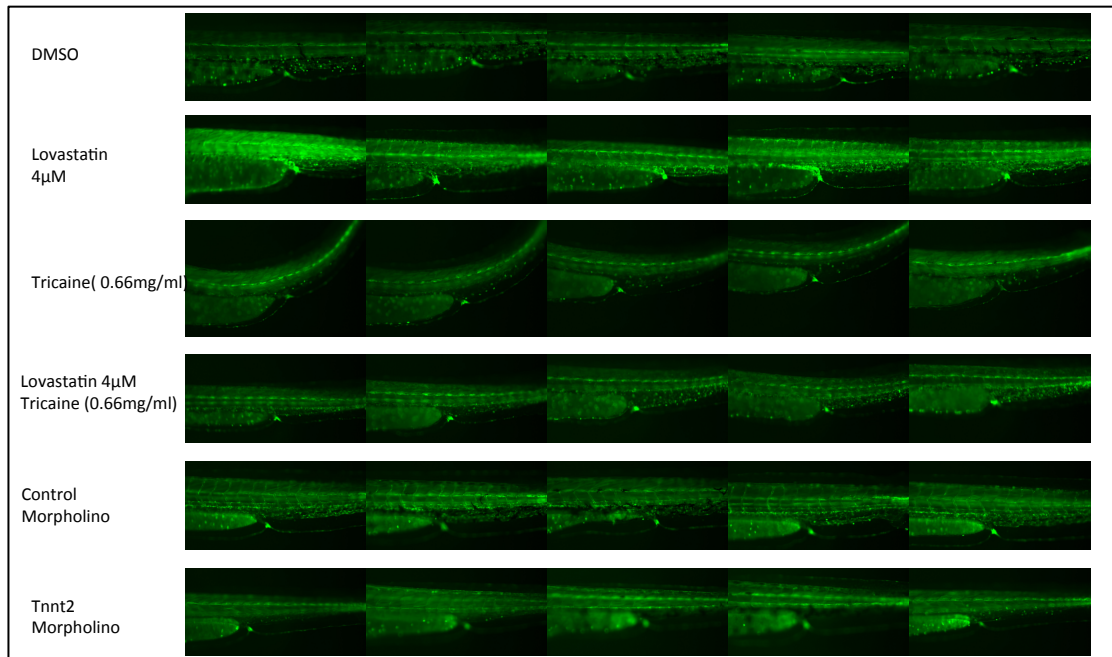


Figure 3.16 Image panels of positive and negative control groups obtained using a fluorescent microscope.. Image panels showing GFP expression in positive control groups (lovastatin 4µM, Tnnt2 morpholino injected, tricaine and tricaine with lovastatin) and negative controls (DMSO treated and control morpholino injected). Lovastatin treated embryos show increased green fluorescence, Tnnt2 morpholino injected and tricaine treated embryos show lower green fluorescence as compared to negative controls.

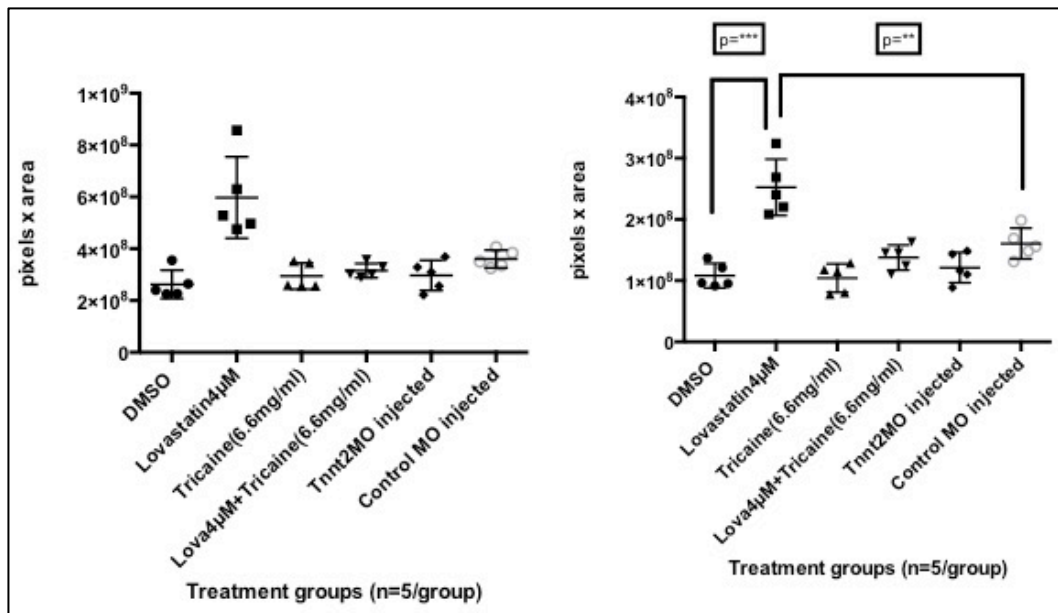


Figure 3.17: Graphs showing Corrected total fluorescence.

Graphs replicating observations in the image panels in figure 3.16.

Left graph shows significant increase in corrected total fluorescence in lovastatin treated 2dpf embryos when fluorescence was measured over the body of zebrafish embryo.

Right graph shows corrected total fluorescence calculated over a selected area over aorta to measure green fluorescence restricted to the vasculature. Again Lovastatin treated embryos had significant increase in GFP fluorescence as compared to negative controls.

I also explored the possibility of using Resveratrol as another positive control. Resveratrol, a plant sterol, is a nicotinamide dinucleotide dependent deacetylase, known to induce *KLF2* through activation of SIRT1 (Sirtulin 1). SIRT1 acts on MEK5 and MEF2 pathways thereby upregulating *KLF2* in HUVECs (Human Umbilical Vascular Endothelial Cells (Gracia-Sancho et al., 2010).

I was not able to show any significant increase in GFP fluorescence in 2dpf embryos that were treated with resveratrol for sixteen hours prior to imaging. Resveratrol was used in concentrations of 20 μM, 40 μM, 60 μM, 80 μM and 100 μM. This result was contrary to that seen by Gracia- Sancho et al.

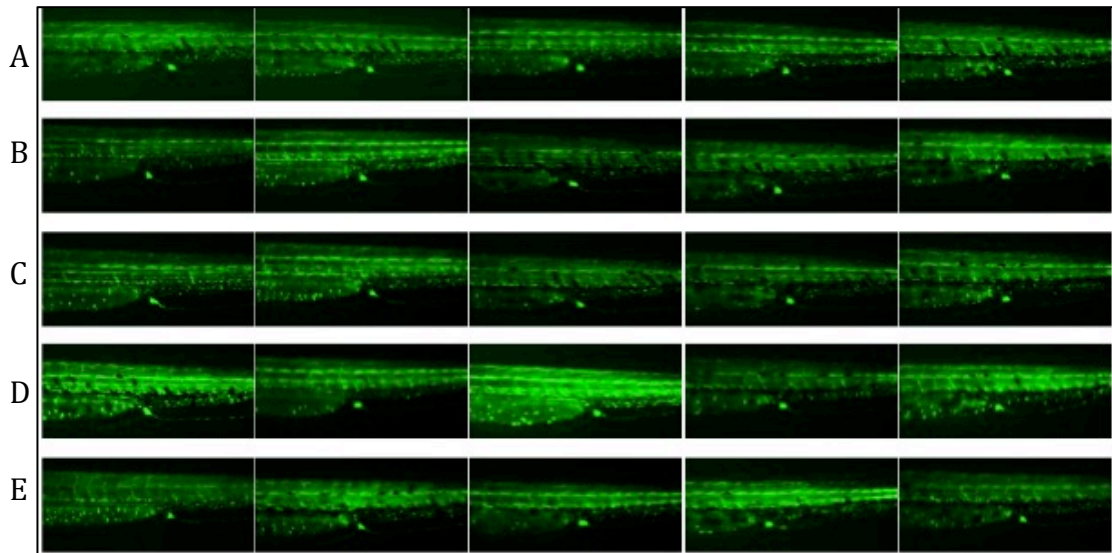


Figure 3.18 Image panels of resveratrol treated embryos
 2dpf embryo treated images after resveratrol treatment with concentrations varying from 40 to 100 μM .
 A. (DMSO treated). B. Resveratrol 40 μM
 C. Resveratrol 60 μM D. Resveratrol 80 μM
 E. Resveratrol 100 μM

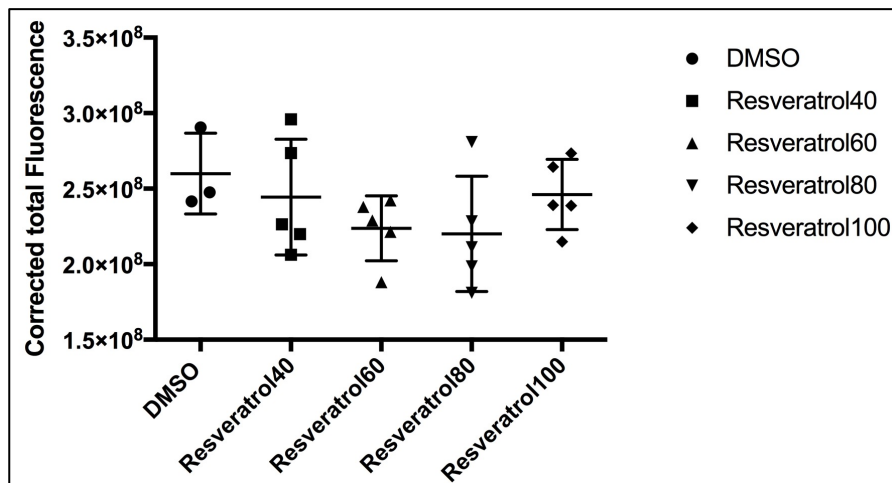


Figure 3.19 Effect of Resveratrol on GFP expression
 Graphs showing no increase in GFP fluorescence in resveratrol treated groups as compared to DMSO treated controls.

3.4.1.2 Validating positive and negative controls on plate-reader

To develop the assay further, I tested the feasibility of the ImageXpress plate-reader for validating the positive and negative controls. Three 1dpf zebrafish embryos per well were placed in each row (n =12) of a 96 well plate with a clear bottom and black walls (Greiner). One row treated with DMSO (Dimethyl Sulfoxide) was used as a negative control. Three further rows were treated with 1 μ M, 4 μ M and 10 μ M concentrations of lovastatin and used as positive controls. Embryos were incubated overnight at 28 $^{\circ}$ C in 250 μ l (microlitres) of DMSO in E3 and 1, 4 and 10 μ M concentrations of lovastatin in E3. On 2dpf 25 μ l of tricaine were added to each well. Embryos were prodded to occupy central area of the wells using a hair-tool. Images were obtained on ImageXpress high throughput plate-reader using a 2X objective with exposure times of 1500 milliseconds for red channels and 2000 milliseconds for green channel. Each well was divided into four quadrants to increase the possibility of capturing images of all three embryos.

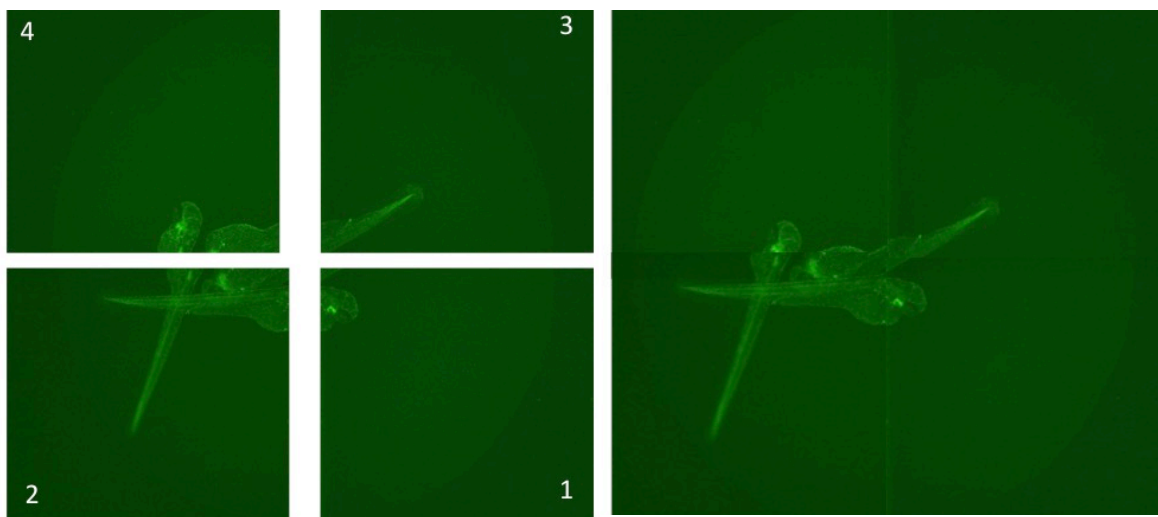


Figure 3.19 Reconstruction of images of each well of a 96 well plate.

Left panel showing the images of four quadrants of a well.

Right panel image showing a reconstructed well.

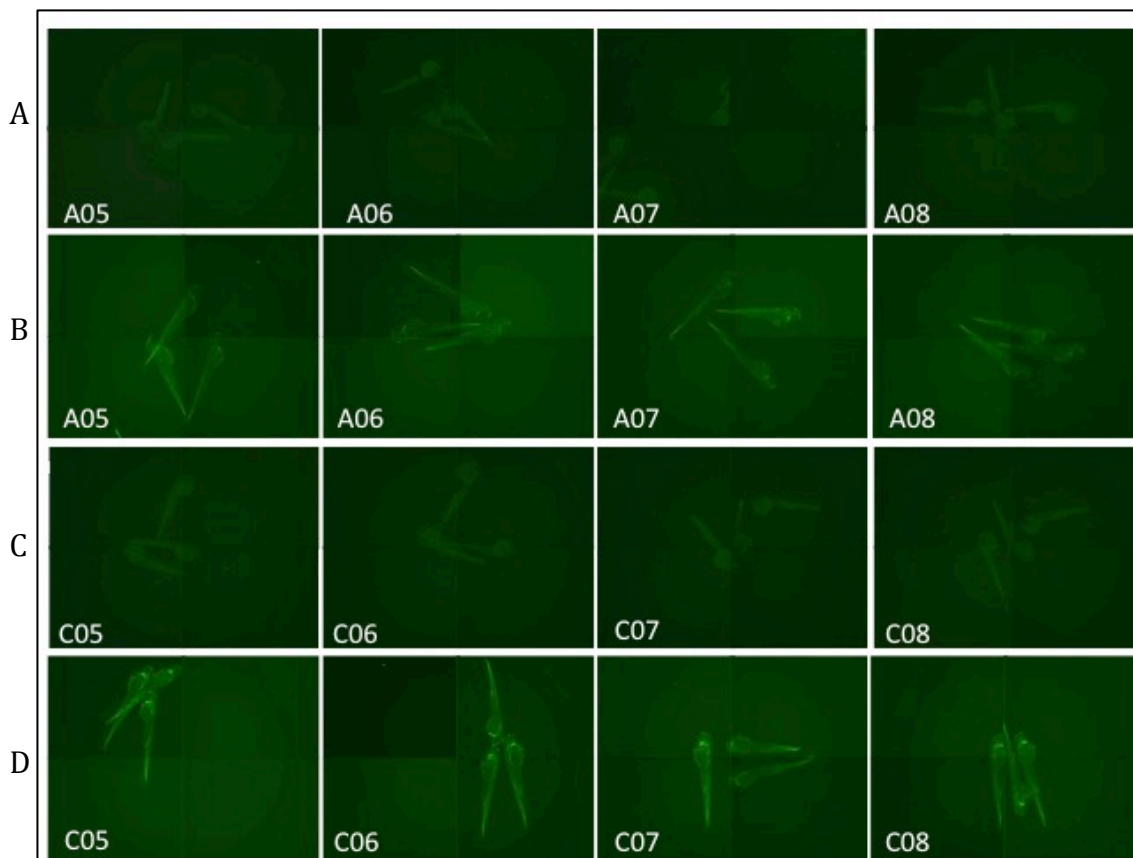


Figure 3.21 Measuring fluorescence in a plate-reader

Panels A and B are pre and post-treatment images of DMSO treated control group.

Panels C and D represent pre and post treatment images of embryos treated with 4µM lovastatin.

Settings on which images were acquired:

Objective 2X,

Exposure for RFP channel 1500 milliseconds,

Exposure for 2000milliseconds

Image analysis using MetaXpress 5.0 software and MWCS (multi wavelength cell scoring) algorithm was able to read a significant increase in GFP expression in 2dpf embryos treated with 1µM, 4µM and 10µM concentrations of Lovastatin for 15 hours as compared with DMSO treated controls. It was amply clear that ImageXpress plate-reader was able to replicate the results obtained by imaging on a stereomicroscope and quantifying fluorescence using FIJI software. Hence the assay was taken to next stage and was used to screen drugs from Spectrum library.

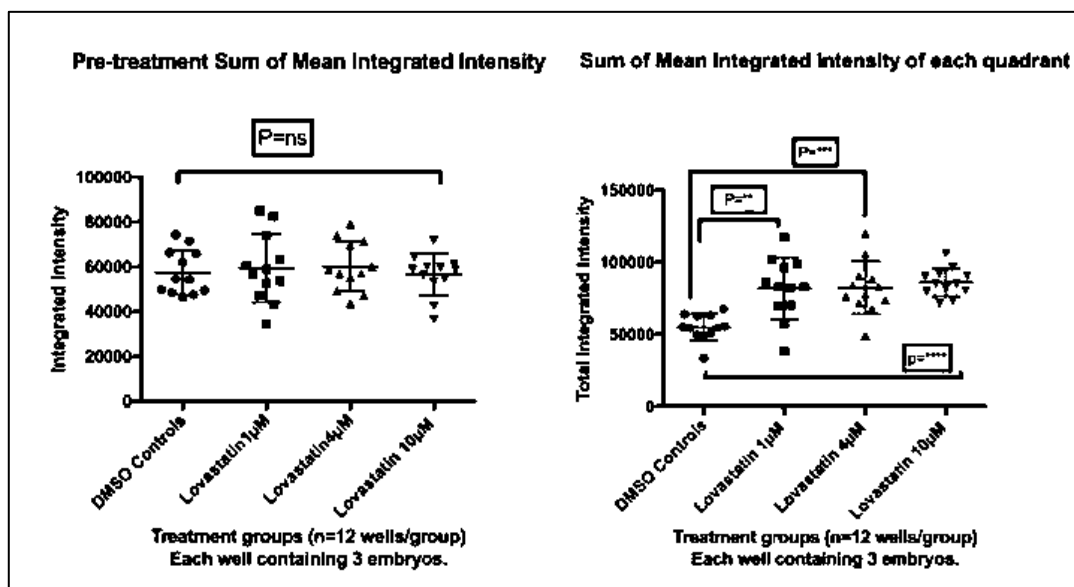


Figure 3.22 Scatter plots of the fluorescence data acquired on ImageXpress.

Right Graph: Scatter plots of post treatment GFP fluorescence showing significant increase in post-treatment (2dpf) GFP expression in embryos treated with Lovastatin as compared to DMSO controls.

Left graph: Shows pretreatment (1dpf) GFP expression, which is same in all the groups.

These results replicate the results obtained with a fluorescent stereomicroscope.

3.4.1.3 Quality control measures

To assure quality control of the assay I calculated “Z” factor for the assay. Z factor is a measure of “statistical effect size”. It compares the mean values of positive or maximum signal control to negative or minimum signal control. “Z” factor was calculated using the following formula

$$Z = 1 - 3(\sigma_p + \sigma_n) / \mu_p - \mu_n$$

where σ_p is standard deviation of the integrated density values of lovastatin (4µM) treated embryos and σ_n is the standard deviation of integrated density values of

DMSO treated controls, and μ_p is the mean integrated density of lovastatin treated embryos and μ_n is the mean of the integrated density of DMSO treated controls.

I obtained a value of 0.17 for Z. (See Appendix1). This qualified my assay as a marginal one. As is evident from the above formula that the Z prime calculation involves a constant factor of 3. This is based on the assumption that the distribution is normal, and 99% of the values are within 3 standard deviations. It is known that, in high throughput screening there is a high chance of distribution to be non-normal. Also the extreme values can adversely affect "Z" value resulting in a situation where the assay may perform well in actual screening and the Z factor is unfavorable {Zhang, 1999}

To overcome some of the short-comings mentioned above, a relatively new statistical parameter, Strictly Standardized Mean Difference (SSMD) is also used in high throughput screens. I calculated the SSMD for my positive and negative control groups using the following formula.

$$\text{SSMD } (\beta) = \mu_p - \mu_n / \sqrt{\sigma_p^2 + \sigma_n^2}$$

Where μ_p is mean value of positive controls, μ_n is the mean value of the negative controls, σ_p^2 is the variance in the positive controls and σ_n^2 is the variance of the negative controls.

SSMD of my assay was 4.5. SSMD not only ranks the size effect but also has a predictor value for classifying effects. A value of 4.5 is classified as a very strong threshold for positive SSMD.

Conclusion

The above experiment, statistical analysis and the quality control evaluation further validated the feasibility of performing drug screen, using ImageXpress plate-reader for mid to high throughput assays.

3.5 Mid to High throughput assay for Drug Screening

Having established positive and negative controls and feasibility of plate-reader as a screening tool, I planned a mid-throughput drug screen using test plates from spectrum drug library (Sigma).

3.5.1 Screening of drugs from Spectrum SP100122 drug library

Three 1dpf embryos were placed in each well of a 96 well plate in 225 microlitres of clear E3 solution and 25 microlitres of tricaine (0.66mg/ml). All wells were imaged on ImageXpress high throughput plate reader using a 2X objective and exposures fixed to 2750 milliseconds for GFP(green fluorescent protein) channel and 1500 milliseconds for RFP (red fluorescent protein) channel. Once pretreatment images were obtained fluid was aspirated out of the wells and 1dpf embryos were treated with 10 μ M concentration of drugs from spectrum library test plate and controls. Total volume of the test drugs and E3 medium in each well was 250 microlitres. The embryos were incubated overnight. Twenty five microlitres of tricaine (4mg/ml) were added to each well. Embryos were prodded to occupy the centre of the wells for optimal image capture. The pre-treatment and the post-treatment images were acquired using the same settings on the plate-reader.

Integrated intensity of green fluorescence was measured by using MetaXpress software. Data thus obtained was analysed using One way ANOVA statistical tests in Graphpad Prism software.

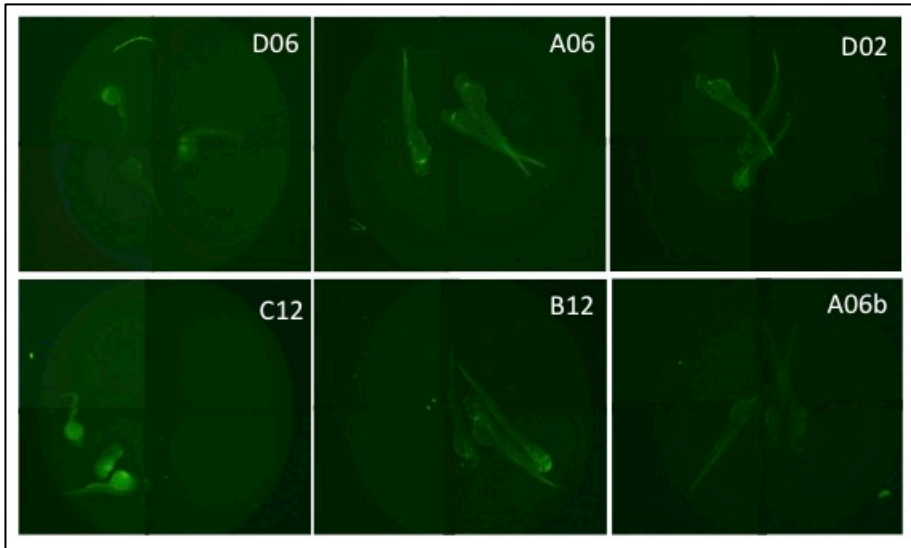


Figure 3.23 Spectrum library drug screening.

Representative images from drug screening plates DMSO (D06, C12) Lovastatin (A06, B12) and Spectrum drugs (D02, A06b).

Images were obtained with following settings

Objective: 2X, Exposure GFP channel: 2750 ms and Exposure RFP channel: 1500 ms

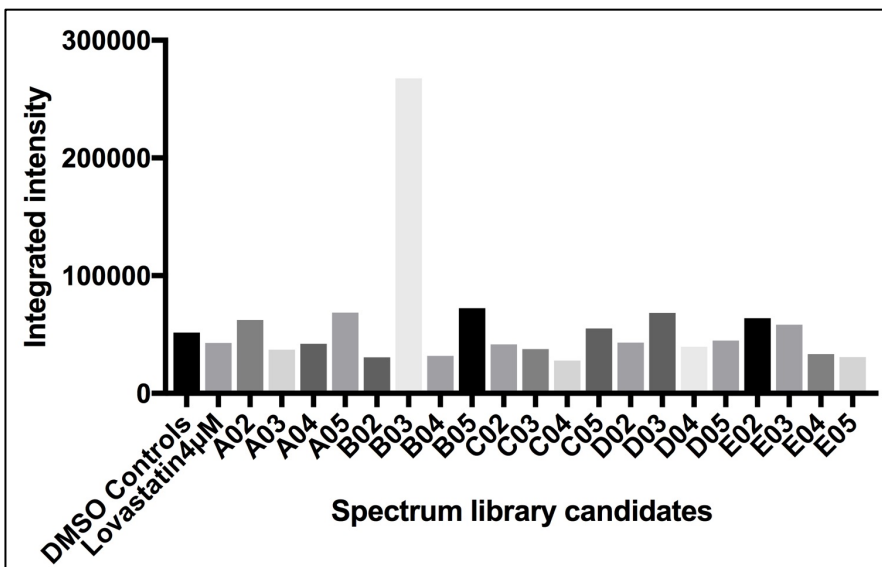


Figure 3.24 Integrated intensity of different drug screen candidates.

Column graph comparing GFP fluorescence (integrated intensity) of 2dpf embryos treated with Spectrum library candidates, DMSO and lovastatin. It is obvious from the plot that the screen did not work as the integrated intensity of lovastatin treated embryos is lower than the negative controls (DMSO group).

Multi-Wavelength Cell Scoring algorithm was used to calculate integrated density

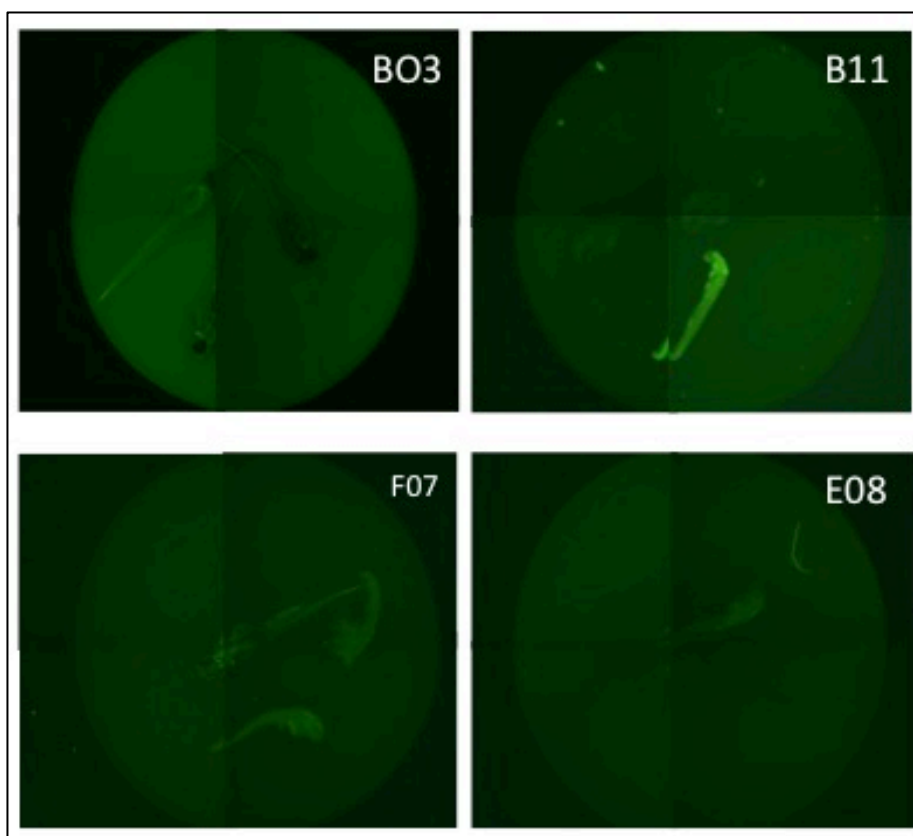


Figure 3.25 Representative images of drug screen.

Images of wells with fluorescent drug (B03) damaged embryo with lots of fluorescence (B11, F07 and E08)

Images were obtained with following settings

Objective: 2X, Exposure GFP channel: 2750 ms and Exposure RFP channel: 1500 ms

(Alpha-numeric are the well numbers).

Integrated intensity of green fluorescence was measured by using MetaXpress software.

Data thus obtained was analysed using Graphpad Prism statistical software.

The above results show a failed drug screen. In the above column graph fluorescence of Lovastatin treated positive controls is less than the DMSO treated negative controls. I cross-checked these results with the images obtained on the plate reader. The reasons that came to light by looking at the images were, fluorescence caused by the drug under investigation itself, as in case of well B03. Lots of embryos appeared damaged. One of the possibilities was that 10 μ M dose for screening was too high or it was a bad batch of

embryos. In order to re-validate the controls, I repeated the experiment by blinding positive and negative controls and comparing the fluorescence to Tnnt2 morphants. I also filled some wells with clear E3 medium only. Using the values of integrated density from these wells I plotted the following graphs for integrated density and net integrated density. Net integrated density was calculated by subtracting the integrated density values obtained from the wells containing E3 medium only from the values obtained from the wells containing treatments A or B.

On analyzing the data for total and net integrated density. Treatment A significantly increased the fluorescence in 2dpf zebrafish embryos as compared to Tnnt2 morphants. On decoding, treatment “A” was lovastatin in 4 μ M concentration and treatment “B” was DMSO only. This further endorsed the validity of controls.

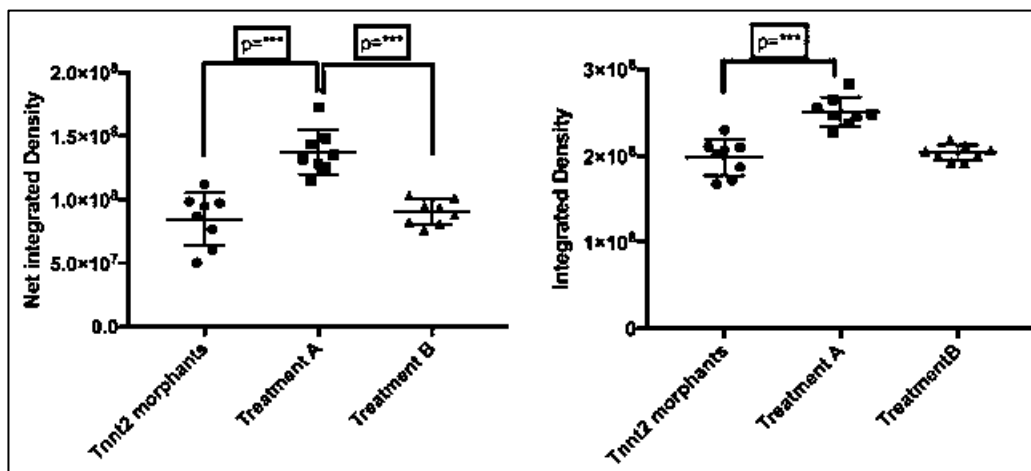


Figure 3.26 Blinded positive and negative controls.

Graphs comparing effects of Tnnt2 morpholino injection, treatment A and treatment B on GFP expression in 2dpf embryos. The treatments A and B were blinded to validate positive and negative controls. Both the graphs show significant increase in integrated intensity and net integrated intensity in treatment Group A.

(Net integrated fluorescence was calculated by subtracting integrated density values of the wells containing E3 medium only from integrated density values of the wells containing treatments A or B. One way ANOVA was used for statistical analysis.)

On decoding treatment A was lovastatin in 4 μ M concentration and treatment B was DMSO.

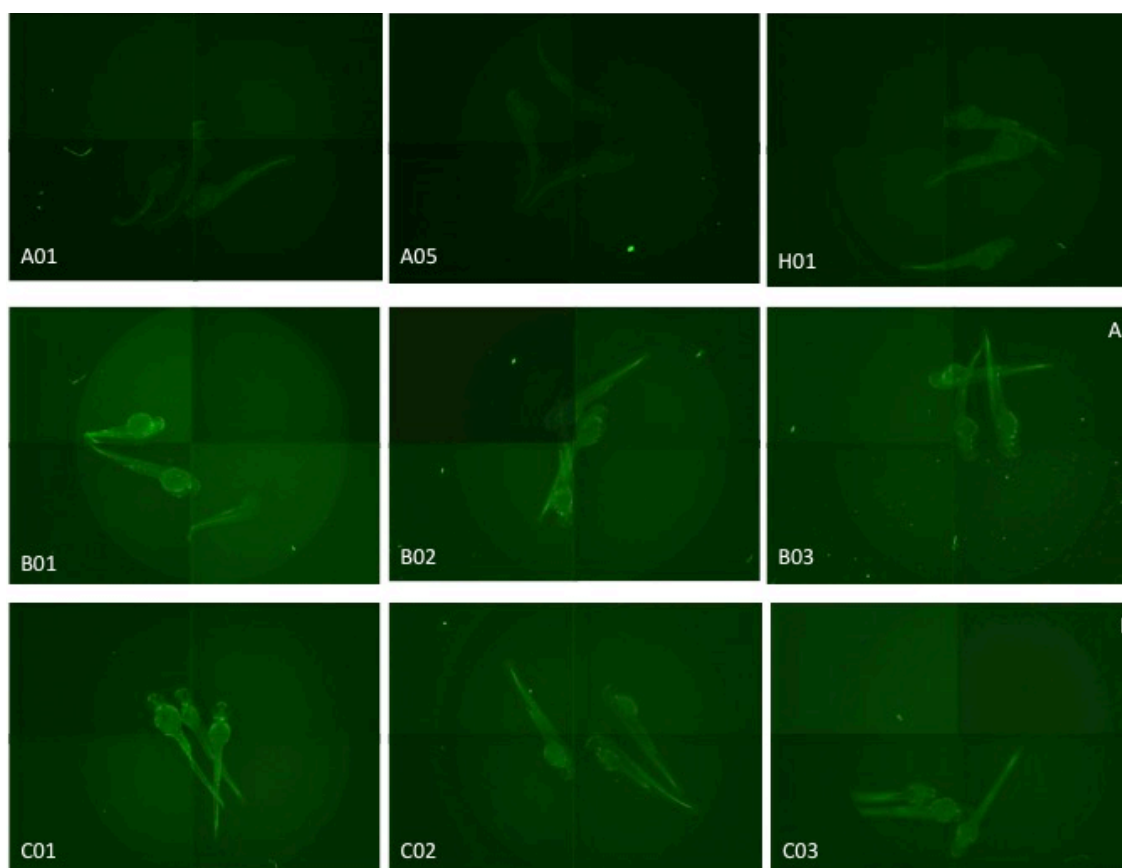


Figure 3.27 Revalidating positive and negative controls.
 Representative images of 2dpf embryos from three groups
 Top panel : Tnnt2morphants, Middle panel: Treatment A ,
 Bottom panel: Treatment B.

Next I repeated the drug screen using 5 μ M concentration of drugs. The micro-assay plate containing the drugs was thawed at room temperature. 200 μ ls of clear E3 solution were added to each well. 100 μ ls were used to treat the embryos in each well. 150 μ ls of E3 medium was added to each well achieving a 5 times dilution. 25 μ ls of tricaine (6.6mg/ml) was added to each well before imaging. Mean integrated intensity of wells treated with DMSO was used as a negative control for comparison. Similarly mean integrated intensity of wells containing Lovastatin treatment was used as a positive control. On screening plate 08 from spectrum library and using the integrated density as a measure of GFP fluorescence I noted there were possible hits in wells A03, C03 D05 and H09

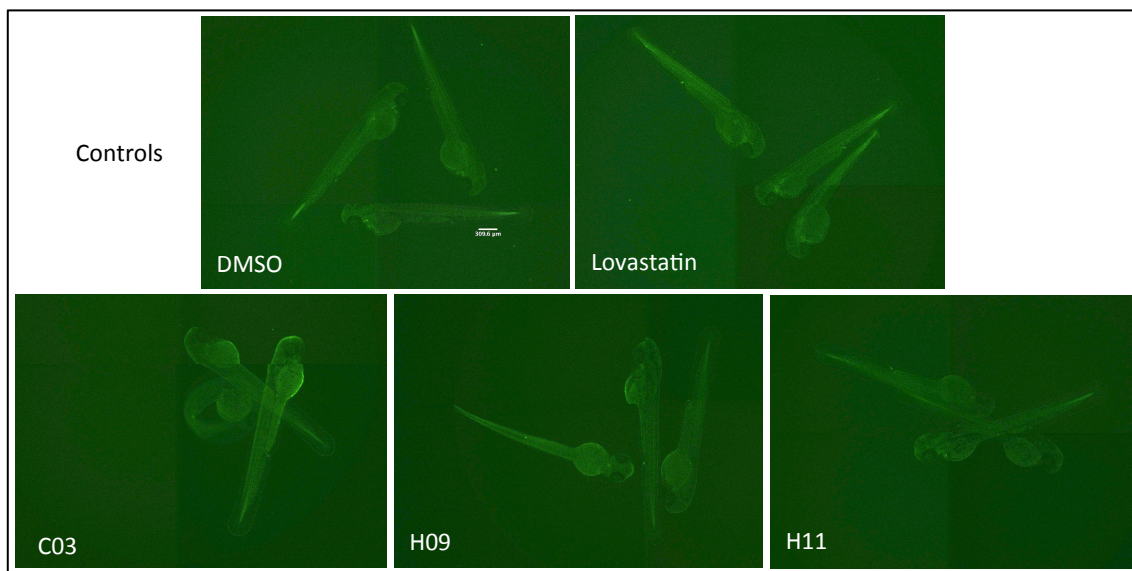


Figure 3.28 Representative images of Mid-throughput screen of Spectrum 100122 plate 8 candidates.

Top panel: (Right image is showing a positive control (lovastatin treated). Left image represents negative (DMSO treated) controls. Bottom panel represents possible hits from the screen.

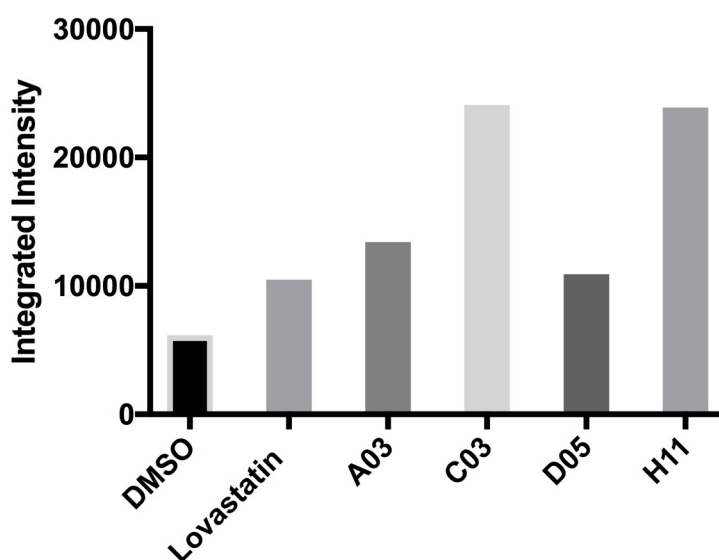


Figure 3.29 Possible hits from the drug screen.

Column graph showing integrated intensity of DMSO treated negative controls (first column) Lovastatin treated positive controls (second column) and integrated intensities of wells (alpha-numeric) that could be possible "hits" in the screen.

On decoding the spectrum library the drugs that came up as possible hits were warfarin, vitamin K antagonist (C03), fenoterol hydrobromide, a beta agonist (H09), mebeverine hydrochloride, anticholinergic (H11), triamcinolone acetonide, a synthetic corticosteroid (A03) and yohimibine hydrochloride, an alpha blocker (D05).

Triamcinolone is a potent topical steroid preparation. It is possible that increased GFP expression could be due to its strong anti-inflammatory effects resulting in suppression of IL1 and TNF α .

Yohimibine is extracted from tree bark of yohimbe tree found in west Africa . It has vasoactive properties because of its alpha adrenergic blocking activities. I may postulate that yohimibine has upregulated GFP expression because of altering mechano-transductory signals in developing blood vessels.

Both the above postulates need to be further explored. On looking up the literature to find any reported associations between any of the above drugs I was not able to find any publications substantiating my postulation.

Chapter 4

Discussion

Discussion

Klf2 expression is dependent on blood flow in the developing vasculature. In my experiments I measured the intensity of a GFP signal as a surrogate for *kfl2a* expression. Novel orientation tools for zebrafish embryo imaging have been described but this did not work well in the context of developing a mid to high throughput screen. I resorted to a much quicker way of loading embryos into a 96 well plate for imaging by just pipetting embryos in clear E3 medium and imaging them. By dividing each well into four quadrants the chances of capturing fluorescence from all three embryos was increased. But I found that embryos adjacent to the wall were not captured. To overcome this problem I first tried to vigorously shake the 96 well plate to move the embryos to the middle of the well. This did not work either. Hence, I used a hair tool to prod the embryos as much to the middle of the well so as to capture all three embryos for imaging and subsequent analysis.

Whilst performing dose response analysis to find the optimal lovastatin dose, 1dpf zebrafish embryos when treated with varied concentrations of lovastatin for 15 hours showed significant increase in GFP fluorescence, a surrogate for *kf2a* expression. On performing a dose response analysis the relation was not linear and I found a 4 μ M concentration of lovastatin gave maximum increase in fluorescence. Not getting a proportionally, increased response in doses higher than 4 μ M could be attributed to statin toxicity affecting myotome architecture in embryos. Campos et al have shown that, zebrafish embryos, when treated with higher concentrations of simvastatin showed morphological alterations. These alterations in development included embryo size, somite size and shape of the septa between the myotomes. There was also a reduction in total cell number in developing zebrafish embryos. (Campos et al., 2016)

I also found that embryos treated with tricaine and lovastatin showed more GFP fluorescence than the embryos that were treated with tricaine alone or *tnnt2* morphants. The increase was not statistically significant. This increase could be due to non flow dependent pathways involved in *klf2a* expression.

Zebrafish embryos showed a lot of autofluorescence when imaged for GFP signal. This was particularly so in the area of yolk sac. Background fluorescence can also add to the values obtained. To prevent this error I selected a finite rectangular area over the body of the embryos and excluded the yolk sac area. Further background fluorescence was calculated by drawing a similar rectangle over the image that did not contain any parts of embryo. Corrected total fluorescence was calculated to achieve a more accurate measure of fluorescence.

Similarly algorithms that were designed for plate-reader, used subtraction methods to exclude yolk sac and measured GFP signal, mostly in vasculature of 2dpf embryo. Line graphs were used to include lowest and highest gray scale values to set the parameters for measuring GFP signal.

Like any other living organisms zebrafish embryos grow at different rates. This can confound the results simply because of less GFP positive cells rather than lower GFP expression. Statistical methods have been applied to compute "z " values that factor in this variability in controls and then applied to treatments groups.

What I have done is very basic development of this assay and tried to be as meticulous as possible. Having established the feasibility of this assay on a high-throughput plate-reader this can be further developed into a high-throughput assay.

Limitations in my experimentation were as follows:

- Lots of human handling was required which could subject this assay to human error. This can range from handling the delicate embryos to mixing treatments. Using robotic systems can get rid of the human error.
- As evident from the methods that I adopted, these were time consuming, and therefore, decreased the efficiency of the assay.
- The double transgenics we used were out-crossed with fish of the nacre line. We did not use any phenylthiourea (PTU) to prevent melanin production in embryos. The reason was to prevent any interaction between the drugs and PTU. Hence there is a possibility that some of the fluorescence was masked by developing melanin pigment. We used one well per treatment making sample size small. So masking of fluorescence can have significant effect on fluorescence quantification.
- Linear DNA based and Tol2-mediated transgenesis was used in the generation of the double transgenic zebrafish (*klf2a:GFP;kdr1:RFP*) used in this assay. However, the integration of multiple copies of transgenes at random genomic locations makes long term transgene stability unpredictable with variable expression. The variability in GFP expression in individual zebrafish embryos in the treatment and control groups can also be attributed to the fact that our transgenic zebrafish line was not single copy for GFP expression. To overcome this limitation in future I screened our *klf2a:GFP;kdr1:GFP* double transgenic zebrafish embryos for single copy GFP expression. Since I out-crossed the *klf2a:GFP;kdr1:GFP* transgenic zebrafish with the fish of nacre line we expect some of the offsprings will have lost the pigment. Keeping this in mind, we have raised 60-70 fish to adulthood. The aim of this exercise is to establish a transgenic nacre line that will be single

copy for GFP with nacre features. This may bring about uniformity in the GFP expression and better capture of GFP fluorescence in future experiments.

- Another aspect of this assay that can be further developed is imaging. Using a 2X objective does not give enough resolution to detail the structure of 2dpf embryos. This results in GFP expressing cells group together as a blob rather than a discrete dot. This can affect the fluorescence calculated by segmentation methods. In future it may be useful to try using a 10x or a 20X objectives for better resolution and more accurate fluorescence quantification.

Future Directions

Zebrafish embryos are going to be used more and more in future for initial drug screening. This assay model can help in finding drugs that will enhance GFP fluorescence a surrogate for *klf2a* expression. *Klf2* is an atheroprotective gene and its increased expression can prevent progression of atherosclerosis. The advantage of screening already licensed drugs for upregulatory effect on *klf2a* expression is that the possible hit can be fast tracked into a therapeutic option.

During embryonic development *klf2a* is expressed in pectoral fins and squamous cells in epidermis. So further drug screens can be developed which are relevant to skin and limb development.

In view of the sequence divergence between zebrafish and human receptor proteins one would expect a modest conservation of pharmacological effects. Actually the rates of conservation are high mostly due to high target similarity at active sites. 82% of disease causing human proteins have an orthologue in zebrafish (Howe et al., 2013). Due to the ease with which zebrafish can be genetically modified zebrafish screening will become more and more relevant in drug screening and developing treatment strategies.

Automation leading to use of robots for zebrafish embryo handling and drug delivery are finding increasing use in drug screening thus making drug screens more efficient and precise. Fecundity of zebrafish can be manipulated to produce more eggs. This can result in large drug screens involving thousands of drugs. (Rennekamp and Peterson, 2015).

Using TALENs and CRISPR-Cas technologies it has been possible to create human disease in zebrafish.(Xiao et al., 2013) (Irion et al., 2014). Geneticists have discovered thousands of mutations associated with human disease. Successful teaming of zebrafish and traditional drug development approaches will help in developing individualized therapeutics.

Though the role of zebrafish in drug screening is on an increase, there are significant challenges that need to be overcome. Controlling and quantifying drug exposure is one of them. It is easy to determine the concentration of drug in plate water, but quantifying drug concentrations in microscopic larvae is very difficult. This can result in false negatives, where a drug cannot show its efficacy for lack of absorption by zebrafish embryos. False negatives will negatively affect a toxicity screen as, toxic compounds may not be identified for lack of absorption.

As more experience is gathered assays will become more standardized and will bear better formal relationship with other pre-clinical models. Also toxicity or efficacy of a drug will have to be measured in a standard fashion, which can then help in comparing the results.

Zebrafish drug screening in my opinion will be an important tool in developing individualized therapeutics.

I would like to conclude by stating that the drug-screening assay I developed can be used for initial whole organism drug screening. This assay will be able to find hits resulting in increased GFP expression. Once hits are established they will need to be further tested by molecular biology methods to prove that increased GFP fluorescence is definitely a surrogate of *klf2a* upregulation.

Chapter 5

References

5. References

- ANDERSON, K. P., KERN, C. B., CRABLE, S. C. & LINGREL, J. B. 1995. Isolation of a gene encoding a functional zinc finger protein homologous to erythroid Kruppel-like factor: identification of a new multigene family. *Mol Cell Biol*, 15, 5957-65.
- ARANY, Z., SELLERS, W. R., LIVINGSTON, D. M. & ECKNER, R. 1994. E1A-associated p300 and CREB-associated CBP belong to a conserved family of coactivators. *Cell*, 77, 799-800.
- ASIMAKI, A., KAPOOR, S., PLOVIE, E., KARIN ARNDT, A., ADAMS, E., LIU, Z., JAMES, C. A., JUDGE, D. P., CALKINS, H., CHURKO, J., WU, J. C., MACRAE, C. A., KLEBER, A. G. & SAFFITZ, J. E. 2014. Identification of a new modulator of the intercalated disc in a zebrafish model of arrhythmogenic cardiomyopathy. *Sci Transl Med*, 6, 240ra74.
- ATKINS, G. B., WANG, Y., MAHABELESWAR, G. H., SHI, H., GAO, H., KAWANAMI, D., NATESAN, V., LIN, Z., SIMON, D. I. & JAIN, M. K. 2008. Hemizygous deficiency of Kruppel-like factor 2 augments experimental atherosclerosis. *Circ Res*, 103, 690-3.
- BANERJEE, S. S., FEINBERG, M. W., WATANABE, M., GRAY, S., HASPEL, R. L., DENKINGER, D. J., KAWAHARA, R., HAUNER, H. & JAIN, M. K. 2003. The Kruppel-like factor KLF2 inhibits peroxisome proliferator-activated receptor-gamma expression and adipogenesis. *J Biol Chem*, 278, 2581-4.
- BASU, P., MORRIS, P. E., HAAR, J. L., WANI, M. A., LINGREL, J. B., GAENSLER, K. M. & LLOYD, J. A. 2005. KLF2 is essential for primitive erythropoiesis and regulates the human and murine embryonic beta-like globin genes in vivo. *Blood*, 106, 2566-71.
- BHATTACHARYA, R., SENBANERJEE, S., LIN, Z., MIR, S., HAMIK, A., WANG, P., MUKHERJEE, P., MUKHOPADHYAY, D. & JAIN, M. K. 2005. Inhibition of vascular permeability factor/vascular endothelial growth factor-mediated angiogenesis by the Kruppel-like factor KLF2. *J Biol Chem*, 280, 28848-51.
- BI, W., DRAKE, C. J. & SCHWARZ, J. J. 1999. The transcription factor MEF2C-null mouse exhibits complex vascular malformations and reduced cardiac expression of angiopoietin 1 and VEGF. *Dev Biol*, 211, 255-67.
- BONAUER, A., CARMONA, G., IWASAKI, M., MIONE, M., KOYANAGI, M., FISCHER, A., BURCHFIELD, J., FOX, H., DOEBELE, C., OHTANI, K., CHAVAKIS, E., POTENTE, M., TJWA, M., URBICH, C., ZEIHNER, A. M. & DIMMELER, S. 2009. MicroRNA-92a controls angiogenesis and functional recovery of ischemic tissues in mice. *Science*, 324, 1710-3.
- BOON, R. A., FLEDDERUS, J. O., VOLGER, O. L., VAN WANROOIJ, E. J., PARDALI, E., WEESIE, F., KUIPER, J., PANNEKOEK, H., TEN DIJKE, P. & HORREVOETS, A. J. 2007.

- KLF2 suppresses TGF-beta signaling in endothelium through induction of Smad7 and inhibition of AP-1. *Arterioscler Thromb Vasc Biol*, 27, 532-9.
- BOTELLA, L. M., SANCHEZ-ELSNER, T., SANZ-RODRIGUEZ, F., KOJIMA, S., SHIMADA, J., GUERRERO-ESTEO, M., COOREMAN, M. P., RATZIU, V., LANGA, C., VARY, C. P., RAMIREZ, J. R., FRIEDMAN, S. & BERNABEU, C. 2002. Transcriptional activation of endoglin and transforming growth factor-beta signaling components by cooperative interaction between Sp1 and KLF6: their potential role in the response to vascular injury. *Blood*, 100, 4001-10.
- BREY, C. W., NELDER, M. P., HAILEMARIAM, T., GAUGLER, R. & HASHMI, S. 2009. Kruppel-like family of transcription factors: an emerging new frontier in fat biology. *Int J Biol Sci*, 5, 622-36.
- CAMPOS, L. M., RIOS, E. A., GUAPYASSU, L., MIDLEJ, V., ATELLA, G. C., HERCULANO-HOUZEL, S., BENCHIMOL, M., MERMELSTEIN, C. & COSTA, M. L. 2016. Alterations in zebrafish development induced by simvastatin: Comprehensive morphological and physiological study, focusing on muscle. *Exp Biol Med (Maywood)*, 241, 1950-1960.
- CARLSON, C. M., ENDRIZZI, B. T., WU, J., DING, X., WEINREICH, M. A., WALSH, E. R., WANI, M. A., LINGREL, J. B., HOGQUIST, K. A. & JAMESON, S. C. 2006. Kruppel-like factor 2 regulates thymocyte and T-cell migration. *Nature*, 442, 299-302.
- CHICO, T. J., INGHAM, P. W. & CROSSMAN, D. C. 2008. Modeling cardiovascular disease in the zebrafish. *Trends Cardiovasc Med*, 18, 150-5.
- CHIPLUNKAR, A. R., CURTIS, B. C., EADES, G. L., KANE, M. S., FOX, S. J., HAAR, J. L. & LLOYD, J. A. 2013. The Kruppel-like factor 2 and Kruppel-like factor 4 genes interact to maintain endothelial integrity in mouse embryonic vasculogenesis. *BMC Dev Biol*, 13, 40.
- CHNG, H. T., HO, H. K., YAP, C. W., LAM, S. H. & CHAN, E. C. 2012. An investigation of the bioactivation potential and metabolism profile of Zebrafish versus human. *J Biomol Screen*, 17, 974-86.
- CONKRIGHT, M. D., WANI, M. A. & LINGREL, J. B. 2001. Lung Kruppel-like factor contains an autoinhibitory domain that regulates its transcriptional activation by binding WWP1, an E3 ubiquitin ligase. *J Biol Chem*, 276, 29299-306.
- CORNHILL, J. F. & ROACH, M. R. 1976. A quantitative study of the localization of atherosclerotic lesions in the rabbit aorta. *Atherosclerosis*, 23, 489-501.
- CUTLER, C., MULTANI, P., ROBBINS, D., KIM, H. T., LE, T., HOGGATT, J., PELUS, L. M., DESPONTIS, C., CHEN, Y. B., REZNER, B., ARMAND, P., KORETH, J., GLOTZBECKER, B., HO, V. T., ALYEA, E., ISOM, M., KAO, G., ARMANT, M., SILBERSTEIN, L., HU, P., SOIFFER, R. J., SCADDEN, D. T., RITZ, J., GOESSLING, W., NORTH, T. E., MENDLEIN, J., BALLEEN, K., ZON, L. I., ANTIN, J. H. & SHOEMAKER, D. D. 2013. Prostaglandin-modulated umbilical cord blood hematopoietic stem cell transplantation. *Blood*, 122, 3074-81.

- DAI, G., KAAZEMPUR-MOFRAD, M. R., NATARAJAN, S., ZHANG, Y., VAUGHN, S., BLACKMAN, B. R., KAMM, R. D., GARCIA-CARDENA, G. & GIMBRONE, M. A., JR. 2004. Distinct endothelial phenotypes evoked by arterial waveforms derived from atherosclerosis-susceptible and -resistant regions of human vasculature. *Proc Natl Acad Sci U S A*, 101, 14871-6.
- DANG, D. T., PEVSNER, J. & YANG, V. W. 2000. The biology of the mammalian Kruppel-like family of transcription factors. *Int J Biochem Cell Biol*, 32, 1103-21.
- DAS, H., KUMAR, A., LIN, Z., PATINO, W. D., HWANG, P. M., FEINBERG, M. W., MAJUMDER, P. K. & JAIN, M. K. 2006. Kruppel-like factor 2 (KLF2) regulates proinflammatory activation of monocytes. *Proc Natl Acad Sci U S A*, 103, 6653-8.
- DAVIES, P. F. 1995. Flow-mediated endothelial mechanotransduction. *Physiol Rev*, 75, 519-60.
- DAVIES, P. F., CIVELEK, M., FANG, Y. & FLEMING, I. 2013. The atherosusceptible endothelium: endothelial phenotypes in complex haemodynamic shear stress regions in vivo. *Cardiovasc Res*, 99, 315-27.
- DEKKER, R. J., BOON, R. A., RONDAIJ, M. G., KRAGT, A., VOLGER, O. L., ELDERKAMP, Y. W., MEIJERS, J. C., VOORBERG, J., PANNEKOEK, H. & HORREVOETS, A. J. 2006. KLF2 provokes a gene expression pattern that establishes functional quiescent differentiation of the endothelium. *Blood*, 107, 4354-63.
- DEKKER, R. J., VAN SOEST, S., FONTIJN, R. D., SALAMANCA, S., DE GROOT, P. G., VANBAVEL, E., PANNEKOEK, H. & HORREVOETS, A. J. 2002. Prolonged fluid shear stress induces a distinct set of endothelial cell genes, most specifically lung Kruppel-like factor (KLF2). *Blood*, 100, 1689-98.
- DEKKER, R. J., VAN THIENEN, J. V., ROHLENA, J., DE JAGER, S. C., ELDERKAMP, Y. W., SEPPEN, J., DE VRIES, C. J., BIESSEN, E. A., VAN BERKEL, T. J., PANNEKOEK, H. & HORREVOETS, A. J. 2005. Endothelial KLF2 links local arterial shear stress levels to the expression of vascular tone-regulating genes. *Am J Pathol*, 167, 609-18.
- DRIESSEN, M., VITINS, A. P., PENNING, J. L., KIENHUIS, A. S., WATER, B. & VAN DER VEN, L. T. 2015. A transcriptomics-based hepatotoxicity comparison between the zebrafish embryo and established human and rodent in vitro and in vivo models using cyclosporine A, amiodarone and acetaminophen. *Toxicol Lett*, 232, 403-12.
- DUCHARME, N. A., REIF, D. M., GUSTAFSSON, J. A. & BONDESSON, M. 2015. Comparison of toxicity values across zebrafish early life stages and mammalian studies: Implications for chemical testing. *Reprod Toxicol*, 55, 3-10.
- EGOROVA, A. D., VAN DER HEIDEN, K., VAN DE PAS, S., VENNEMANN, P., POELMA, C., DERUITER, M. C., GOUMANS, M. J., GITTENBERGER-DE GROOT, A. C., TEN DIJKE, P., POELMANN, R. E. & HIERCK, B. P. 2011. Tgfbeta/Alk5 signaling is required for shear stress induced klf2 expression in embryonic endothelial cells. *Dev Dyn*, 240, 1670-80.

- FANG, Y. & DAVIES, P. F. 2012. Site-specific microRNA-92a regulation of Kruppel-like factors 4 and 2 in atherosusceptible endothelium. *Arterioscler Thromb Vasc Biol*, 32, 979-87.
- FISCH, S., GRAY, S., HEYMANS, S., HALDAR, S. M., WANG, B., PFISTER, O., CUI, L., KUMAR, A., LIN, Z., SEN-BANERJEE, S., DAS, H., PETERSEN, C. A., MENDE, U., BURLEIGH, B. A., ZHU, Y., PINTO, Y. M., LIAO, R. & JAIN, M. K. 2007. Kruppel-like factor 15 is a regulator of cardiomyocyte hypertrophy. *Proc Natl Acad Sci U S A*, 104, 7074-9.
- FLEDDERUS, J. O., BOON, R. A., VOLGER, O. L., HURTTILA, H., YLA-HERTTUALA, S., PANNEKOEK, H., LEVONEN, A. L. & HORREVOETS, A. J. 2008. KLF2 primes the antioxidant transcription factor Nrf2 for activation in endothelial cells. *Arterioscler Thromb Vasc Biol*, 28, 1339-46.
- FLEDDERUS, J. O., VAN THIENEN, J. V., BOON, R. A., DEKKER, R. J., ROHLENA, J., VOLGER, O. L., BIJNENS, A. P., DAEMEN, M. J., KUIPER, J., VAN BERKEL, T. J., PANNEKOEK, H. & HORREVOETS, A. J. 2007. Prolonged shear stress and KLF2 suppress constitutive proinflammatory transcription through inhibition of ATF2. *Blood*, 109, 4249-57.
- FLEMING, A., DIEKMANN, H. & GOLDSMITH, P. 2013. Functional characterisation of the maturation of the blood-brain barrier in larval zebrafish. *PLoS One*, 8, e77548.
- GIMBRONE, M. A., JR. & GARCIA-CARDENA, G. 2013. Vascular endothelium, hemodynamics, and the pathobiology of atherosclerosis. *Cardiovasc Pathol*, 22, 9-15.
- GRACIA-SANCHO, J., VILLARREAL, G., JR., ZHANG, Y. & GARCIA-CARDENA, G. 2010. Activation of SIRT1 by resveratrol induces KLF2 expression conferring an endothelial vasoprotective phenotype. *Cardiovasc Res*, 85, 514-9.
- GUTIERREZ, A., PAN, L., GROEN, R. W., BALEYDIER, F., KENTSIS, A., MARINEAU, J., GREBLIUNAITE, R., KOZAKEWICH, E., REED, C., PFLUMIO, F., POGGIO, S., UZAN, B., CLEMONS, P., VERPLANK, L., AN, F., BURBANK, J., NORTON, S., TOLLIDAY, N., STEEN, H., WENG, A. P., YUAN, H., BRADNER, J. E., MITSIADES, C., LOOK, A. T. & ASTER, J. C. 2014. Phenothiazines induce PP2A-mediated apoptosis in T cell acute lymphoblastic leukemia. *J Clin Invest*, 124, 644-55.
- HAMIK, A., LIN, Z., KUMAR, A., BALCELLS, M., SINHA, S., KATZ, J., FEINBERG, M. W., GERZSTEN, R. E., EDELMAN, E. R. & JAIN, M. K. 2007. Kruppel-like factor 4 regulates endothelial inflammation. *J Biol Chem*, 282, 13769-79.
- HAYASHI, M., KIM, S. W., IMANAKA-YOSHIDA, K., YOSHIDA, T., ABEL, E. D., ELICEIRI, B., YANG, Y., ULEVITCH, R. J. & LEE, J. D. 2004. Targeted deletion of BMK1/ERK5 in adult mice perturbs vascular integrity and leads to endothelial failure. *J Clin Invest*, 113, 1138-48.
- HERGENREIDER, E., HEYDT, S., TREGUER, K., BOETTGER, T., HORREVOETS, A. J., ZEIHNER, A. M., SCHEFFER, M. P., FRANGAKIS, A. S., YIN, X., MAYR, M., BRAUN, T., URBICH, C., BOON, R. A. & DIMMELER, S. 2012. Atheroprotective communication

between endothelial cells and smooth muscle cells through miRNAs. *Nat Cell Biol*, 14, 249-56.

HOWE, K., CLARK, M. D., TORROJA, C. F., TORRANCE, J., BERTHELOT, C., MUFFATO, M., COLLINS, J. E., HUMPHRAY, S., MCLAREN, K., MATTHEWS, L., MCLAREN, S., SEALY, I., CACCAMO, M., CHURCHER, C., SCOTT, C., BARRETT, J. C., KOCH, R., RAUCH, G. J., WHITE, S., CHOW, W., KILIAN, B., QUINTAIS, L. T., GUERRA-ASSUNCAO, J. A., ZHOU, Y., GU, Y., YEN, J., VOGEL, J. H., EYRE, T., REDMOND, S., BANERJEE, R., CHI, J., FU, B., LANGLEY, E., MAGUIRE, S. F., LAIRD, G. K., LLOYD, D., KENYON, E., DONALDSON, S., SEHRA, H., ALMEIDA-KING, J., LOVELAND, J., TREVANION, S., JONES, M., QUAIL, M., WILLEY, D., HUNT, A., BURTON, J., SIMS, S., MCLAY, K., PLUMB, B., DAVIS, J., CLEE, C., OLIVER, K., CLARK, R., RIDDLE, C., ELLIOT, D., THREADGOLD, G., HARDEN, G., WARE, D., BEGUM, S., MORTIMORE, B., KERRY, G., HEATH, P., PHILLIMORE, B., TRACEY, A., CORBY, N., DUNN, M., JOHNSON, C., WOOD, J., CLARK, S., PELAN, S., GRIFFITHS, G., SMITH, M., GLITHERO, R., HOWDEN, P., BARKER, N., LLOYD, C., STEVENS, C., HARLEY, J., HOLT, K., PANAGIOTIDIS, G., LOVELL, J., BEASLEY, H., HENDERSON, C., GORDON, D., AUGER, K., WRIGHT, D., COLLINS, J., RAISEN, C., DYER, L., LEUNG, K., ROBERTSON, L., AMBRIDGE, K., LEONGAMORNERT, D., MCGUIRE, S., GILDERTHORP, R., GRIFFITHS, C., MANTHRAVADI, D., NICHOL, S., BARKER, G., et al. 2013. The zebrafish reference genome sequence and its relationship to the human genome. *Nature*, 496, 498-503.

HUDDLESON, J. P., SRINIVASAN, S., AHMAD, N. & LINGREL, J. B. 2004. Fluid shear stress induces endothelial KLF2 gene expression through a defined promoter region. *Biol Chem*, 385, 723-9.

IRION, U., KRAUSS, J. & NUSSLEIN-VOLHARD, C. 2014. Precise and efficient genome editing in zebrafish using the CRISPR/Cas9 system. *Development*, 141, 4827-30.

JIANG, J., CHAN, Y. S., LOH, Y. H., CAI, J., TONG, G. Q., LIM, C. A., ROBSON, P., ZHONG, S. & NG, H. H. 2008. A core Klf circuitry regulates self-renewal of embryonic stem cells. *Nat Cell Biol*, 10, 353-60.

JOHNSON, B. D., MATHER, K. J. & WALLACE, J. P. 2011. Mechanotransduction of shear in the endothelium: basic studies and clinical implications. *Vasc Med*, 16, 365-77.

KAWANAMI, D., MAHABELESWAR, G. H., LIN, Z., ATKINS, G. B., HAMIK, A., HALDAR, S. M., MAEMURA, K., LAMANNA, J. C. & JAIN, M. K. 2009. Kruppel-like factor 2 inhibits hypoxia-inducible factor 1alpha expression and function in the endothelium. *J Biol Chem*, 284, 20522-30.

KLIMEK, V. M., DOLEZAL, E. K., SMITH, L., SOFF, G. & NIMER, S. D. 2012. Phase I trial of sodium salicylate in patients with myelodysplastic syndromes and acute myelogenous leukemia. *Leuk Res*, 36, 570-4.

KOBUS, K., KOPYCINSKA, J., KOZLOWSKA-WIECHOWSKA, A., URASINSKA, E., KEMPINSKA-PODHORODECKA, A., HAAS, T. L., MILKIEWICZ, P. & MILKIEWICZ, M. 2012. Angiogenesis within the duodenum of patients with cirrhosis is

- modulated by mechanosensitive Kruppel-like factor 2 and microRNA-126. *Liver Int*, 32, 1222-32.
- KOMARAVOLU, R. K., ADAM, C., MOONEN, J. R., HARMSEN, M. C., GOEBELER, M. & SCHMIDT, M. 2015. Erk5 inhibits endothelial migration via KLF2-dependent down-regulation of PAK1. *Cardiovasc Res*, 105, 86-95.
- KUMAR, A., LIN, Z., SENBANERJEE, S. & JAIN, M. K. 2005. Tumor necrosis factor alpha-mediated reduction of KLF2 is due to inhibition of MEF2 by NF-kappaB and histone deacetylases. *Mol Cell Biol*, 25, 5893-903.
- KUO, C. T., VESELITS, M. L. & LEIDEN, J. M. 1997. LKLF: A transcriptional regulator of single-positive T cell quiescence and survival. *Science*, 277, 1986-90.
- LEE, J. S., YU, Q., SHIN, J. T., SEBZDA, E., BERTOZZI, C., CHEN, M., MERICKO, P., STADTFELD, M., ZHOU, D., CHENG, L., GRAF, T., MACRAE, C. A., LEPORE, J. J., LO, C. W. & KAHN, M. L. 2006. Klf2 is an essential regulator of vascular hemodynamic forces in vivo. *Dev Cell*, 11, 845-57.
- LIN, Z., KUMAR, A., SENBANERJEE, S., STANISZEWSKI, K., PARMAR, K., VAUGHAN, D. E., GIMBRONE, M. A., JR., BALASUBRAMANIAN, V., GARCIA-CARDENA, G. & JAIN, M. K. 2005. Kruppel-like factor 2 (KLF2) regulates endothelial thrombotic function. *Circ Res*, 96, e48-57.
- LINGREL, J. B., PILCHER-ROBERTS, R., BASFORD, J. E., MANOHARAN, P., NEUMANN, J., KONANIAH, E. S., SRINIVASAN, R., BOGDANOV, V. Y. & HUI, D. Y. 2012. Myeloid-specific Kruppel-like factor 2 inactivation increases macrophage and neutrophil adhesion and promotes atherosclerosis. *Circ Res*, 110, 1294-302.
- LORD, A. M., NORTH, T. E. & ZON, L. I. 2007. Prostaglandin E2: making more of your marrow. *Cell Cycle*, 6, 3054-7.
- MARTIN, K. M., METCALFE, J. C. & KEMP, P. R. 2001. Expression of Klf9 and Klf13 in mouse development. *Mech Dev*, 103, 149-51.
- MCCONNELL, B. B. & YANG, V. W. 2010. Mammalian Kruppel-like factors in health and diseases. *Physiol Rev*, 90, 1337-81.
- MEADOWS, S. M., SALANGA, M. C. & KRIEG, P. A. 2009. Kruppel-like factor 2 cooperates with the ETS family protein ERG to activate Flk1 expression during vascular development. *Development*, 136, 1115-25.
- MEHTA, T. S., LU, H., WANG, X., URVALEK, A. M., NGUYEN, K. H., MONZUR, F., HAMMOND, J. D., MA, J. Q. & ZHAO, J. 2009. A unique sequence in the N-terminal regulatory region controls the nuclear localization of KLF8 by cooperating with the C-terminal zinc-fingers. *Cell Res*, 19, 1098-109.
- MILLER, I. J. & BIEKER, J. J. 1993. A novel, erythroid cell-specific murine transcription factor that binds to the CACCC element and is related to the Kruppel family of nuclear proteins. *Mol Cell Biol*, 13, 2776-86.

- NANDAN, M. O. & YANG, V. W. 2009. The role of Kruppel-like factors in the reprogramming of somatic cells to induced pluripotent stem cells. *Histol Histopathol*, 24, 1343-55.
- NICOLI, S., STANDLEY, C., WALKER, P., HURLSTONE, A., FOGARTY, K. E. & LAWSON, N. D. 2010. MicroRNA-mediated integration of haemodynamics and Vegf signalling during angiogenesis. *Nature*, 464, 1196-200.
- NUSSLEIN-VOLHARD, C. & WIESCHAUS, E. 1980. Mutations affecting segment number and polarity in *Drosophila*. *Nature*, 287, 795-801.
- OATES, A. C., PRATT, S. J., VAIL, B., YAN, Y., HO, R. K., JOHNSON, S. L., POSTLETHWAIT, J. H. & ZON, L. I. 2001. The zebrafish *klf* gene family. *Blood*, 98, 1792-801.
- OWENS, K. N., SANTOS, F., ROBERTS, B., LINBO, T., COFFIN, A. B., KNISELY, A. J., SIMON, J. A., RUBEL, E. W. & RAIBLE, D. W. 2008. Identification of genetic and chemical modulators of zebrafish mechanosensory hair cell death. *PLoS Genet*, 4, e1000020.
- PARMAR, K. M., LARMAN, H. B., DAI, G., ZHANG, Y., WANG, E. T., MOORTHY, S. N., KRATZ, J. R., LIN, Z., JAIN, M. K., GIMBRONE, M. A., JR. & GARCIA-CARDENA, G. 2006. Integration of flow-dependent endothelial phenotypes by Kruppel-like factor 2. *J Clin Invest*, 116, 49-58.
- PARMAR, K. M., NAMBU DIRI, V., DAI, G., LARMAN, H. B., GIMBRONE, M. A., JR. & GARCIA-CARDENA, G. 2005. Statins exert endothelial atheroprotective effects via the KLF2 transcription factor. *J Biol Chem*, 280, 26714-9.
- PEAL, D. S., MILLS, R. W., LYNCH, S. N., MOSLEY, J. M., LIM, E., ELLINOR, P. T., JANUARY, C. T., PETERSON, R. T. & MILAN, D. J. 2011. Novel chemical suppressors of long QT syndrome identified by an in vivo functional screen. *Circulation*, 123, 23-30.
- PEARSON, R., FLEETWOOD, J., EATON, S., CROSSLEY, M. & BAO, S. 2008. Kruppel-like transcription factors: a functional family. *Int J Biochem Cell Biol*, 40, 1996-2001.
- PETERSON, R. T., LINK, B. A., DOWLING, J. E. & SCHREIBER, S. L. 2000. Small molecule developmental screens reveal the logic and timing of vertebrate development. *Proc Natl Acad Sci U S A*, 97, 12965-9.
- POPOVIC, M., ZAJA, R., FENT, K. & SMITAL, T. 2014. Interaction of environmental contaminants with zebrafish organic anion transporting polypeptide, *Oatp1d1* (*Slco1d1*). *Toxicol Appl Pharmacol*, 280, 149-58.
- RADER, D. J. & DAUGHERTY, A. 2008. Translating molecular discoveries into new therapies for atherosclerosis. *Nature*, 451, 904-13.
- RAJAMANNAN, N. M., SUBRAMANIAM, M., ABRAHAM, T. P., VASILE, V. C., ACKERMAN, M. J., MONROE, D. G., CHEW, T. L. & SPELSBERG, T. C. 2007. TGFbeta inducible early gene-1 (*TIEG1*) and cardiac hypertrophy: Discovery and characterization of a novel signaling pathway. *J Cell Biochem*, 100, 315-25.

- RAZANI, B., ENGELMAN, J. A., WANG, X. B., SCHUBERT, W., ZHANG, X. L., MARKS, C. B., MACALUSO, F., RUSSELL, R. G., LI, M., PESTELL, R. G., DI VIZIO, D., HOU, H., JR., KNEITZ, B., LAGAUD, G., CHRIST, G. J., EDELMANN, W. & LISANTI, M. P. 2001. Caveolin-1 null mice are viable but show evidence of hyperproliferative and vascular abnormalities. *J Biol Chem*, 276, 38121-38.
- RENNEKAMP, A. J. & PETERSON, R. T. 2015. 15 years of zebrafish chemical screening. *Curr Opin Chem Biol*, 24, 58-70.
- ROSEN, J. N., SWEENEY, M. F. & MABLY, J. D. 2009. Microinjection of zebrafish embryos to analyze gene function. *J Vis Exp*.
- ROTH, B. L., SHEFFLER, D. J. & KROEZE, W. K. 2004. Magic shotguns versus magic bullets: selectively non-selective drugs for mood disorders and schizophrenia. *Nat Rev Drug Discov*, 3, 353-9.
- SANDOVAL, I. T., MANOS, E. J., VAN WAGONER, R. M., DELACRUZ, R. G., EDES, K., WINGE, D. R., IRELAND, C. M. & JONES, D. A. 2013. Juxtaposition of chemical and mutation-induced developmental defects in zebrafish reveal a copper-chelating activity for kalihinol F. *Chem Biol*, 20, 753-63.
- SCHUH, R., AICHER, W., GAUL, U., COTE, S., PREISS, A., MAIER, D., SEIFERT, E., NAUBER, U., SCHRODER, C., KEMLER, R. & ET AL. 1986. A conserved family of nuclear proteins containing structural elements of the finger protein encoded by Kruppel, a Drosophila segmentation gene. *Cell*, 47, 1025-32.
- SEBZDA, E., ZOU, Z., LEE, J. S., WANG, T. & KAHN, M. L. 2008. Transcription factor KLF2 regulates the migration of naive T cells by restricting chemokine receptor expression patterns. *Nat Immunol*, 9, 292-300.
- SEN-BANERJEE, S., MIR, S., LIN, Z., HAMIK, A., ATKINS, G. B., DAS, H., BANERJEE, P., KUMAR, A. & JAIN, M. K. 2005. Kruppel-like factor 2 as a novel mediator of statin effects in endothelial cells. *Circulation*, 112, 720-6.
- SENBANERJEE, S., LIN, Z., ATKINS, G. B., GREIF, D. M., RAO, R. M., KUMAR, A., FEINBERG, M. W., CHEN, Z., SIMON, D. I., LUSCINSKAS, F. W., MICHEL, T. M., GIMBRONE, M. A., JR., GARCIA-CARDENA, G. & JAIN, M. K. 2004. KLF2 is a novel transcriptional regulator of endothelial proinflammatory activation. *J Exp Med*, 199, 1305-15.
- SHINDO, T., MANABE, I., FUKUSHIMA, Y., TOBE, K., AIZAWA, K., MIYAMOTO, S., KAWAI-KOWASE, K., MORIYAMA, N., IMAI, Y., KAWAKAMI, H., NISHIMATSU, H., ISHIKAWA, T., SUZUKI, T., MORITA, H., MAEMURA, K., SATA, M., HIRATA, Y., KOMUKAI, M., KAGECHIKA, H., KADOWAKI, T., KURABAYASHI, M. & NAGAI, R. 2002. Kruppel-like zinc-finger transcription factor KLF5/BTEB2 is a target for angiotensin II signaling and an essential regulator of cardiovascular remodeling. *Nat Med*, 8, 856-63.
- STREISINGER, G., WALKER, C., DOWER, N., KNAUBER, D. & SINGER, F. 1981. Production of clones of homozygous diploid zebra fish (*Brachydanio rerio*). *Nature*, 291, 293-6.

- SUMMERTON, J. & WELLER, D. 1997. Morpholino antisense oligomers: design, preparation, and properties. *Antisense Nucleic Acid Drug Dev*, 7, 187-95.
- SWINNEY, D. C. & ANTHONY, J. 2011. How were new medicines discovered? *Nat Rev Drug Discov*, 10, 507-19.
- VILELLA, A. J., SEVERIN, J., URETA-VIDAL, A., HENG, L., DURBIN, R. & BIRNEY, E. 2009. EnsemblCompara GeneTrees: Complete, duplication-aware phylogenetic trees in vertebrates. *Genome Res*, 19, 327-35.
- WANG, B., HALDAR, S. M., LU, Y., IBRAHIM, O. A., FISCH, S., GRAY, S., LEASK, A. & JAIN, M. K. 2008. The Kruppel-like factor KLF15 inhibits connective tissue growth factor (CTGF) expression in cardiac fibroblasts. *J Mol Cell Cardiol*, 45, 193-7.
- WANG, L., FAN, C., TOPOL, S. E., TOPOL, E. J. & WANG, Q. 2003. Mutation of MEF2A in an inherited disorder with features of coronary artery disease. *Science*, 302, 1578-81.
- WANG, W., HA, C. H., JHUN, B. S., WONG, C., JAIN, M. K. & JIN, Z. G. 2010. Fluid shear stress stimulates phosphorylation-dependent nuclear export of HDAC5 and mediates expression of KLF2 and eNOS. *Blood*, 115, 2971-9.
- WANG, X. Q., NIGRO, P., WORLD, C., FUJIWARA, K., YAN, C. & BERK, B. C. 2012. Thioredoxin interacting protein promotes endothelial cell inflammation in response to disturbed flow by increasing leukocyte adhesion and repressing Kruppel-like factor 2. *Circ Res*, 110, 560-8.
- WANI, M. A., CONKRIGHT, M. D., JEFFRIES, S., HUGHES, M. J. & LINGREL, J. B. 1999a. cDNA isolation, genomic structure, regulation, and chromosomal localization of human lung Kruppel-like factor. *Genomics*, 60, 78-86.
- WANI, M. A., WERT, S. E. & LINGREL, J. B. 1999b. Lung Kruppel-like factor, a zinc finger transcription factor, is essential for normal lung development. *J Biol Chem*, 274, 21180-5.
- WESTHOFF, J. H., GISELBRECHT, S., SCHMIDTS, M., SCHINDLER, S., BEALES, P. L., TONSHOFF, B., LIEBEL, U. & GEHRIG, J. 2013. Development of an automated imaging pipeline for the analysis of the zebrafish larval kidney. *PLoS One*, 8, e82137.
- WHITE, D. T., EROGLU, A. U., WANG, G., ZHANG, L., SENGUPTA, S., DING, D., RAJPUROHIT, S. K., WALKER, S. L., JI, H., QIAN, J. & MUMM, J. S. 2016. ARQiv-HTS, a versatile whole-organism screening platform enabling in vivo drug discovery at high-throughput rates. *Nat Protoc*, 11, 2432-2453.
- WITTBRODT, J. N., LIEBEL, U. & GEHRIG, J. 2014. Generation of orientation tools for automated zebrafish screening assays using desktop 3D printing. *BMC Biotechnol*, 14, 36.

- XIAO, A., WANG, Z., HU, Y., WU, Y., LUO, Z., YANG, Z., ZU, Y., LI, W., HUANG, P., TONG, X., ZHU, Z., LIN, S. & ZHANG, B. 2013. Chromosomal deletions and inversions mediated by TALENs and CRISPR/Cas in zebrafish. *Nucleic Acids Res*, 41, e141.
- YAMAMOTO, Y., VERMA, U. N., PRAJAPATI, S., KWAK, Y. T. & GAYNOR, R. B. 2003. Histone H3 phosphorylation by IKK-alpha is critical for cytokine-induced gene expression. *Nature*, 423, 655-9.
- YAN, C., TAKAHASHI, M., OKUDA, M., LEE, J. D. & BERK, B. C. 1999. Fluid shear stress stimulates big mitogen-activated protein kinase 1 (BMK1) activity in endothelial cells. Dependence on tyrosine kinases and intracellular calcium. *J Biol Chem*, 274, 143-50.
- YU, P. B., HONG, C. C., SACHIDANANDAN, C., BABITT, J. L., DENG, D. Y., HOYNG, S. A., LIN, H. Y., BLOCH, K. D. & PETERSON, R. T. 2008. Dorsomorphin inhibits BMP signals required for embryogenesis and iron metabolism. *Nat Chem Biol*, 4, 33-41.
- ZHANG, X., SRINIVASAN, S. V. & LINGREL, J. B. 2004. WWP1-dependent ubiquitination and degradation of the lung Kruppel-like factor, KLF2. *Biochem Biophys Res Commun*, 316, 139-48.
- ZHANG, Y., YEH, J. R., MARA, A., JU, R., HINES, J. F., CIRONE, P., GRIESBACH, H. L., SCHNEIDER, I., SLUSARSKI, D. C., HOLLEY, S. A. & CREWS, C. M. 2006. A chemical and genetic approach to the mode of action of fumagillin. *Chem Biol*, 13, 1001-9.

Appendix

Appendix 1: Plate-reader feasibility

Lovastatin titration data from plate-reader using MetaXpress software

Plate-reader feasibility images

Calculating Z factor and SSMD for the assay.

Appendix 2: Validating blinded positive and negative controls

Data from plate-reader using MetaXpress software

Appendix 3: Spectrum Library (100122) plate 8 screening data.